CHALMERS

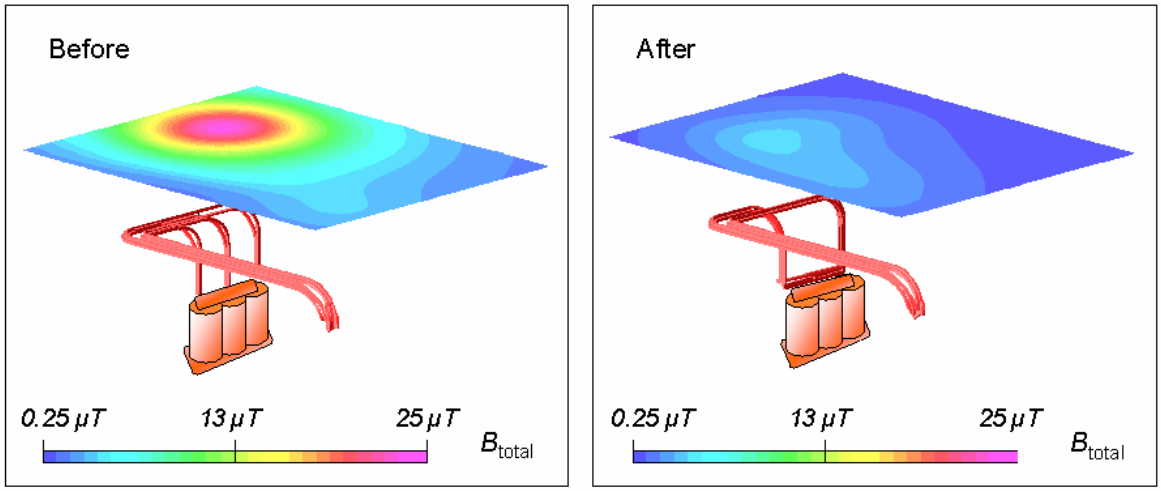

Mitigation of Power-Frequency Magnetic Fields

With Applications to Substations and Other Parts of the Electric Network

ENER SALINAS

Department of Electric Power Engineering
Chalmers University of Technology
Göteborg, Sweden 2001

Mitigation of Power-Frequency Magnetic Fields

With Applications to Substations and Other Parts of the Electric Network

av

Ener Salinas

Akademisk avhandling som för avläggande av
teknisk doktorsexamen vid Chalmers tekniska högskola
försvaras vid en offentlig disputation i IT-rummet, Hörsalsvägen 11
Chalmers tekniska högskolan, Göteborg,
fredagen den 24: e augusti 2001, kl 10.00.

Fakultetsopponent är Michel Ianoz,
Laboratoire de Réseaux d'Energie Electrique
Ecole Polytechnique Federale de Lausanne, Schweiz.

Avhandlingen finns tillgänglig på
Institutionen för Elkraftteknik
CHALMERS TEKNISKA HÖGSKOLA
412 96 Göteborg

Telefon 031-7721660

Abstract

In recent times, electromagnetic emissions from various electrical components have induced more than one debate whether they represent a harmful influence to our health. In addition, interferences caused by power frequency magnetic fields (PFMFs) on electron beam based electronic equipment (e.g. cathode ray tubes found in TV screens and computer monitors, electron microscopes) become evident at levels over 1 microtesla. These issues have caused some concern with the general public but also to the utilities, their customers and the electromagnetic compatibility community. On the other hand, they have also spurred efforts to study and mitigate these fields.

Although most published studies and debates are concerned with fields from power transmission lines, similar levels of PFMFs can be found in a city neighbourhood. For this reason this study focuses on the fields originating from the last stages of the power network before reaching the customer, in particular the components of in-house secondary substations. However the methods developed in this study can also be applied more generally.

Conductive and ferromagnetic shielding, passive and active compensation and other techniques are described. These techniques make use of modern methods of analysis such as algebraic computing and 2D/3D modelling. It was found that shielding using thin conductive plates and a proper design can provide for cost-effective mitigation of PFMFs. It was shown that the choice of either ferromagnetic or conductive shielding is dependant on a number of variables, which can only be determined by a proper 2D or 3D modelling. It was also found that cable and busbar connections and not the transformers are the main cause of large PFMF emission from substations.

These and other results were applied to actual cases where the measured values were considered as problematic, or where low emission was a requirement already at the design stages.

Keywords: busbars, eddy currents, EMC, FEM, field mitigation, power-frequency magnetic fields, substation, transformers.

Preface

In this thesis a research project is described which was both pleasant and rewarding. The project started as an initiative to deal with a difficult and an interesting issue: How to mitigate power-frequency magnetic fields? Search for solutions could work best if efforts were combined. This resulted in a co-operation between industry and the academic world. The departments of Electric Power Engineering and Electromagnetics at Chalmers University of Technology, Elforsk, ABB and Göteborg Energi, together initiated this project.

I would like to thank Elforsk for financing this project. My gratitude goes to the members of the steering group: Lars Hammarsson (Göteborg Energi Nät AB), Sven Hörnfeldt (ABB Corporate Research AB) and Jan-Olov Sjödin (Vattenfall Transmission AB), for the continuous assessment of the project, their good advice and helpful meetings.

In order to find the optimal solution of a problem sometimes more than one point of view is needed. In this respect it has been quite an experience to have the advise of my three supervisors, Professors Jaap Daalder, Anders Bondeson and Yngve Hamnerius, each of them with a rather different, yet necessary, background for a of project of this nature. I would like to express my gratitude to each of you.

I would like to thank Lars Aspemyr and professor Jorma Luomi for their cooperation during the initial stages of the project, professor Eskil Möller for our discussions about modelling with Opera 3D, Aleksander Bartnicki, for the help and checks in some of our experiments, and the personal at Göteborg Energi for their technical support.

I am grateful to Kjell Siimon, Jan-Olov Lantto and Alexander Wolgast, for countless times of assistance in computer magic.

Finally, dear colleagues and friends at this institute, whom through discussions at the coffee room (some of them about electricity), *brännboll games,* and lunches at *Primavera,* created such a nice working atmosphere, to all of you: Thanks!

Table of contents

1 Introduction

Some time ago, during a conversation with an experimental physicist we arrived at the conclusion that there are two things one certainly always remembers. One of them is the first time you saw a magnet – I still vividly recall playing with iron fillings on a paper while moving a magnetized screw under it. The other one is of a non-technical nature and is not the subject of this thesis.

This report is about magnetism, a subject that has fascinated humans for centuries, and still does. Recently I managed to establish a little record of 7.5 minutes in levitating a spinning magnet that was constructed in collaboration with my first year students [1]. No batteries, superconductors or cold temperatures were involved, just a trick of pure magnetism: one magnet on top of another facing the same poles. Rotation and precession, contribute to the stability of this "toy". Devices such as this were thought to be physically impossible until just a couple of decades ago.

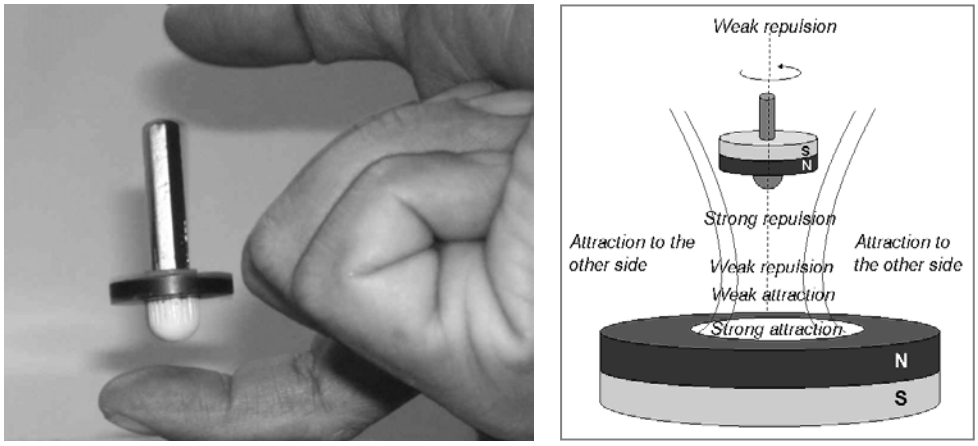

Fig. 1.1 A magnetic spinning top is stably levitating above a larger ring magnet. No batteries, cold temperatures or superconductors are added. Just pure magnetism!

Magnetism itself has of course been known since ancient times. The Chinese called the magnetic stones *tzhu shih,* or “love”. In French a magnet goes by the name *aimant,* the word for “loving” or “affectionate”. In my hometown, Arequipa, the word is *imán,* which also means “very popular” or “attractive”. Then again, we won’t go deeper into this subject.

As advanced as our science and technology is, one may think that nearly everything is known about magnetism. However, there are still interesting, yet unresolved problems. Take for example something we have all heard of: the earth’s magnetism. First of all, in most of our school textbooks, earth’s magnetism is portrayed as our planet being a big magnet. This may be a misconception. To our best knowledge the representation of earth’s magnetism is closest to an electromagnet: circulating ionic currents (billions of amperes) furnish the magnetic field. Yet, we are not very sure about the details of this model. Another example: if we were ever sure that the magnetism of rocks called magnetite or lodestone were originated by the earth’s magnetic field, then we have to be prepared to encounter another problem; namely that the earth’s magnetic field is simply too weak to produce the magnetization found in some of these stones. A scenario involving lightning may solve this puzzle: hundreds of millions volts and hundreds of thousands amperes certainly are able to induce high magnetization in rocks rich in iron. To work out the details of this hypothesis is the exciting part.

1.1 The electromagnetic revolution

The moment that represented the start of one of the most important revolutions in science and in due time having profound implications on technology, was not an *Eureka!* in the Archimedes style, nor a logically deducted theoretical result more in the spirit of Newton or Einstein. No, it was simply an "accident", during a routine preparation for a physics demonstration. The Danish physicist Hans Christian Oersted, observed in 1820 that when an electric current was switched on, a nearby magnetic compass needle started to move. Although he was not able to explain this phenomenon, he published his perception never realizing that 18 years before (!), Gian Dominico Romognosi had already made the very same observation. Moreover Romognosi published it in *La Gazetta de Trentino*. Unfortunately, two things contributed for this observation to be overlooked: Romognosi was a jurist, and he published in a newspaper.

Only a few days passed since the receipt of the news of Oersted's discovery in Paris, when André Marie Ampère presented to the French academy a list of new results based on Oersted's observations; including the one involving attraction between conductors. In England Michael Faraday constructed the first device that could move continuously with electricity [2], and, not much later, he proved the existence of electromagnetic induction, inventing at the same time the transformer. A flurry of investigation ignited and soon other results were obtained, culminating brilliantly with the synthesis and unification of all electromagnetic phenomena by James C. Maxwell in 1871. Strangely enough, no conservative opposition arose to this revolution; neither was

there a time of gradual acceptance as for example happened with the Copernican revolution [3]. In fact it seemed the world was prepared and waiting for it.

1.2 Power-frequency magnetic fields – an uninvited guest?

The electromagnetic revolution changed technology to the world of electricity, electronics and communication we know today. This technical world brought also circuit boards, cables, data transferring devices, power transmission lines, antennas and highly packed circuits – to mention a few. Oersted's and Faraday's observations imply that these devices, due to their electromagnetic properties, are fated to interfere with each other. Moreover, there are propagating electric and magnetic fields that escape the working frequency band of a device or a circuit (i.e. fields due to harmonics).

These fields, depending on their frequency, have different types of interactions with matter and are in general, for more than one reason, undesirable. It is natural to ask if these fields can be hostile to living organisms and if they can produce interference to electronic equipment. As will be seen in chapter 3 the answers to these questions are not trivial. Total elimination of these fields could mean to influence the cause of them so drastically that the devices producing them would not be of much use (e.g. some field may leak off a motor inducing disturbances on some electronic devices, but altering the currents that originate this stray field could also make the motor stop). However it is clear that reducing these fields in a suitable way would be very much desired.

1.3 Mitigation of power-frequency magnetic fields

Imagine you are very annoyed by the noise caused by your neighbour who is fond of music and dance. One way to solve the problems is by covering the walls with sound-masking material (such as fibre-glass sound attenuator laminates or cellulose treated with borax or aluminium sulphate). You can also talk to your neighbour about possible solutions, modifying his music schedule, turning down the volume of the devices or simply moving that big stereo to the other side of the room.

Noise attenuation is just an analogy to illustrate the methodology used in this project. The standard method in magnetic field reduction is to shield affected areas, often using aluminium or iron laminations. The project described in this report goes beyond this criterion. Properties of magnetic field sources are studied; reasons leading to the generation of high fields are investigated; subsequently a cost-efficient strategy to reduce these fields is developed. Simple tools sometimes sufficiently attain large field reductions. However, extensive experimentation and laborious numerical simulations are, not infrequently, necessary to reach modest – but valuable – mitigation factors.

Although this report focuses on the magnetic field reduction from secondary substations, the methods explained here can be applied to other parts of the electric network. An electrical secondary substation is described as the last segment of the distribution stages and closest to the customer.

1.4 Outline of this report

Chapter 2 studies typical sources of power frequency magnetic fields. Deduced properties from this study are essential for developing field reduction strategies. Chapter 3 is dedicated to the interaction between electromagnetic fields and matter, biological effects and electromagnetic compatibility (EMC). Chapter 4 presents simple experiments to intuitively visualize some of the techniques used in this project such as shielding (conductive and ferromagnetic) and active compensation. Chapter 5 describes the fields produced by a substation. The relevance of field reduction by phase arrangement, phase splitting, and optimal positioning of the sources is analysed in chapter 6.

Numerical methods and fundamentals of finite element codes are described in chapter 7. A set of properties for the field of busbars is obtained in chapter 8. In chapter 9, 2D and 3D FEM codes are applied to the conductive and ferromagnetic shielding of magnetic fields from various sources, especially of busbars. Analysis of induced currents in conductive shielding suggests the structure of some of the circuits to be used in passive and active compensation, the subject of chapter 10. Chapter 11 deals with the field mitigation of transformers. Chapter 12 presents applications to actual cases of field reduction, among others, from newly built, modified and renovated substations. Screens for shielding can also be built using a multiple-layer structure. These and other additional characteristics are presented in the appendixes. Chapter 13 discusses future extensions of this work. Chapter 14 presents the main conclusions. At the end published articles are attached.

Throughout this report, the main physical quantity involved is the magnetic flux density (B). In most cases, for simplicity, it is called merely magnetic field. MKS units are used thorough out. Moreover, for B, microtesla (μT) is the most useful sub-unit. Another quantity used is the magnetic field strength (H), with units: A/m. If there is no material around, then there is no actual reason to prefer H or B since they are related by $B = \mu_0 H$. However, inside materials, the distinction can be important.

Some abbreviations used in this report are:
PFMFs: Power frequency magnetic fields
EMC: Electromagnetic compatibility

Mitigation, *reduction* and *attenuation* are used as synonyms, as are *shielding* and *screening* but the latter entail the application of metallic plates.

References

[1] E. Salinas, et al, "Mechanical and Magnetic Levitation", in: *First Quest,* First year students project at the ED-Section, Chalmers University of Technology, Sweden, 2000.

[2] J. F. Keithley *The Story of Electrical and Magnetic Measurements* IEEE Press, New York, 1999.

[3] T. S. Kuhn, *The Structure of Scientific Revolutions*, The University of Chicago Press, 1962.

2 Sources of power frequency magnetic fields

The sources of PFMFs associated with electric energy flows are: transmission lines, overhead distribution services, underground cables, busbars (often carrying currents of the order of few to several thousands amperes), transformers, and in-house cables (Fig. 2.1). In order to design strategies of field reduction it is important to study the properties, similarities and differences of these sources. Although sometimes difficult it is possible – at least in principle – to estimate the magnetic field emitted by most of these sources rather accurately, the most difficult one being the field of a transformer. Different degrees of approximation are required depending on each particular case. For long systems, as in the case of transmission lines or underground cables, a two-dimensional (2D) treatment suffices. However for short busbars, where edge effects are important, or in the case of transformers, three-dimensional (3D) treatments are necessary. These estimations can, in a few cases, be obtained analytically, or using symbolic manipulation programs. However, numerical codes are usually very effective for complex cases.

To evaluate the field from the devices mentioned above it is helpful to find the magnetic field produced by a small element (i.e. of infinitesimal length) of current. This can be done using the Ampere-Laplace law [1], often also called the Biot-Savart formula [2]:

$$d\boldsymbol{B} = \left(\frac{\mu_0 i}{4\pi} \right) \frac{d\boldsymbol{l} \times \boldsymbol{e}_r}{r^2} \tag{2.1}$$

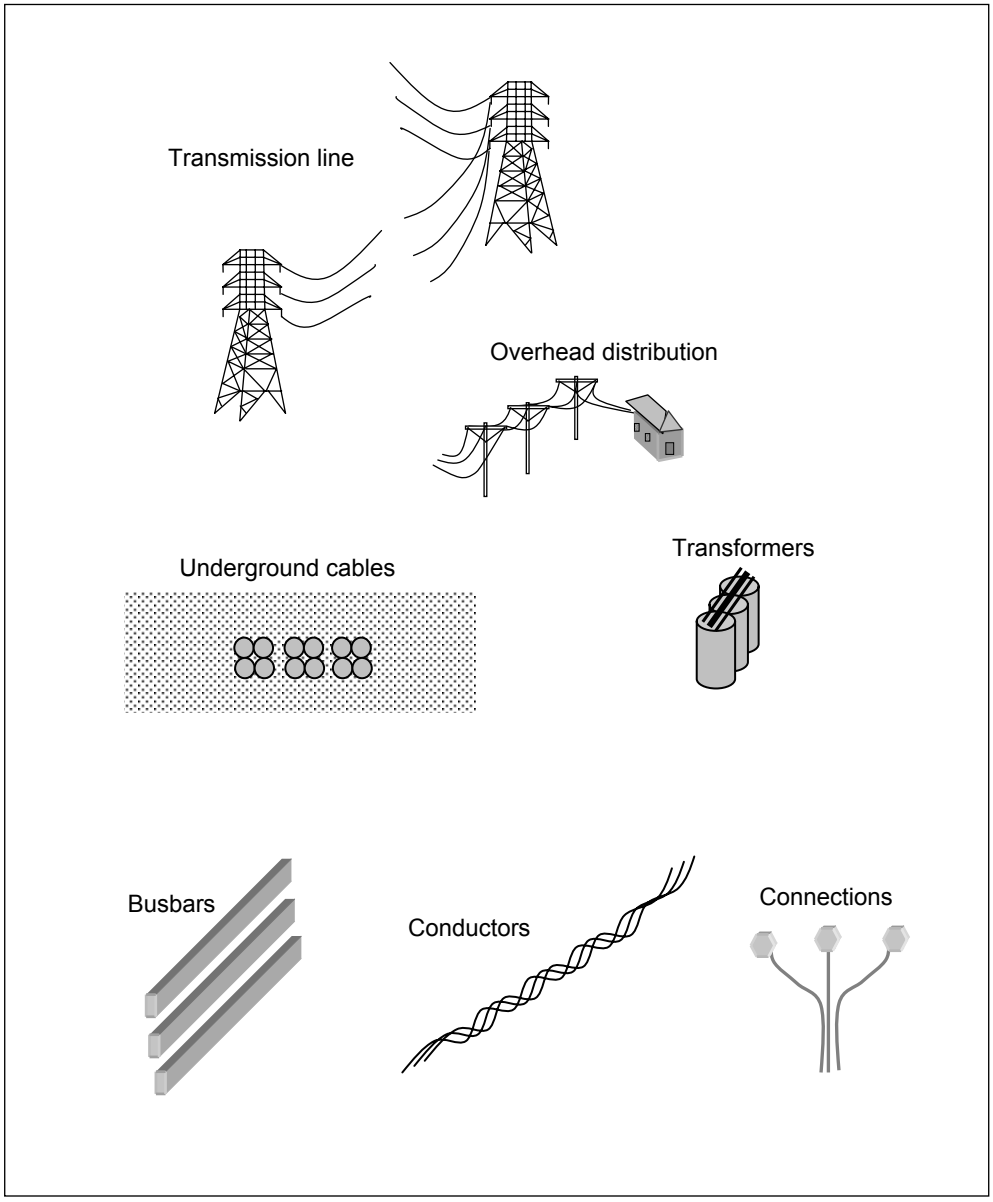

Fig. 2. 1 Major sources of PFMFs at the transmission and distribution stages.

The direction of the current i is represented by $d\boldsymbol{l}$, and $\boldsymbol{r} = r\,\boldsymbol{e}_r$ is the position where the field $\boldsymbol{B}$ is evaluated (Fig. 2.2). Once the field from this element of current is determined, it is a matter of using the superposition

principle and integration to obtain the magnetic field from a more complex source. However, an inspection of this picture and Eq. 2.1 gives what appears to be a physical impossibility, or a contradiction, as the segment represents a broken circuit the current appears on one edge and disappears on the other edge (Fig. 2.2). Consequently the system seems to violate the continuity equation and charge conservation.

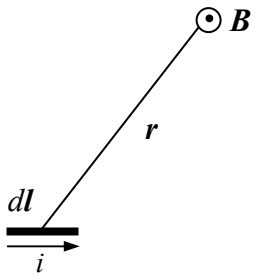

Fig. 2. 2 The field of a small element of current.

Two different ways to solve this apparent contradiction are presented in appendix I.

2.1 Magnetic field of a straight wire of length L

A finite, very thin, and straight conductor of length L carries a current *i*. It is placed along the z-axis (Fig. 2.3). The magnetic field [3] at the location (ρ, z) is independent of the coordinate φ. Its magnitude and direction, in cylindrical coordinates, is given by:

$$\mathbf{B}(\rho,z)=\frac{\mu_0 i}{4\pi\rho}\left[\frac{L/2+z}{\sqrt{(L/2+z)^2+\rho^2}}+\frac{L/2-z}{\sqrt{(L/2-z)^2+\rho^2}}\right]\mathbf{e}_\phi \qquad (2.2)$$

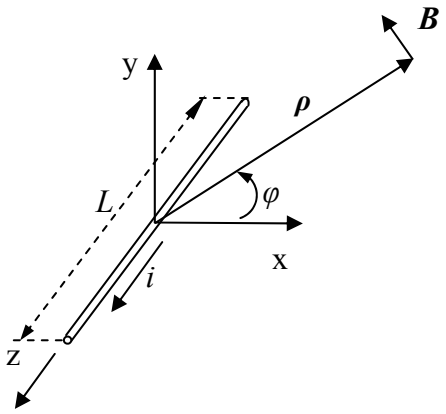

Fig. 2.3 Magnetic field of a thin, straight wire of length *L*.

2.2 Magnetic field of an infinite wire

In order to obtain the field of an infinite (or very long) wire, it is helpful to evaluate Eq. 2.2 in the plane perpendicular to the centre of the wire (i.e. at z = 0). The result is a simplified expression

$$\mathbf{B}(\rho,0)=\frac{\mu_0 i}{4\pi\rho}\left[\frac{L}{\sqrt{(L/2)^2+\rho^2}}\right]\mathbf{e}_\phi \tag{2.3}$$

Hence when $L \to \infty$, or when $\rho << L$, the last equation expresses the field of an infinite long wire. For this limit, the equation becomes even simpler

$$\mathbf{B}(\rho)=\frac{\mu_0 i}{2\pi\rho}\mathbf{e}_\phi \tag{2.4}$$

The decay of the magnetic field from this source is explicitly – unlike the field for short wires – inversely proportional to the distance.

2.2 Magnetic field of two finite wires carrying a mono-phase current

The aim is to evaluate the magnetic field, and its dependence on the distance, of two parallel wires carrying a single phase current, one wire carries a current *i* and the other carries the return *-i*. First of all, the field of two finite wires (with length *L*) is evaluated. In practical situations, it can be advantageous to use Cartesian coordinates (x, y, z). In such case Eq. 2.2 has the following expression

$$\mathbf{B}(x,y,z)=\frac{\mu_0 i}{4\pi}(-y\mathbf{e}_x+x\mathbf{e}_y)f(x,y,z) \tag{2.5}$$

where

$$f(x,y,z)=\frac{1}{(x^2+y^2)}\left[\frac{L/2+z}{\sqrt{x^2+y^2+(L/2+z)^2}}+\frac{L/2-z}{\sqrt{x^2+y^2+(L/2-z)^2}}\right]$$

For a two wires configuration with a separation *a* (Fig. 2.4) both field contributions will superimpose

$$\mathbf{B}=\frac{\mu_0 i}{4\pi}\left\{\left[(-y_1 f(x_1,y_1,z_1)+y_2 f(x_2,y_2,z_2)\right]\mathbf{e}_x+\left[(x_1 f(x_1,y_1,z_1)-x_2 f(x_2,y_2,z_2)\right]\mathbf{e}_y\right\}$$

The following relations hold: $x_1=x-a/2$; $x_2=x+a/2$; $y_1=y_2=y$; $z_1=z_2=z$.

In order to study the field decay with distance, e.g. along the y-axis, the calculation is specialized for $z=0$ and $x=0$ (i.e. $x_1=-a/2$, $x_2=a/2$).

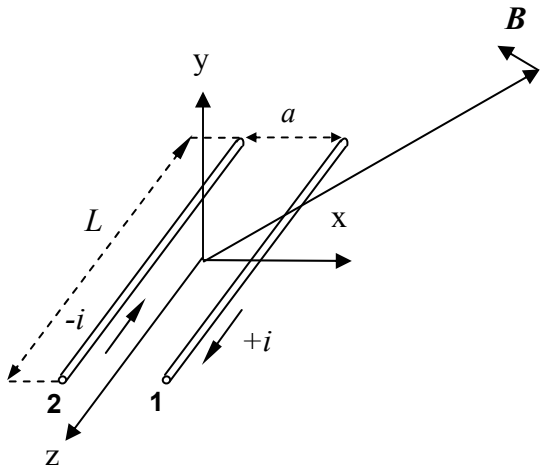

Fig. 2.4 Magnetic field of two parallel wires of length L, the directions of the instantaneous currents are also shown.

Then the field component along the x-axis vanishes, leaving a simple expression for the field of two parallel wires of finite length

$$\mathbf{B}(0,y,0) = -\frac{\mu_0 i}{4\pi}\left\{\frac{aL}{\left[(a/2)^2 + y^2\right]\sqrt{(a/2)^2 + y^2 + (L/2)^2}}\right\}\mathbf{e}_y \qquad (2.6)$$

Furthermore, for long wires $y << L$ the formula reduces to:

$$\mathbf{B}(0,y,0) = -\frac{\mu_0 i}{2\pi}\left\{\frac{a}{\left[(a/2)^2 + y^2\right]}\right\}\mathbf{e}_y \qquad (2.7)$$

For vertical distances y much larger than the separation a (Fig. 2.5), which is often the case of interest, two facts can be deduced: firstly, the magnetic field depends linearly on the separation a; and secondly, the magnetic field decays as $1/(distance)^2$, this is a much faster decay than the dependence on the distance of the field of a single line.

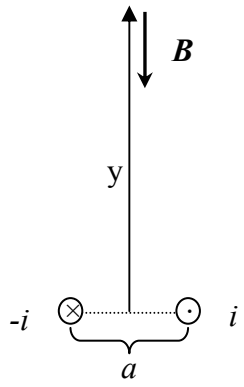

Fig. 2.5 Instantaneous magnetic field of two infinite parallel wires along the vertical distance.

2.2 Magnetic field of a three-phase system of conductors with length *L*

In this case three segments are parallel and carry currents with different phase angles (Fig. 2.6) In general the resultant field will be a rotating vector, i.e. an elliptically polarized field. A frequently used measure of the magnitude of B is given by the following expression

$$B_{result} = \sqrt{B_{\text{major}}{}^2 + B_{\text{minor}}{}^2} \tag{2.8}$$

Where B_{major} and B_{minor} are the maximum and the minimum magnitudes of **B** in the ellipse.

However, under certain conditions (e.g. if the distance between segments is much smaller than the distance to the plane X-Z) one can sometimes assume that the polarization of the magnetic field in the region of interest (the plane X-Z, at some metres above the system) is approximately linear. The field at the point ***P*** is calculated adding the vector-field contribution of each current of the three-busbars system.

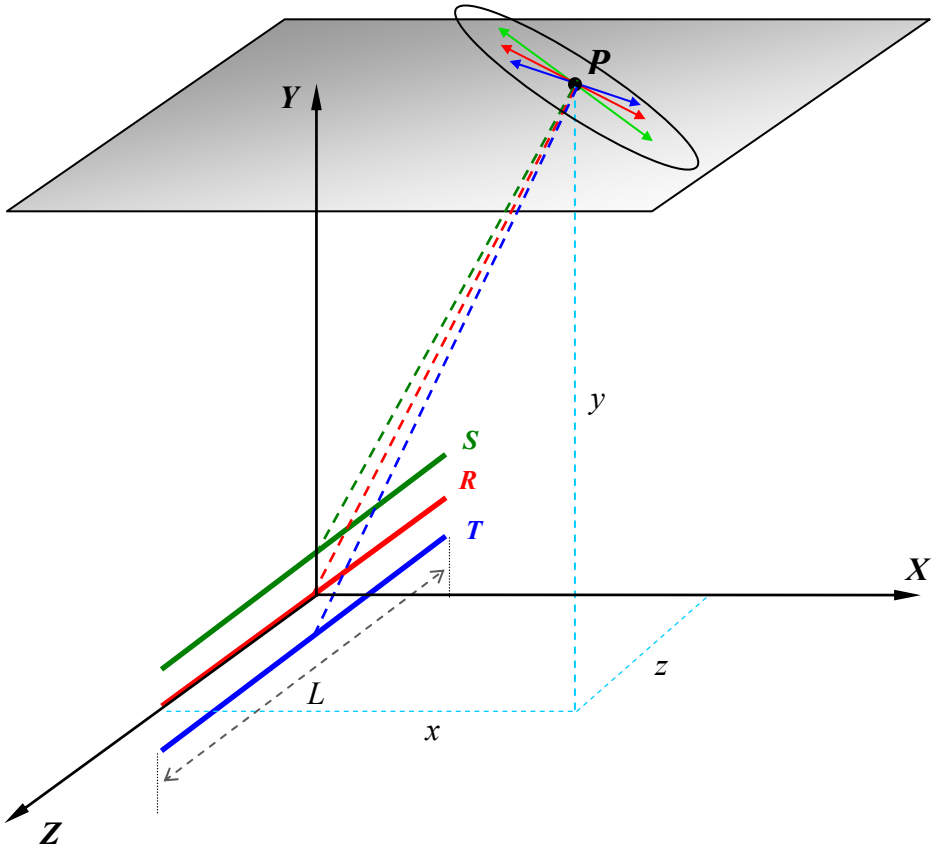

Fig. 2. 6 Magnetic field of a three-phase system of wires evaluated at the point ***P***. The resulting field is rotating and elliptically polarized.

After some lengthy but straightforward calculations, using Eq. 2.5, the rms-value of the magnetic field, in microtesla, acquires the following expression:

$$\left|\vec{B}_{Total}(x,y)\right|_{rms} = \frac{i_{rms}}{10}\cdot\left\{\left(A_1-\frac{A_2}{2}-\frac{A_3}{2}\right)^2+\left(C_1-\frac{C_2}{2}-\frac{C_3}{2}\right)^2+\frac{3}{4}\left[(A_2-A_3)^2+(C_2-C_3)^2\right]\right\}^{1/2}$$

where,

$$A_k(x,y)=\frac{x}{x^2+y_k^2}\left[\frac{L/2+z}{\sqrt{x^2+y_k^2+(L/2+z)^2}}+\frac{L/2-z}{\sqrt{x^2+y_k^2+(L/2-z)^2}}\right]$$

$$C_k(x,y)=\frac{-y_k}{x^2+y_k^2}\left[\frac{L/2+z}{\sqrt{x^2+y_k^2+(L/2+z)^2}}+\frac{L/2-z}{\sqrt{x^2+y_k^2+(L/2-z)^2}}\right], k=1,2,3 \qquad (2.9)$$

This equation is easy to program for a computer, for example MAPLE VI (which is a symbolic manipulation language), thus making it possible to evaluate the field from any geometrical arrangement of straight conductors within the mentioned approximation. By analysing the dependence on some parameters (e.g. the distance between busbars, the length of the busbars, the distance from the busbars system to the measuring point) it is possible to gain some understanding of the properties of busbars.

For a more realistic study of busbars (e.g. considering their finite thickness); for the computation of the field originating from coils of transformers, and other complex problems involving conductors, 2D and 3D numerical simulations are used (to be described in subsequent chapters). However even the formulations of numerical codes that can be able to perform such computations are based on the results discussed in this chapter.

References

[1] J. D. Jackson, *Classical Electrodynamics*, Third Edition, John Wiley & Sons, Inc. N.Y. 1999, pp. 175-180.

[2] D. K. Cheng, *Field and Wave Electromagnetics*, Addison-Wesley Massachusetts, 1989, pp. 600-605.

[3] E. Salinas, *Reduction of Power Frequency Magnetic Fields from Electrical Secondary Substations*, Tek. Lic. Thesis, Chalmers University of Technology, ED section, 1999, pp. 25-32.

3 Interactions

Sources of electromagnetic fields can produce radiant fields and non-radiant fields. A radiant field persists even after the source is turned off; this behaviour is typical for distances (D) much larger than the wavelength λ (i.e. $D/\lambda >> 1$ or "far-field" region). A non-radiant field, typical for sources with $D/\lambda << 1$ (also called "near-field" region), produces electric and magnetic fields that can be decoupled and treated as independent entities. The wavelength of a field with a frequency of 50 Hz is $\lambda = c / f = 6000$ Km. This distance is as large as the radius of our planet (Fig. 3.1). The cases of interest in this study are phenomena taking

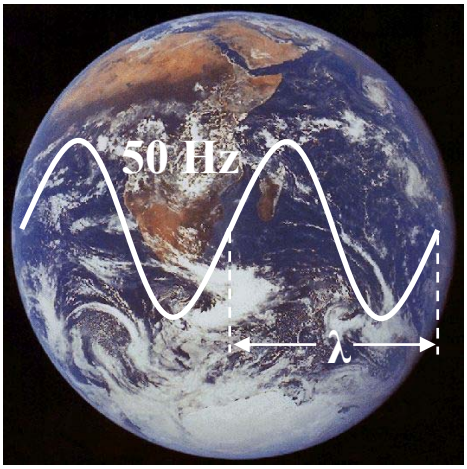

Fig. 3.1 The wavelength of an electromagnetic field with a frequency of 50 Hz is nearly as large as the radius of the earth.

place at a "human-size" scale; thus the frequency is certainly within the near field region. Moreover, the interest is on the magnetic field part of the PFMF. The electric field is also part of it, but is of little interest in

this study. Electric fields caused by free charges can easily be shielded by conducting objects and have poor ability to penetrate walls and even skin.

3.1 The electromagnetic spectrum

In particular for PFMFs, there are two relevant interactions: *i)* the influence of PFMFs on living beings and *ii)* on electronic equipment. In order to determine (or at least try to comprehend) these interactions it is essential to characterize PFMFs in the context of a broad collection of fields, namely the electromagnetic spectrum.

The electromagnetic spectrum represents all possible energies a photon can have (Fig. 3.2). The interest of this study (50/60 Hz) belongs to a narrow range of this spectrum called extremely low frequency (ELF). From the energy point of view these frequencies belong to nearly the lowest end of the spectrum – even far lower than the range of radio waves.

The upper part of the spectrum contains *ionizing radiation.* The frequency (and consequently the energy per quantum) of this type of radiation is substantially higher than that of visible light, and is therefore able to penetrate many materials. When these rays interact with atoms, they send off electrons producing ions, thus the name “ionizing”. High energetic ultraviolet radiation usually manages to kick off external electrons; X-rays penetrate more and can hit electrons belonging to interior energy levels. In extreme cases (*e.g.* gamma radiation) they can affect the nucleus and induce a nuclear reaction. Because ionization of

atoms and molecules change chemical properties, the harmful effect of ionizing radiation on biological tissue is evident.

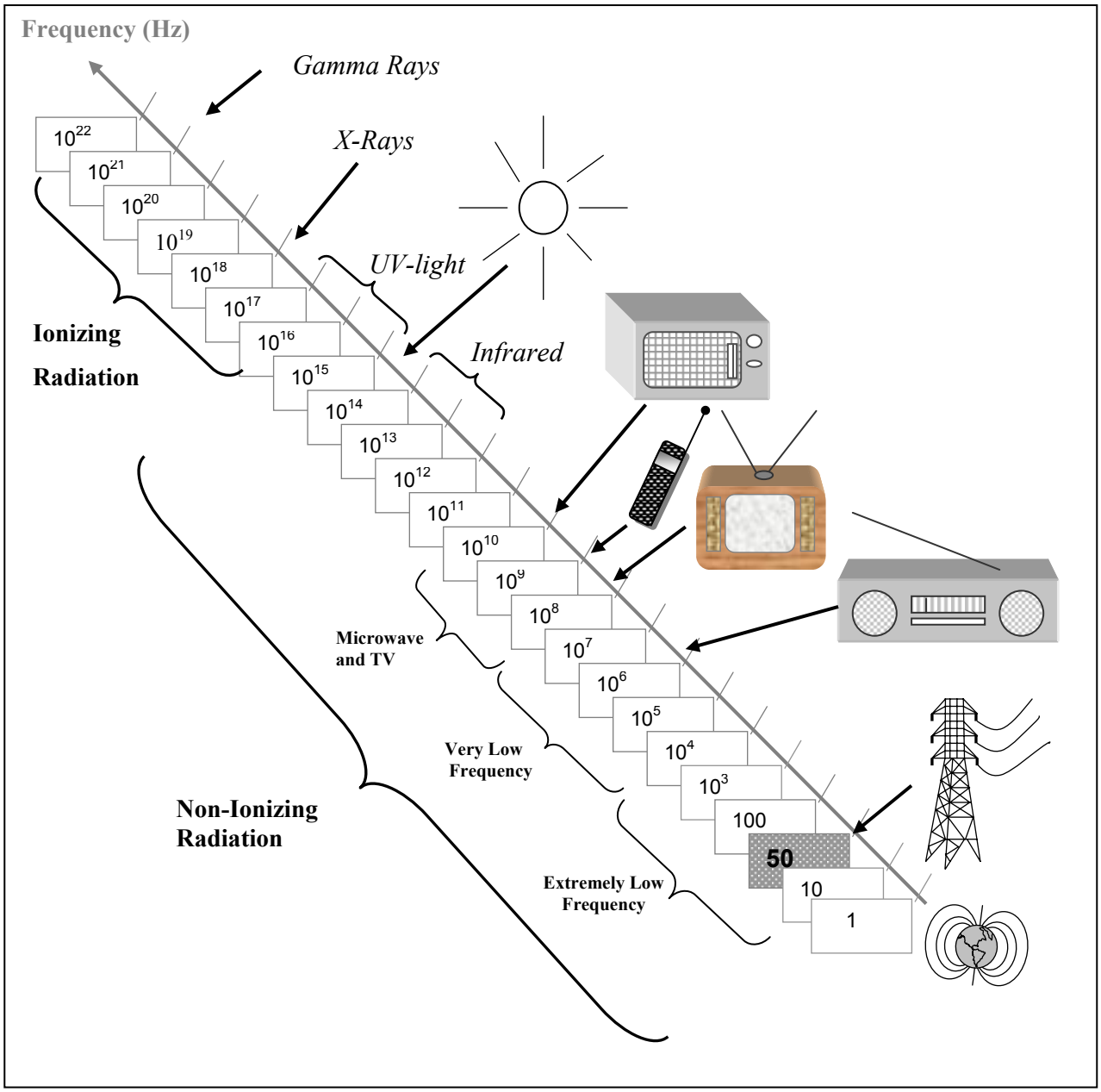

Fig. 3.2 The electromagnetic spectrum; power frequencies (50Hz/60Hz) belong to the extremely low frequency (ELF) part of this spectrum.

Different astrophysical phenomena are the major sources of ionizing radiation. It originates, and remains (thanks to the shielding properties of our atmosphere at these frequencies), mainly in space. However gamma and X-ray emissions occur to some extent in radioactive matter on earth; X-rays are also emitted by certain electronic devices.

Non-ionizing radiation represents electromagnetic waves at lower frequencies, where each quantum is not energetic enough to get electrons away from the atoms. Yet, at some frequencies, some physical mechanism, different from the ones described for the ionizing radiation, can operate. An example is the rapid increase of temperature (induced by rotation of water molecules) in biological tissue when exposed to certain ranges of microwave radiation. A large source of non-ionizing radiation comes from space and especially our sun. Other sources that emit non-ionizing radiation are electronic devices, TV-sets, mobile telephones, radio transmitters, power lines, to name a few.

Static (zero frequency) magnetic fields, such as the geomagnetic, do not induce forces on non-moving charges. However, the real world is dynamic, thus some interaction is expected. Fortunately, this field has been part of the external environment that shaped life on our planet. Thus, even though the average geomagnetic field (around 20-50 microtesla) is fifty times larger than the range of PFMFs considered problematic, living organisms are accustomed to it!

3.2 Biological effects of PFMFs

Studies [1] have shown that power frequency magnetic fields may produce biological effects. Furthermore, it is suspected that different

kinds of diseases might be related to PFMFs, such as: brain cancer and leukaemia. The values of the magnetic field involved are also dependent on the type of analysis. In some epidemiological studies, values as low as 0.2 microtesla, are mentioned to correlate with significant increase in cancer incidence among populations living nearby power lines [2]. Today several experiments are being conducted on animals and researchers have indicated that under certain circumstances exposure to PFMFs may promote tumour development. However other investigators have failed in reproducing these results.

IARC (International Agency for Research on Cancer) recently [3] evaluated possible carcinogenic hazards to human beings from exposures to static and extremely low frequency ELFelectric and magnetic fields, issuing that:

"Overall, ELF magnetic fields were evaluated *as possibly carcinogenic to humans*, based on the statistical association of higher level residential ELF magnetic fields and increased risk for chilhood leukaemia".

Even if a relationship exists at all between PFMFs at the microtesla level and certain forms of cancer, the risk must be very small. But even a small risk must be looked at seriously. Because large numbers of people are exposed to EMF, a small risk could add up to a substantial number of additional cancer cases nation-wide.

3.3 Electromagnetic compatibility

Electromagnetic compatibility (EMC) has been also called the "science of electric/electronic systems coexistence", and it has been defined in the

IEEE Standard Dictionary of Electrical and Electronic terms (IEEE Std. 1000-1992) as:

"The ability of a system to function satisfactorily in its electromagnetic environment without introducing intolerable disturbance to that environment."

Regarding PFMFs, experimental studies [4] show that magnetic field values over 1 microtesla are manifestly able to produce interference in computer terminals and TV screens. This interference is evident in the form of jittering (Fig. 3.3). A jittering screen is not only difficult to use but is annoying to the user, and even produces eye irritation after prolonged use. The productivity of millions of workers in modern society depends on manipulating computer monitors for hours, thus such

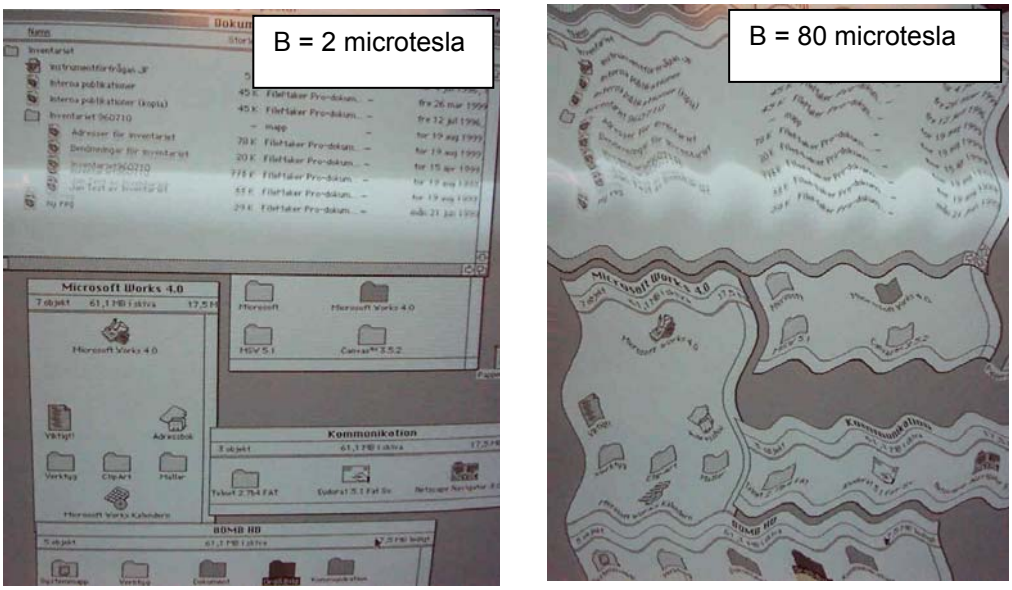

Fig. 3.3 Disturbances on a computer screen, which are produced by two different values of an external magnetic field. Studies show that at the 1 microtesla level there is already a noticeable and annoying disturbance.

disturbances should be considered a serious problem of electromagnetic compatibility.

The value of 1 microtesla is important for it already suggests at what range a power frequency magnetic field can be considered high – independently of the existence of biological effects of PFMFs.

3.4 Recommendations

There are not yet safety standards (issued in terms of biological effects or EMC) regulating the admissible values for PFMFs. However, the International Committee on Non-Ionizing Radiation Protection (ICNIRP) recommends, for the general public, that the current densities caused by magnetic (or electric) fields in the human body should be lower than 2 mA/m^2. From here it is possible to derive some regulations, which can be applied to the general public and are intended to define access to restricted areas. For example the ICNIRP [5] mentions a worse-case reference value (for 50 Hz) of 100 microtesla for general public. This is not the policy followed in this work –At such magnitude of the magnetic field, a computer monitor simply will not work (see Fig. 3.3).

The Swedish authorities have adopted the policy of "prudent avoidance" [6] i.e. taking simple steps to reduce the exposure to electromagnetic fields in daily life without going out on an economic limb. To this an "engineering approach" can be added i.e. in specific cases of public buildings and residential areas it is advisable to study the sources of PFMFs and try to reduce them in a cost-effective way. Of course this only leads to the question: Which values are acceptable?

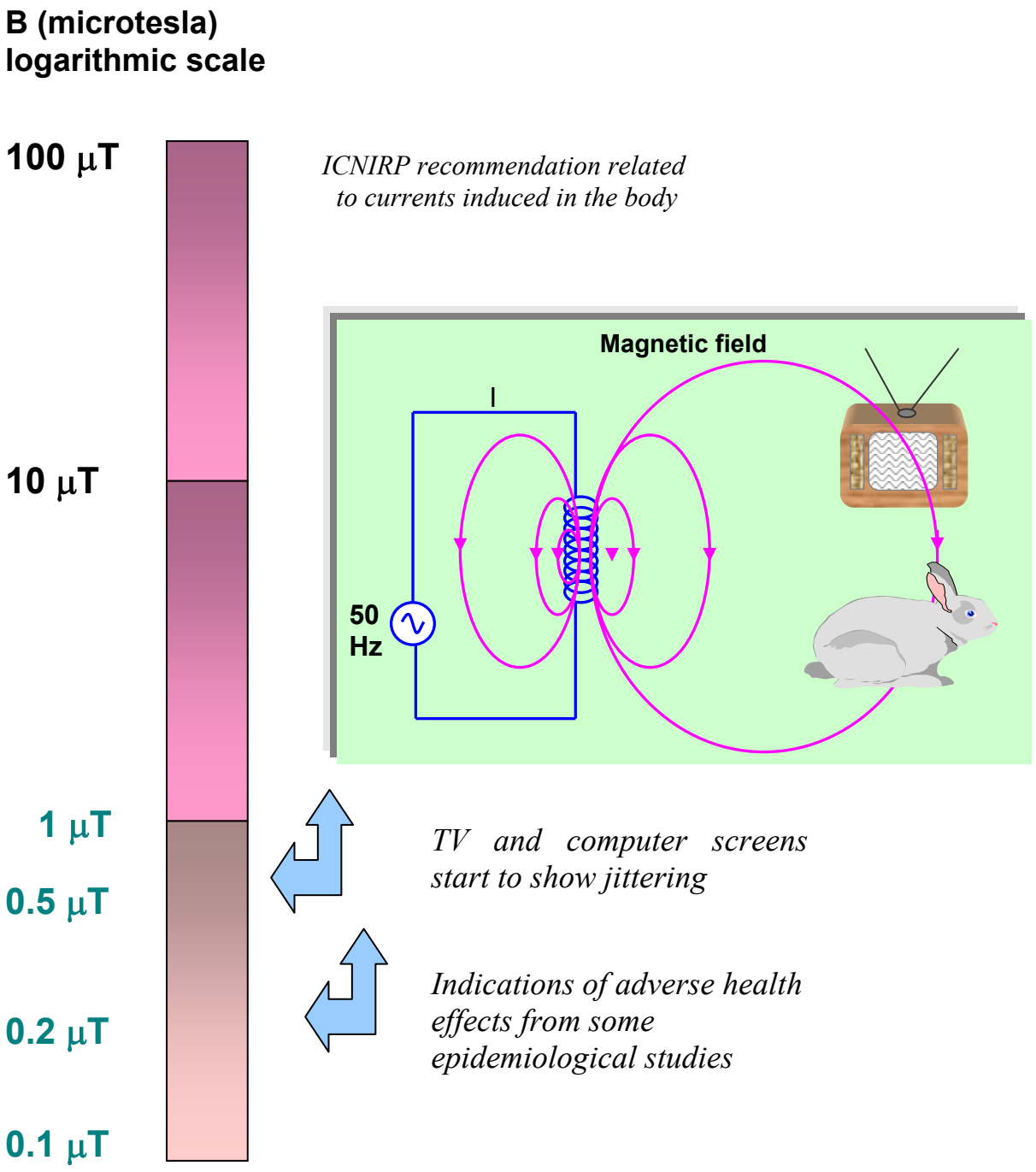

Fig. 3.4 Values and interactions of power-frequency magnetic fields with electronic equipment and living organisms.

The fact that interference of PFMFs with electronic equipment and suspected biological effects fall both within the same range of values (Fig. 3.4) allows to put forward the following "working principle"[7]:

The maximum rms-values of PFMFs (in areas of residence, places where people are staying extended periods of time, or sensitive equipment is located) should be kept at the sub-microtesla level.

References

[1] C. J. Portier, M. S. Wolfe, Eds. "Assessment of Health Effects from Exposure to Power-Line Frequency Electric and Magnetic Fields", *NIH Publication* No. 98-3981, North Carolina (1998).

[2] M. Feychting, and A. Ahlbom, *Magnetic Fields and Cancer in People Residing Near Swedish High Voltage Power Lines, IMM-rapport 6/92,* Institutet för miljömedicin, Karolinska Institutet, Stockholm, 1992.

[3] IARC, *Static and Extremely Low Frequency Electric and magnetic Fields*, Monograms on the Evaluation of the Carcinogenic Risk in Humans, Vol. 80, Lyon, 2001.

[4] M. Sandström, K. Hansson Mild, and A Berglund, "Induced Jitter on VDT Screens from external 50/60 Hz Magnetic Fields", in *Abstract book work with display units*, Tech. Univ. Berlin, Sept. 1992, pp. C5-7.

[5] ICNIRP (International Committee on Non-Ionizing Radiation Protection), *Guidelines for limiting exposure to time-varying electric, magnetic and electromagnetic fields (up to 300 Hz)*, Health Physics, Vol 74, Number 4, 1988.

[6] The Swedish: National Board of Occupational Safety and Health, National Board of Housing, Building and Planning, National Electrical Safety Board, National Board of Health and Welfare, Radiation Protection Institute, *Low-Frequency Electrical and Magnetic Fields*: *"The Precautionary Principle for National Authorities",* Solna, Sweden, 1996.

[7] E. Salinas, J. Daalder, and Y. Hamnerius in: Proceedings of the CIRED-99 Conference on Electricity Distribution, *Special Reports*, Nice, 1999, pp. 208-209.

4 Visualization of mitigation methods

To mitigate power-frequency magnetic fields some properties of electromagnetism and its interaction with matter can be used – resulting in different solutions to mitigate these fields. In this report the following methods are discussed:

- Conductive shielding
- Ferromagnetic shielding
- Passive compensation
- Active compensation
- Design modification of electrical facilities and equipment

In order to visualize these methods it is worth to notice that magnetic fields with extremely low frequency (e.g. 50 Hz) can also be obtained by rotating a permanent magnet. In fact a power frequency is not difficult to achieve mechanically (Fig. 4.1) by means of an appropriate combination

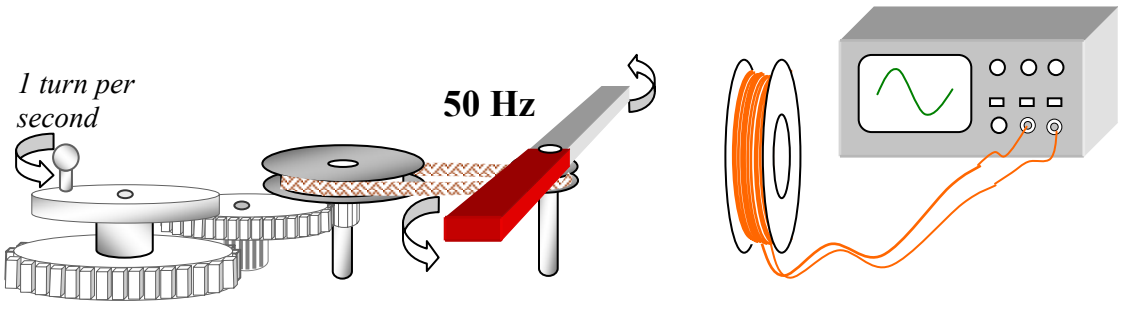

Fig 4.1 Mechanical generation and measurement of 50 Hz magnetic fields.

of gears. The field is measured with a coil and an oscilloscope. Although this way of generating a magnetic field with extremely low frequency differs from the sources described in chapter 2, it can provide a helpful insight on mitigation methods.

When a plate made of ferromagnetic material (with high relative permeability) is placed between the magnet and the coil, the magnetic field lines are attracted to the plate and the field diminishes. Fig. 4.2 shows a contour plot of the magnetic field strength where field reduction is attained at the other side of the plate. For example, at 20 cm from the source, on the side containing the plate, the field is reduced by a factor of 5 compared to the value at the same distance on the opposite side.

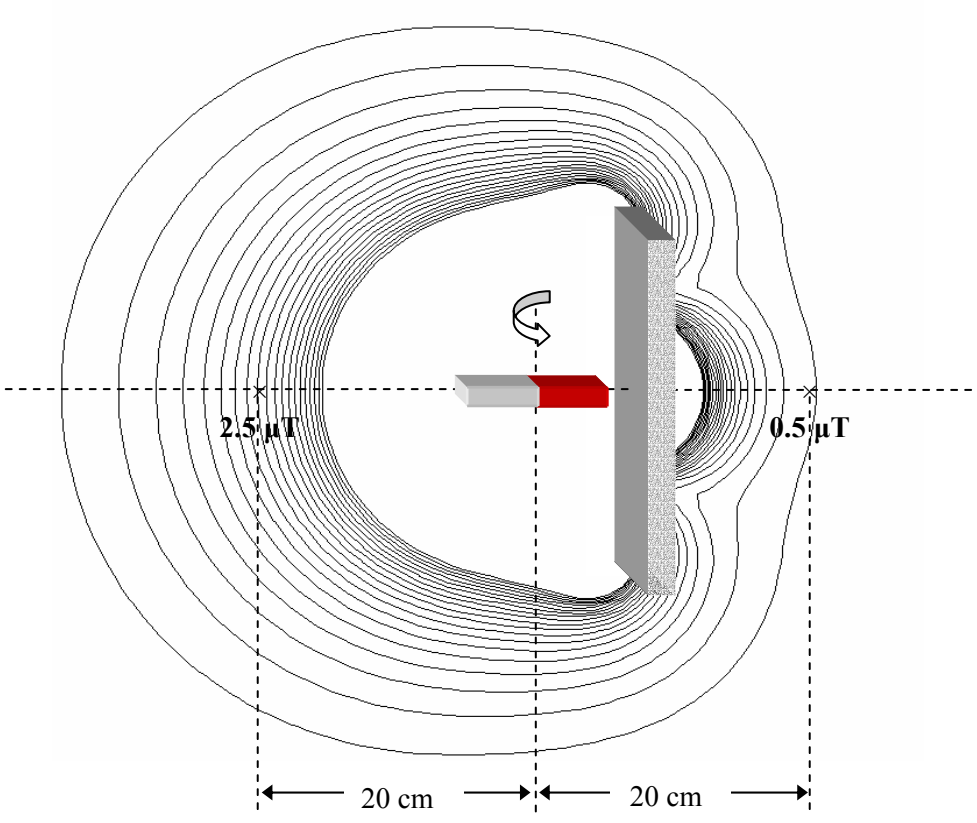

Fig. 4.2 Magnetic field mitigation using a plate made of ferromagnetic material.

Another way to reduce the field of a rotating magnet[1] is to place a conductive plate (e.g. made of aluminum or copper) in front of the magnet. According to Faraday's law a varying magnetic flux induces eddy currents, mainly on the surface of the plate (Fig. 4.3-a). The direction of

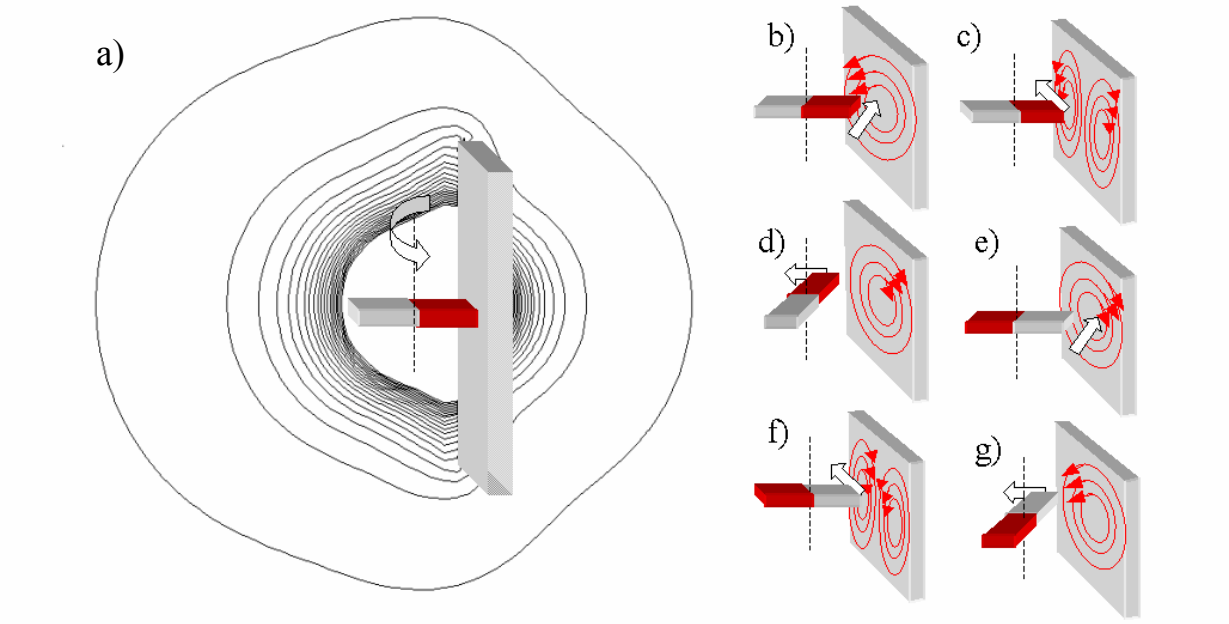

Fig. 4.3 Magnetic field mitigation using a plate made of conductive material.

these currents changes. When the magnet's north-pole approaches the plate, the flux through it increases and the induced currents on the surface create a magnetic flux that counteracts the incident one (Fig. 4.3-b). When it passes closest to the plate two loops are formed –this happens

[1] It should be pointed out that to develop these analogies and the properties discussed here, small-scale experiments were carried out using actual rotating magnets and electronic measuring devices. However the contour plots and field values in figures 4.2 and 4.3 were obtained by modeling the shielding of a dipolar field of a solenoid at 50 Hz. These plots do not accurately represent the field of a rotating magnet and are used only for illustration purposes.

because on the plate there is a region where the flux increases and another region where the flux diminishes. When the north-pole leaves the plate (Fig. 4.3-c) the currents are opposite to the case (b). Conversely, when the magnet's south-pole approaches, reaches its maximum or moves away from the plate, eddy currents are shifted towards 0°, as the currents try to increase the diminishing magnetic flux (Fig. 4.3-c). An analogous situation occurs when the magnet's south pole approaches and moves away from the plate (Fig. 4.3 - d, e). The net time-averaged effect is a reduction of the field that is shown as a contour plot in Fig. 4.3-a. As in the ferromagnetic case, the reduction is more evident on the other side of the shield even though the field is globally affected.

It is important to note, especially in practical applications, that the continuity of the shielding plate is crucial. Any cuts, openings, holes, slits or

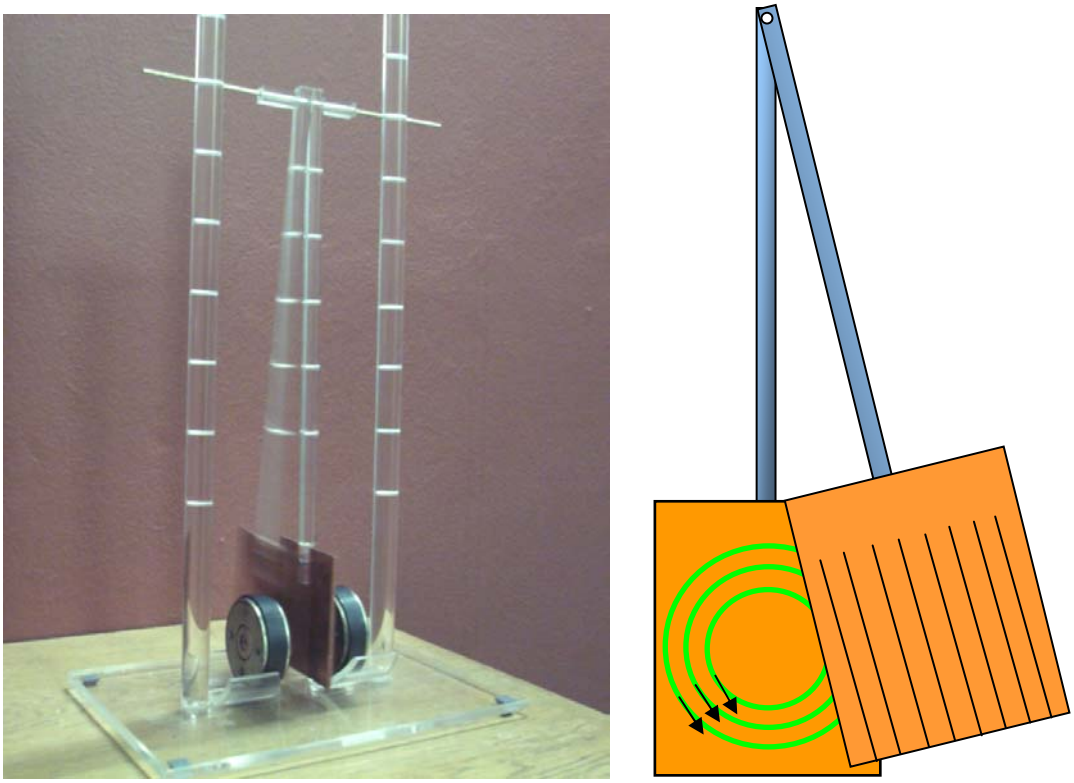

Fig. 4.4 Experiment to show the efficiency of induced currents generation in a continuous conductive plate compared with a non-continuous plate.

even cracks may drastically reduce the shielding effect, as the induced current paths will be obstructed. This can be illustrated in the experiment shown in Fig. 4.4. Two parallel pendulums, one containing a solid copper plate and the other containing a plate of the same material and dimensions but with several slits. They oscillate in the field of two permanent magnets with a frequency of the order of 1 Hz, leading to the formation of eddy currents (the interaction between plates is negligible). The result of this experiment is that the pendulum with the continuous plate slows down very quickly and stops its oscillation (after a few seconds) while the pendulum with the non-continuous plate continues oscillating for a much longer time until friction forces slows it down [1]. This experiment illustrates that the slits made on the copper plate prevent the formation of efficient loops of eddy currents.

The generation of eddy currents on conductive plates suggests the next two ways of mitigating magnetic fields, namely, passive and active compensation. If an "imitation" of the main current loops formed in the shielding plate is made by constructing closed copper rings and placing them –in the same location– instead of the plate (Fig. 4.5), then field mitigation is expected due to the generation of induction currents in the wire loops.

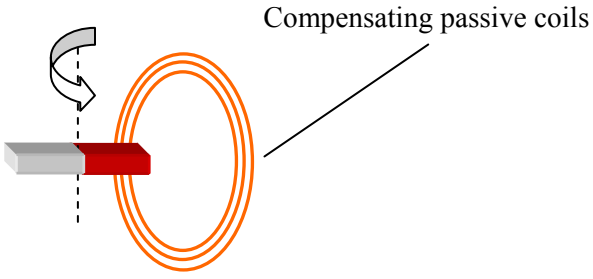

Fig 4.5 The principle of passive compensation: copper loops are placed in front of the rotating magnet as to "imitate" the paths of the induced currents.

It is also possible to cancel the field of the rotating magnet in a specific region completely by the use of a coil carrying a current fed by a control system (Fig. 4.6). A small coil acts as a sensor and is placed in the region of interest. The detected signal is amplified and phase shifted electronically providing an accurate cancellation current.

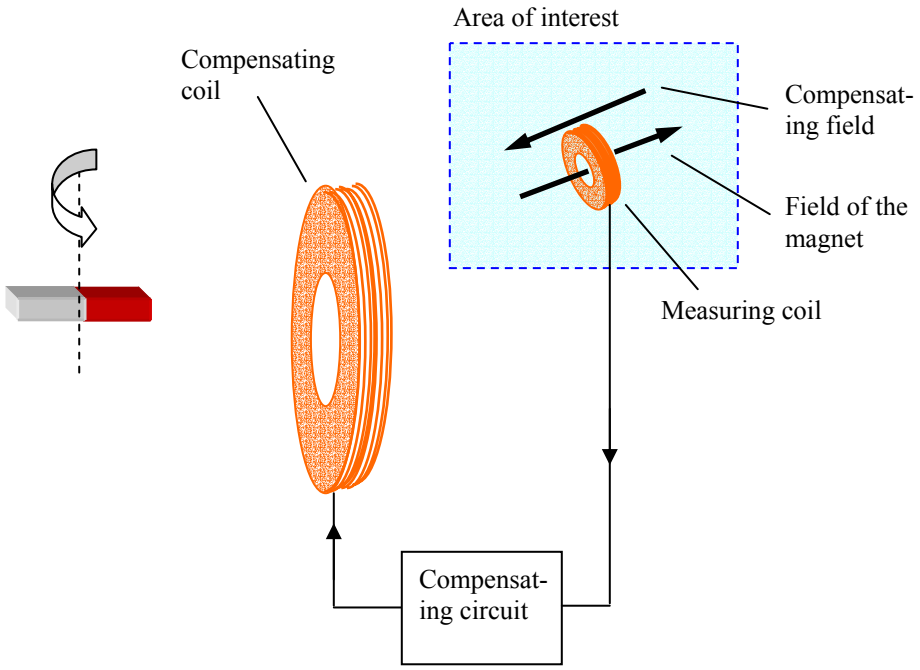

Fig. 4.6 Field mitigation by active compensation: the compensating coil produces a field that cancels, in the area of interest, the original field of the rotating magnet.

The modification of the design of the rotating magnet can yield other options of field mitigation in a desired region. An example of this is the change of the rotation axis to obtain a different geometrical configuration of the field in the area of interest. A rotation around a horizontal axis is shown in Fig. 4.7, the signal is (for small distances to the magnet) drasti-

cally damped near the axis, as there is little variation of the magnetic flux trough the measuring coil. The global field is of the same size as before.

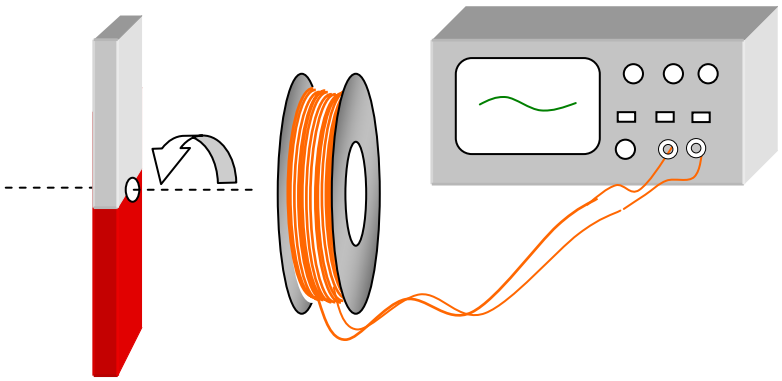

Fig 4.7. Modification of the design to produce a rotation around a horizontal axes; it provides a different, much lower, signal on the oscilloscope; therefore a drastic mitigation of the magnetic field is achieved in the region where the coil is located.

In this chapter PFMFs mitigation techniques have been discussed. Shielding by ferromagnetic material is yet rather effective when the frequency of the rotating magnet decreases ($f < 50$ Hz) or even when it stops ($f = 0$) creating a static magnetic field. On the other hand, shielding by conductive materials does not work unless the magnet is moving in such a way as to produce a time-varying magnetic flux through the shielding surface ($\Delta\varphi/\Delta t \neq 0$). The later can also be said about passive compensation, since the idea is based on conductive shielding. Active compensation works for static fields provided the system can measure these fields.

It can also be observed that in the case of the rotating magnet the mitigating actions can affect directly the way the original field is created. For

example, in conductive shielding the eddy currents generated in the plate do not only try to cancel the field. They also exert a braking torque on the dipole generating the field e.g. in Fig. 4.1. To various extents similar conclusions can be drawn for the other methods as well. This observation illustrates that the mitigation methods could influence the operation of the source. It is generally essential to ensure that this influence is negligible (e.g. avoiding too high mutual inductances in passive compensation) when designing practical applications.

References

[1] R. P. Feynman, M. L. Sands, R. B. Leighton. "The Feynman Lectures on Physics" (Vol. II), Addison Wesley, Reading (1964).

[2] M. McCaig, "Permanent Magnets in Theory and Practice", Pentech Press, London (1977).

5 PFMFs originating from secondary substations

During the last decade both research and the public media have focused on the significance of magnetic fields of power transmission lines [1-2]. However, the final distribution stage of the electrical energy flow before reaching the customer, in particular secondary substations[1], is often a source of similar field values (in areas of concern) as encountered at the transmission stage. This prevails in spite of the fact that secondary substations and power lines have very different voltage ranges (Fig. 1). On one hand, as the electric energy flows from high voltage stages to lower ones, the current branches. Therefore, if this were the only cause, lower magnetic fields would be expected at the end of the electric flow. On the other hand, when the voltage diminishes (via

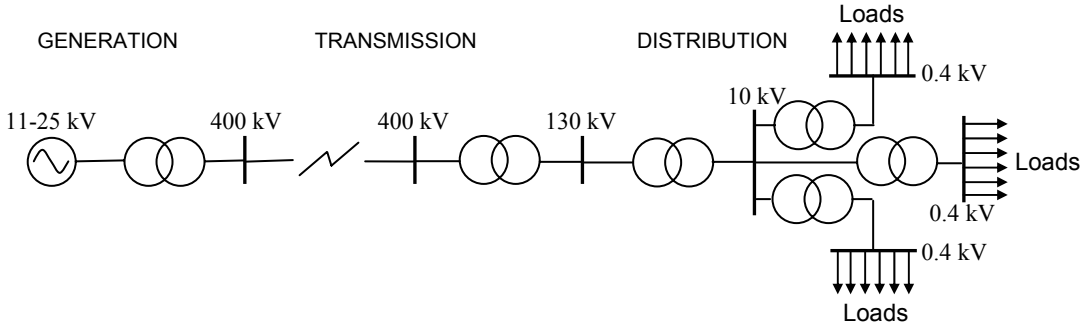

Fig. 5.1 A simplified diagram of the electrical energy flow from the generation plant to the customer.

[1]A substation is called secondary when they convert electrical energy at **primary** distribution voltage levels (e.g. 35 kV, 21 kV, 12.5 kV, 10 kV, or 4.16 kV) to utilization or **secondary** levels (e.g. 460 V, 400 V, 240 V, 208 V, or 120 V).

transformer operation) the current increases [3]. In addition, the distance from sources to affected areas diminishes and the density of population and equipment (sensitive to PFMFs) increases.

Consequently the issue of PFMFs can be considered at least as important in highly populated neighbourhoods, such as in a city environment, as in areas along power lines. Accordingly, the mitigation of fields from secondary substations can contribute to the solution of some of the issues studied in chapter 3.

5.1 In-house secondary substations

In Sweden and other European countries it is not unusual, especially in neighbourhoods with a dense population, to situate secondary substations inside buildings. Common locations are cellars. In other countries (e.g. in USA) the use of pad-mounted transformers is more common. These transformers are inside a metal enclosure and placed on the ground. Hence they are rather visible. Fig 5.2 shows a characteristic situation displaying the sources and some typical field values. The substations analysed in this report contain three-phase transformers (10/0.4 kV, 800 kVA). They also contain high and low voltage switchboards that have covers customarily made of plane steel and they both enclose busbars. However, due to the reduction in voltage, the currents increase with the same factor at the secondary side of the transformers. Therefore cables, and busbars at the low voltage part of the substation constitute major sources of magnetic fields. Hence methods to mitigate their fields will be the goal of the next chapters.

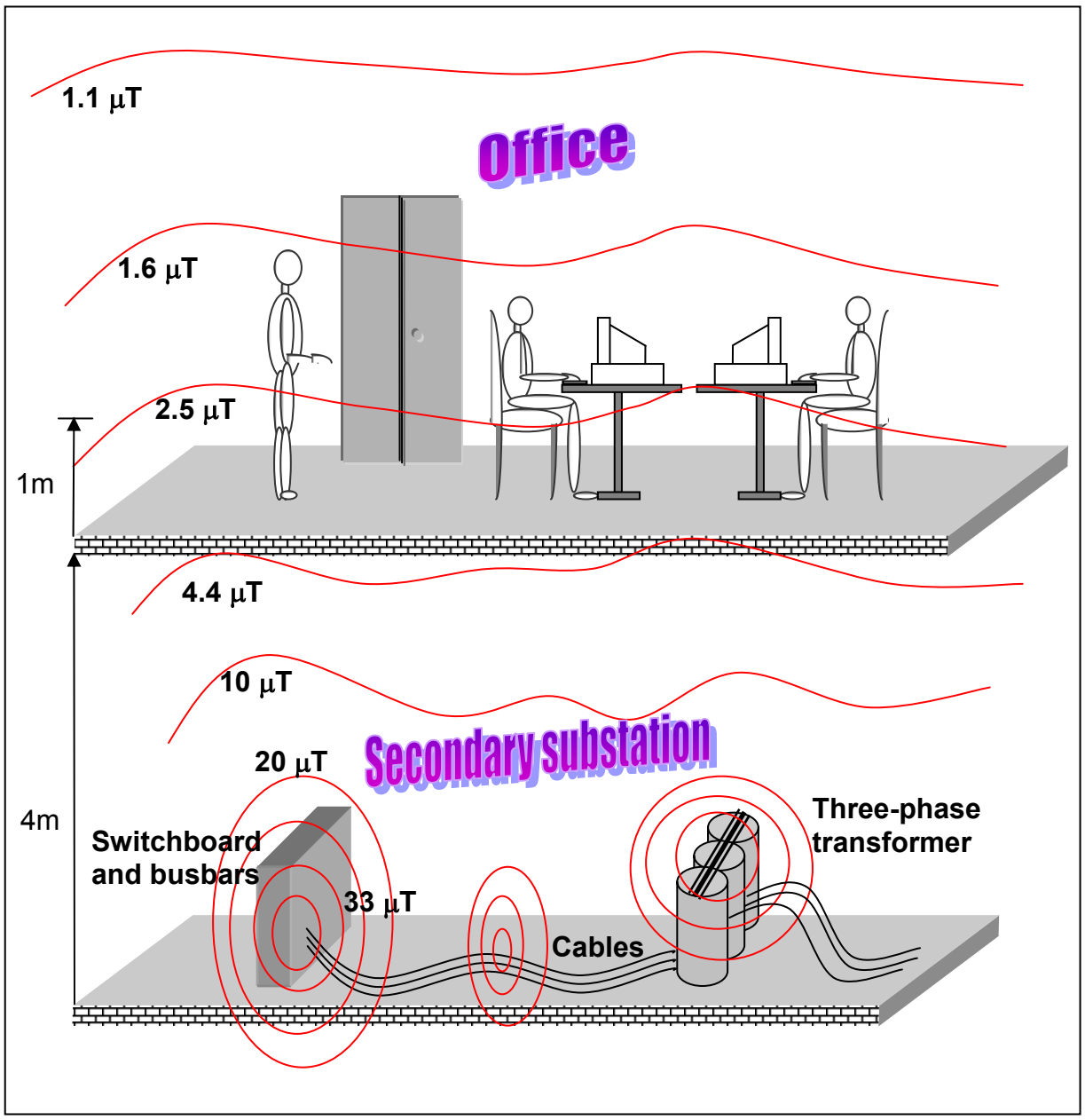

Fig. 5.2 Some typical magnetic field values (in microtesla) from a secondary substation situated in a cellar of a building. A usual configuration of major sources and distances is also shown.

The magnetic field values originated from a secondary substation are the result of an intricate superposition of the fields from various sources. It is

then natural to ask: is it possible to discriminate in advance the magnitude of the contribution of each source by scanning the field values in the affected area (Fig. 5.3)? The answer –as we will learn in the next chapters– is yes. There are two reasons for this: (1) Analysis of the field gradient on the scanned surface could suggest the possible source behaviour. (2) Analysis of the variation of the field values with the distance perpendicular to the scanned surface could provide a 3 dimensional picture of the field decay, and subsequent source identification. Moreover, after a simple inspection of the substation itself (this may include a few extra measurements), the problem can be straightened out, and a mitigation method can be suggested. See applications of these techniques in chapters 11 and 12.

References

[1] M. Feychting and A. Ahlbom, "Magnetic Fields and Cancer in People Residing Near Swedish High Voltage Power Lines", IMM-rapport 6/92, *Institutet för Miljömedicin*, Karolinska institutet, Stockholm, 1992.

[2] G. Theriault et al: "Risk of leukemia among residents close to high voltage transmission electric lines" *Occup Environ Med* 54: 625-628, 1997.

[3] T. Wildi, "Electrical Machines Drives and Power Systems", Second edition, Prentice-Hall International, London, 1991.

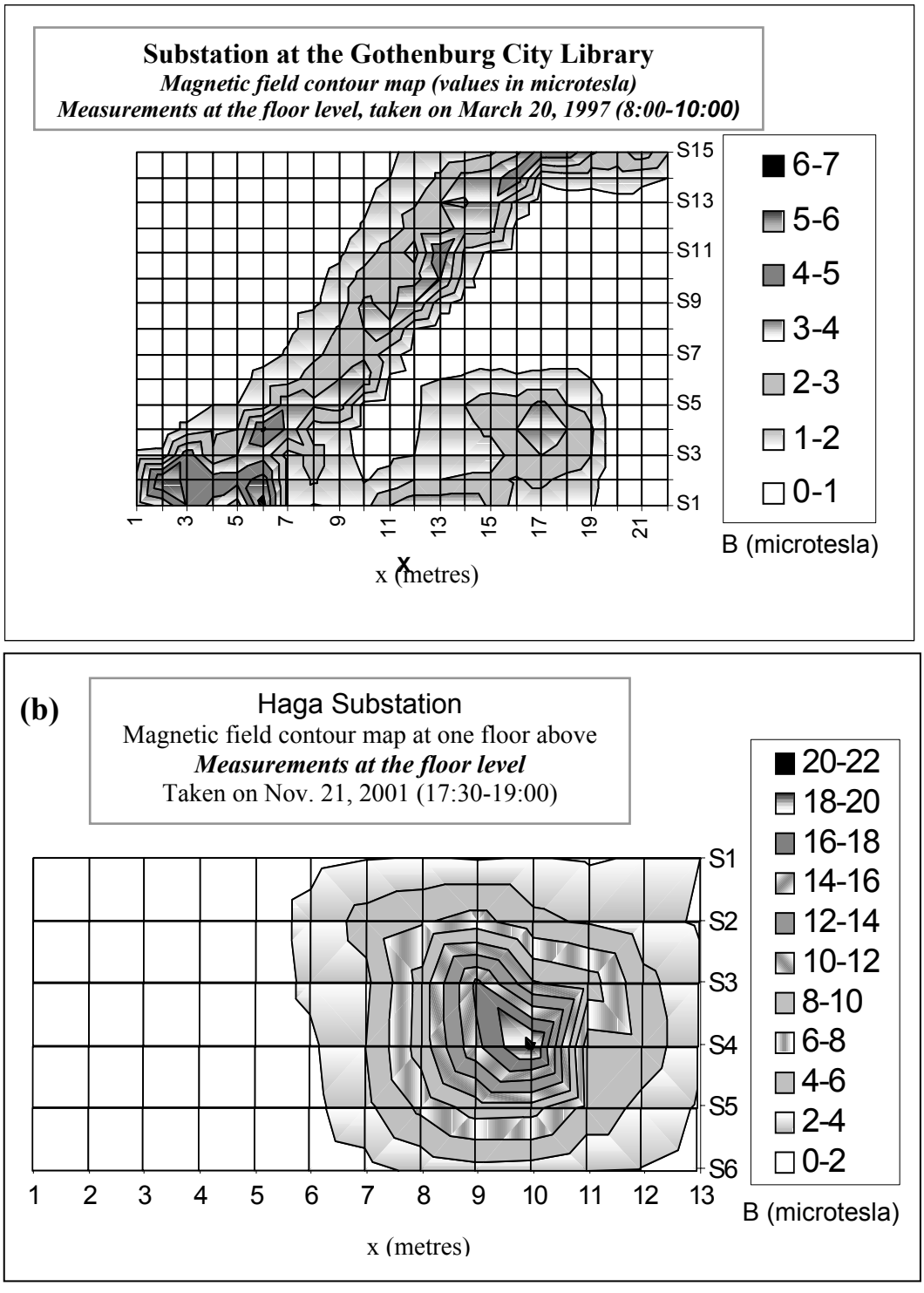

Fig. 5.3 Two typical examples of the magnetic field contour plots on the floor above a substation. It naturally follows the question: what can be deduced from these plots?

6 Phase arrangements

Cables, wires, power lines and busbars are the carriers of electrical energy and sources of PFMFs. Hence, the phase configuration and geometrical positioning of these sources are essential factors in the design of electrical installations with low PFMFs. This is, nevertheless, also valid for old installations. If the initial design did not consider optimal cable arrangements, a set of suitable modifications can yet be made which leads to mitigation of PFMFs.

Here we will give examples of the field around given phase configurations assuming the following: (1) The relative permeability of the surrounding environment is unity, and (2) the conductivity of the surrounding material is zero. The computations are based on direct application of the formulas given in chapter 2 (for instance Eq. 2.10). The field can be obtained analytically (for simple geometries) or, in general, by numerical techniques such as FEM codes. The latter is the method applied in this chapter. The FEM solver code ELEKTRA was used [1], which has the grid generator OPERA 2D/3D. ELEKTRA evaluates the field from a conductor of nearly any shape by integrating the Biot-Savart formula. Current densities and dimensions of conductors are the main inputs. To enable these conductors to be oriented in space correctly, local coordinate systems can be used. To reduce the amount of input data when dealing with several conductors, operations such as reflections and translations can be used to replicate any basic shape.

The computation that follows is an example of how phase arrangement can be used as a field mitigation technique.

6.1 PFMFs from bundles of three-phase conductors

Three bundles of three-phase conductors R (0º), S (120º) and T (240º) carrying a 50 Hz current of 100A (rms) are grouped in different phase arrangements as shown in Fig. 6.1. The aim is to find the arrangement,

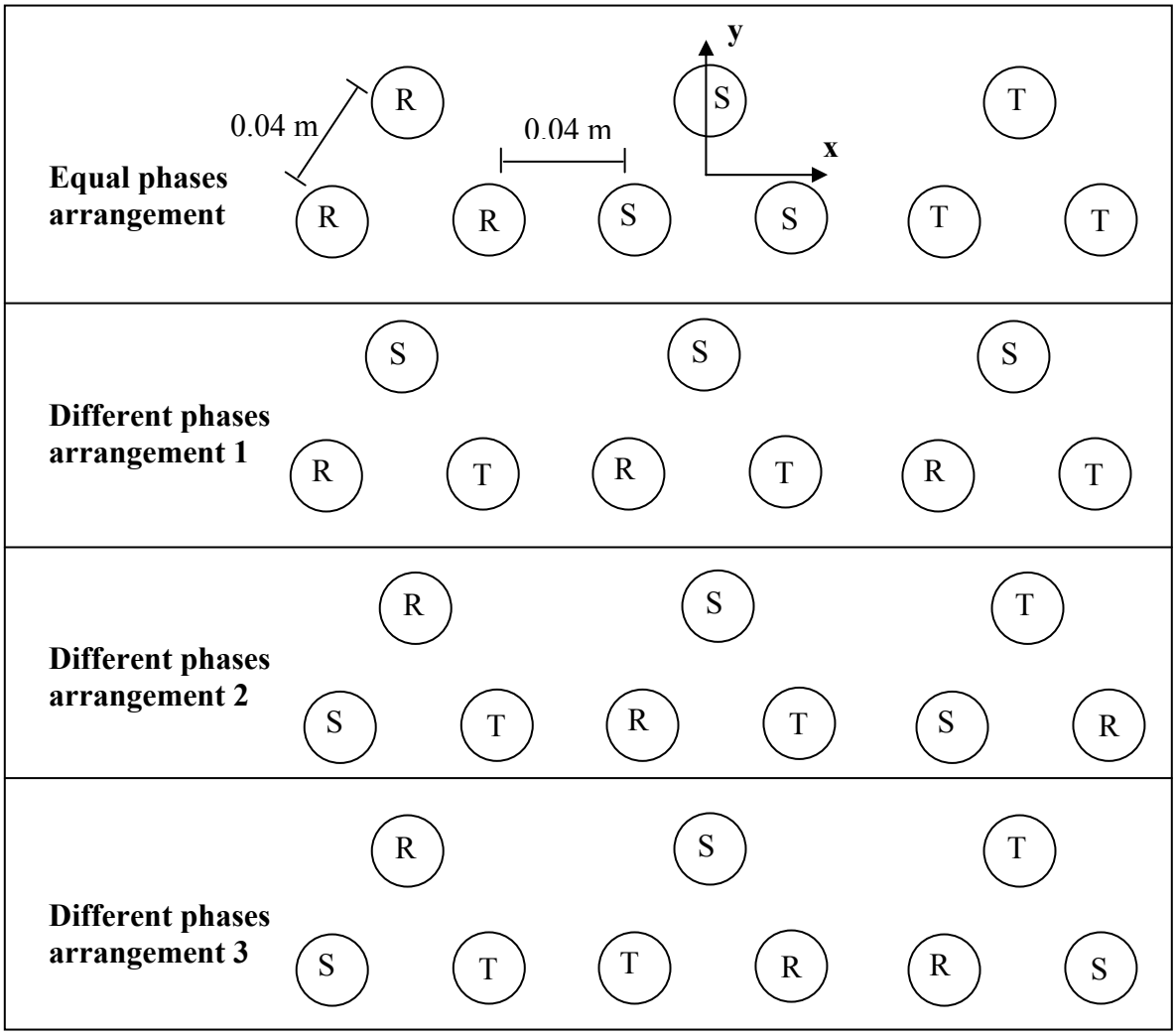

Fig. 6.1 Different phase arrangements for a system of nine conductors, each conductor diameter is 0.02 m, insulation thickness 0.01 m, and the current per phase is I = 100A.

which provides the lowest values of PFMF at a certain distance (y) larger than the cross-sectional dimensions of the arrangement (~ 0.2 m).

The results are presented in Fig. 6.2. The contour plots are all on the same scale, the field values are plotted within the range [0.1 – 1] μT, and the interval between lines is 0.05 μT. It can be observed that the arrangement number 3 of bundles with different phases has the lowest field emission.

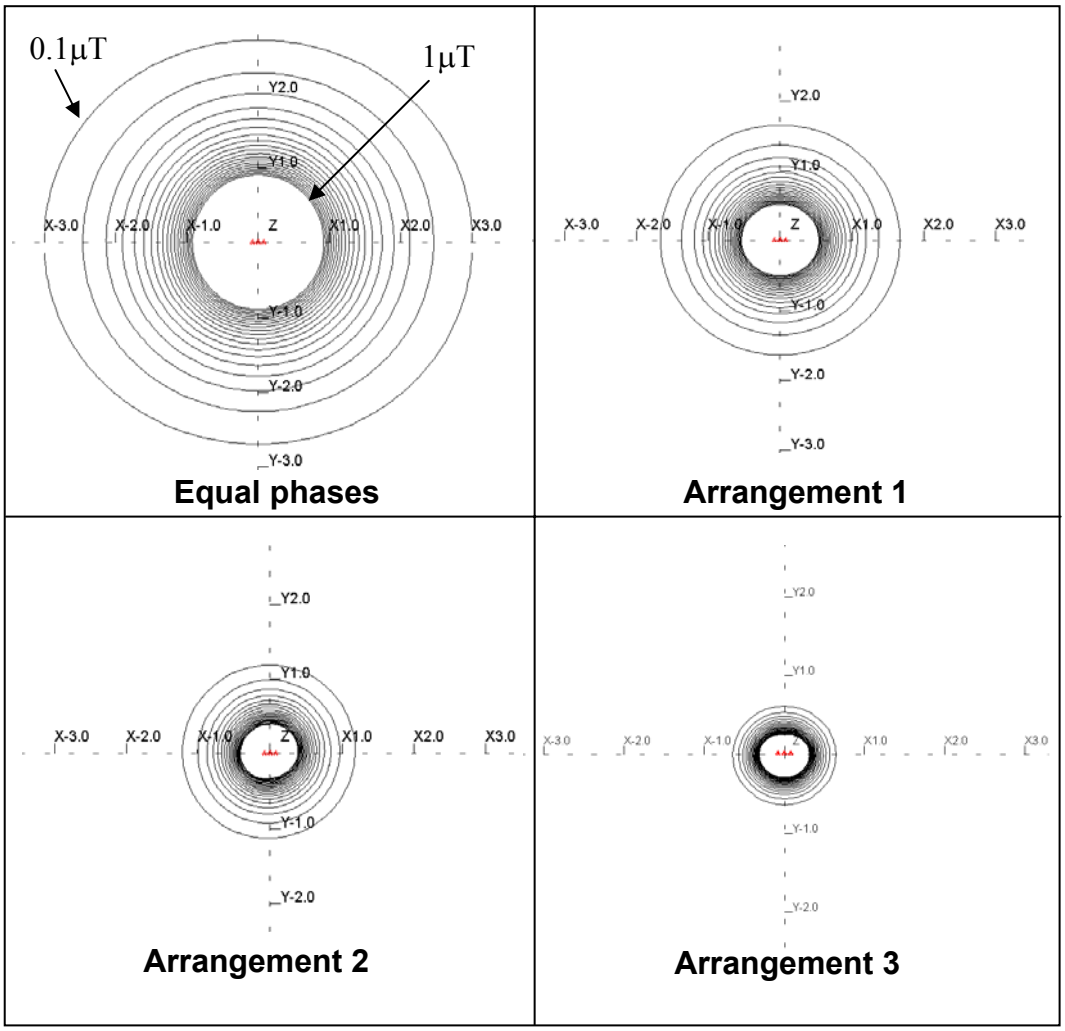

Fig. 6.2 Contour plots for the different phase configurations of Fig. 6.1. The plots are all on the same scale, the field values are plotted within the range [0.1 - 1] μT, and the interval between lines is 0.05 μT. The axis scales are in metres.

The results deduced from the plots of Fig. 6.2, are even more evident in the curves shown in Fig. 6.3 that shows the field variation as a function of the distance along the y-axis.

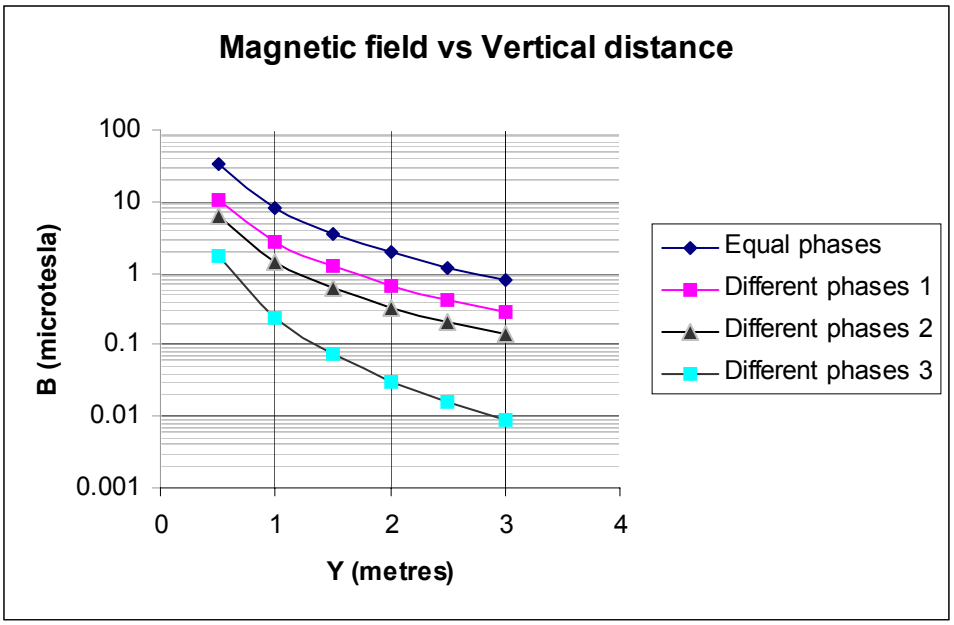

Fig. 6. 3 Variation of the magnetic field as a function of the distance.

An attenuation factor is defined as

$$A(x,y) = B_0(x,y) / B_{att}(x,y) \qquad (6.1)$$

B_0 represents the initial field and the B_{att} denotes the field after a mitigation procedure has been applied; this expression must be evaluated at the same position (x,y) in both cases. The higher the attenuation factor the more successful the mitigation technique is.

In the case studied in this section, it is assumed that the initial field is the one with the bundles of equal phases, and the attenuated field

corresponds to the various cases of combining phases in different bundles. Applying this definition to the values of the different phase arrangements we obtain the following table:

Table 6.1 Field of equal phases and attenuation factors (B_0 / B_{att}) of various arrangements

	y = 0.5 m	y = 1 m	y = 1.5 m	y = 2 m	y = 2.5 m	y = 3 m
Field B_0 (equal phases)	33.70 μT	8.27 μT	3.58 μT	1.95 μT	1.20 μT	0.80 μT
Different phases, A1	***3.11***	***3.0***	***2.93***	***2.87***	***2.79***	***2.67***
Different phases, A2	***5.48***	***5.75***	***5.83***	***5.87***	***5.89***	***5.9***
Different phases, A3	***19.2***	***34.5***	***49.4***	***63.4***	***76.5***	***88.9***

Analysing the variation of the attenuation factors with distance, given in table 6.1, one can see that: the attenuation diminishes for the arrangements 1 whereas it increases for arrangements 2 and 3. That is to say, the latter arrangements (especially arrangement 3) not only provide better mitigation than the first one, but it also improves with the distance – at least in the areas of interest. This property can be very useful since often the interest is to mitigate an affected area which distance from the source is large in comparison with the dimensions of the source.

Three dimensional arrangements with variation in the z direction can also be taken into account. This allows further mitigation by the operation of twisting the conductors. In this way there is a partial cancellation of some of the contribution to the field integration along the z - direction. This action is, however, not always possible, especially for high current conductors, due to the stiffness of the conductors.

The method presented in this chapter, and considerations of heat conduction, can be readily applied to arrangements of underground

cables [2], power lines, connections between the low-voltage side of a substation transformer (Section 11.2) and a switchboard and, in general, to any electrical installation where a field source of high magnetic fields is located in inadequately designed groupings of cables or wires.

An specific application of this technique is to *split-phase configuration.* This operation can reduce drastically the field of –for example– power lines. The line configuration in Fig. 6.4 has very low field emission compared to a standard one. It also has the advantage of being more compact. The computations to design this type of arrangements are basically not different from the ones presented in this section.

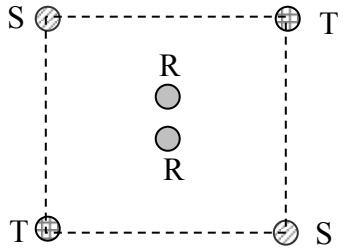

Fig. 6.4 Split-phase configuration of three-phase conductors yields low field emission.

References

[1] Vector Fields Ltd., "Opera 3D user manual", Kidlington, OX5 1JE, England, 1998.

[2] Horton, W.F. and Goldberg, S., Shielding the power Frequency Magnetic Fields Produced by Underground Distribution Cables, Proceedings of the North American Power Symposium, Kansas State University, 1994.

7 Modelling PFMFs using 2D and 3D FEM codes

The behaviour of power devices such as transformers, electrical machines or power lines is governed by electromagnetic fields that obey the Maxwell equations. Consequently, in order to predict the behaviour of these devices (e.g. in the course of their design or in a field mitigation problem) one must solve Maxwell's equations. This involves dealing with a set of differential equations and adequate boundary conditions. Analytical methods [1] (e.g. separation of variables, Laplace transformations or series expansions) cover only a very few cases which involve a high degree of symmetry. Numerical methods are necessary to solve these equations more generally.

The method of finite differences [2] has been rather popular since the very origin of computational electromagnetics. It subdivides the solution region into a rectangular grid or a mesh of points. This method transforms the complicated problem of dealing with differential equations to an approximately equivalent and much easier one: a set of linear algebraic equations. A drawback of this method is its poor flexibility when dealing with oblique and curved boundaries.

As computer capabilities increased other computational methods were developed [2], [3], integral equation formulations [4], often referred as the method of moments (MoM) for which several different formulations exist [5]. However, the method that is nowadays widely accepted as a

powerful technique in electrical engineering problems is the finite element method (FEM) [3], [7]. This chapter will focus on this particular technique.

7.1 Quasi-static electromagnetic fields

When the wavelength of a time-varying field is much larger than the dimensions of the problem (i.e. in the near field zone), then the set of four Maxwell equations simplify. One reason for this is that the *displacement current* term becomes negligible in comparison with the current density **J**. Thus the Ampère law is a good approximation for Ampère-Maxwell equation. The set of equations given in Eq. 7.1 (a) describes electromagnetic phenomena in a quasi-static regime.

The low frequency approximation formally amounts to setting $\varepsilon_0 = 0$; therefore the fourth equation in Eq. 7.1 (a) is also disregarded. In fact, in any modelling of eddy currents only three of the Maxwell equations are involved [6]. Moreover, in this report, the fields have sinusoidal variation, thus one can use the complex formulation of the fields: $\mathbf{E}(t) = Re\{\hat{\mathbf{E}}\exp(j\omega t)\}$, and $\mathbf{H}(t) = Re\{\hat{\mathbf{H}}\exp(j\omega t)\}$, where j is the imaginary unit, and ω is the angular frequency. Consequently, for modelling PFMFs in a medium containing regions with σ and μ, (for example shielding of power sources using ferromagnetic or conductive material) Maxwell's equations simplify ending to the set given by Eq. 7.1(b).

The following additional assumptions are often made in modelling a PFMFs mitigation problem:

(1) The conducting media are linear with respect to the current.

(2) The conducting media are isotropic.

(3) The relative permeability μ_r of the conductive media is constant.

(4) A macroscopic model is used for the conducting media.

(5) Thermal effects are neglected or considered linear.

It should be noted that current research in electromagnetic modelling is concerned with removing most of these assumptions. An example is the inclusion of realistic permeability curves in recent models.

Equations for electromagnetic modelling

Eq. 7.1 (a) Quasi-static fields

$$\nabla \times \mathbf{H} = \mathbf{J} \qquad \textit{Ampere Law}$$

$$\nabla \times \mathbf{E} = -\frac{\partial \mathbf{B}}{\partial t} \qquad \textit{Faraday Law}$$

$$\nabla \cdot \mathbf{B} = 0 \qquad \textit{Gauss law for } \mathbf{B}$$

$$\nabla \cdot \mathbf{D} = \rho \qquad \textit{Gauss law for } \mathbf{E}$$

$$\mathbf{B} = \mu \mathbf{H} \qquad \textit{Constitutive relation}$$

$$\mathbf{D} = \mu \mathbf{E} \qquad \textit{Constitutive relation}$$

$$\mathbf{J} = \sigma \mathbf{E} \qquad \textit{Ohm's law}$$

Eq. 7.1 (b) Eddy current formulation for PFMFs

$$\nabla \times \mathbf{H} = \sigma \mathbf{E} + \mathbf{J}s$$

$$\nabla \times \mathbf{E} = -j\omega\mu \mathbf{H}$$

$$\nabla \cdot (\mu \mathbf{H}) = 0, \nabla \cdot (\sigma \mathbf{E}) = \nabla \cdot \mathbf{J}s$$

7.2 The finite elements method (FEM)

This method is increasingly popular [7], [8] due to its ability to deal with regions with very complex geometries. It divides the region under study into a number of sub-domains (usually triangles, quadrilaterals,

tetrahedra, or hexahedra) called *elements*. The field on each element is approximated by a simple algebraic expression; hence the values of the field on a finite set of nodal points or edges are determined as the solution of a linear set of equations. To deal with an unbounded geometry, several approaches are possible. Boundary elements can accurately model an infinite region, however reasonable approximation can be found using differential equation solvers by surrounding the region of interest by a large box. The accuracy of the solution depends, among other factors, on the size of the limiting box (or external boundary) and the number and distribution of elements. Two commercial codes have been extensively used in the present work: 2D ACE from ABB Research Corporation [9], and 3D ELEKTRA from the company Vector Fields [10]. Both use the method of a large surrounding box.

7.3 Two-dimensional FEM

The two-dimensional program ACE uses the relation $\mathbf{B} = \nabla \times \mathbf{A}$ to calculate the magnetic flux density **B** from the determination of the magnetic vector potential **A.** The formulation uses the fact that the problem to solve is 2-dimensional, and that the frequencies involved are low. Consequently simplifications are possible (e.g. the electric displacement vector is ignored). Applying Maxwell's equations, it is possible to find a differential equation to be solved for **A** involving the known quantities magnetic permeability μ, electric conductivity σ, angular frequency ω and the current density **J**. The imposed condition at the boundary is $\mathbf{n} \times \mathbf{A} = 0$. Finally the 2D-vector **B** located in the

symmetry plane is determined. A good characteristic of the ACE program is that its mesh generator is adaptive, making it possible to run different variations of the geometry of a problem, without having to spend too much time on mesh generation.

7.4 Three-dimensional FEM

The program ELEKTRA uses a combination of vector and scalar potentials to model time varying electromagnetic fields. Vector potentials **A** have to be used in conductive media; reduced scalar potentials ψ can be used in the rest of the space [10]. In a region of free space that does not include source currents, the magnetic field strength can be replaced by the gradient of this potential $\mathbf{H} = -\nabla\psi$. In the case of time-varying fields, the currents induced in conducting media can be computed from the vector potential [11]. The equations for the vector potential are:

$$\nabla \times \frac{1}{\mu} \nabla \times A + \sigma \left(\frac{\partial A}{\partial t} + \nabla V \right) = 0 \tag{7.2}$$

$$\nabla \cdot \sigma \nabla V + \nabla \cdot \sigma \frac{\partial A}{\partial t} = 0 \tag{7.3}$$

where V is the electrical scalar potential. This set of equations allows a gauge transformation

$$\overline{\mathrm{V}} = \mathrm{V} + \mathrm{U}, \quad \overline{A} = A - \int^{t} \nabla U dt$$

Coulomb gauge $\nabla \cdot A = 0$ can be imposed by adding the term

$$-\nabla \frac{1}{\mu} \nabla \cdot A$$

on the left hand side of (7.2). This leads to a formulation suited for nodal elements for A and V.

The equations are simplified and solved for **A** under the condition of steady state alternating current excitation; this condition assumes linear materials. Having determined **A,** the code calculates the distribution of the magnetic flux density within the 3-dimensional domain of the problem.

The boundary conditions are essential in the specification of the problem to be modelled. They can be applied in two situations:

(1) To reduce the size of the geometry of the problem by symmetry.

(2) To approximate the magnetic field at large distances.

The boundary condition used in the far-field boundaries of the problems in this report is TANGENTIAL MAGNETIC, i.e. $\mathbf{H}\cdot\mathbf{n} = 0$, and $\frac{\partial \psi}{\partial n} = 0$, where n is the normal unit vector to the surface being considered and ψ represents either the reduced or the total scalar potential.

One difficulty with the Vector Fields mesh generator (OPERA-3d) is the cumbersome way the mesh has to be generated. This makes undertaking the modelling of a problem that requires the variation of the geometry parameters a very time consuming task.

7.5 Modelling a mitigation problem in a 3D FEM code.

There are several stages to reach the solution of a mitigation problem (or in general of an electromagnetic problem) modelled by a FEM code. The most relevant and useful stages are

1) Specification of the physical model: geometry, shielding materials, conductors are given.

2) Reduction of the various parts to a geometrical structure. They are embedded in a box large enough to permit the decay of the field to negligible values.
3) Formation of the base plane or a section of it (if the problem contains symmetries) with the help of construction lines. The coordinate points are positioned and then *facets*, i.e. close squares or polygons, are constructed.
4) Partition of the sides of the facets into a number of *subdivisions*, which can be uniform or variable, i.e. more dense in certain regions than in others according to the expected field variation.
5) *Extrusion* of the base plane along a direction (the z direction is chosen in all modelling presented in this report). This action creates various layers and generates the required geometrical structure in the third dimension.
6) Material modification: the material properties for each layer are named. They are said to be modified because the default is AIR, which stands for $\sigma = 0$ and $\mu = 1$. The type of the potential is also specified here by choosing between REDUCED (regions containing the source conductors), TOTAL (in regions where the mitigation is high) or VECTOR (for regions where eddy currents are formed).
7) Setting of boundary conditions, they are specified on the external faces.
8) Conductor specification, the conductors are defined by their dimensions, positioning and current density and each one is given a label.

9) Meshing, the program divides the problem space into elements and positions the nodes.

10) An *Analysis* file is created and a *data base* is completed by specifying the phase*s* of the labels of the different conductors and the working frequency. The conductivity, permeability and linearity of materials is specified. Finally the file is saved ending the pre-processing operation.

11) The solver ELEKTRA is activated. This will calculate the matrix coefficients for one equation per node. The coefficients of the equations are formed into a matrix. The program also calculates the right-hand side terms of the equations and finally, by a preconditioned iterative method, solves the equations.

12) The solution is analysed by the post-processor. In the modelling of PFMFs the parameter BMOD evaluates the value of the magnetic flux at phase 0º. However at 90º BMOD can have a rather different value, and this has to be taken into account. Therefore the following expression gives the correct rms values

    #BTOT=SQRT(BMOD**2 + iBx**2 + iBy**2 + iBz**2).

13) Finally the field is evaluated and plotted. This can be done point by point, in contour plots, or in 3D diagrams.

7.6 Modelling a 2D problem using OPERA-3d

The field mitigation modelling in this report is adapted to the operation of extrusion (step 5 in section 7.5.). Moreover, it takes advantage of it by

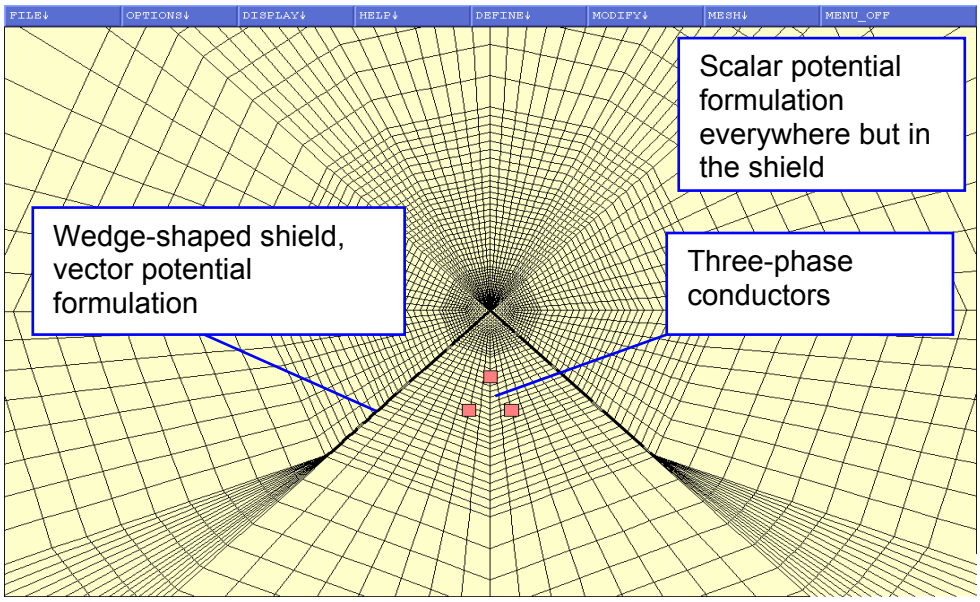

Fig. 7.1 The 2D formulation of a shielding problem in terms of potentials for the case of three- phase underground cables.

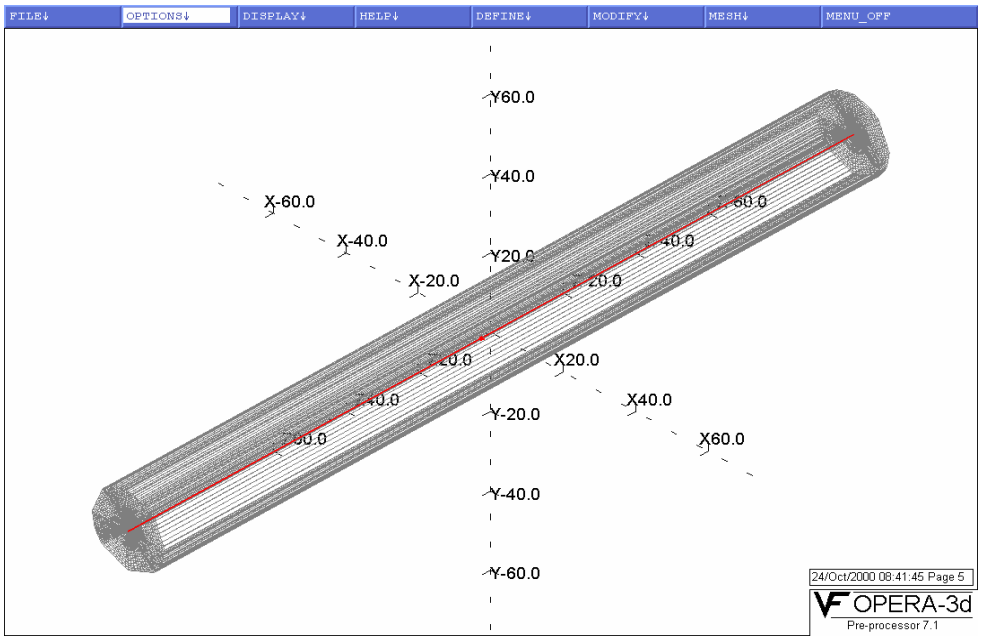

Fig. 7.2 3D approach of the 2D shielding problem. The extrusion in the z-direction has only one subdivision. This approach makes it easier to model other cases of similar cross-section but much shorter dimensions.

reducing the time spend in pre-processing when a large number of cases are modelled. The most difficult part is the generation of subdivisions and meshing on the base plane because the coordinate points. For this reason, even if a problem can be considered as 2D (because of the characteristics of the geometry) as in Fig. 7.1, it is still possible and convenient to approach this as a 3D problem and making an equivalence to a 2D problem. This is achieved by defining a second plane at a rather large distance from the base plane (e.g. 200 metres in the case of modelling of long cables). An extrusion with one element forming only one layer will define an equivalent of a 2D problem (Fig. 7.2). The solution is evaluated in a plane at the middle of the grid. The advantage of this approach is that the grid can be kept and used again in other problems with similar cross-sections but of much shorter length – where edge effects become relevant. This can be attained with very little modifications, mainly shortening the original extrusion and defining more extrusion planes to generate the 3D grid.

References

[1] Binns, K. J., and Laurenson, P.J., *Analysis and Computation of Electric and Magnetic Field Problems*, Pergamon Press, Oxford, 1963.

[2] Booton, R. C., *Computational Methods* John Wiley& Sons, Inc., N.Y., 1992.

[3] J. Jin, *The Finite Element Method in Electromagnetics,* Wiley, New York, 1993.

[4] Mayergoyz, I. D., "A New Approach to the calculation of Three-Dimensional Skin-Effect Problems" IEEE Trans. Magn.Vol. MAG-19, No. 5, 1983, pp. 2198-2200.

[5] Harrington, R. F., *Field Computation by Moment Methods*, Krieger, Florida, 1987.

[6] Stoll, R. L., *The Analysis of eddy Currents*, Claredon Press, Oxford, 1974.

[7] Silvester, P. P. and Ferrari, R. L., *Finite Elements for Electrical Engineers*, Cambridge University Press, New York, 1983.

[8] Chari, M. V. K., and Salon S. J., *Numerical Methods in Electromagnetism*, Academic Press, San Diego, 2000.

[9] ABB Corporate Research, The ABB Common Platform for 2D Field Analysis and Simulation, **Ace 2.2** *User Manual,* 4th Edition, Västerås, 1993.

[10] Vector Fields Ltd., "Opera 3D user manual", Kidlington, OX5 1JE, England, 1998.

[11] Binns, K. J., Lawrenson, P. J., Trowbridge, C. W., *The Analytical and Numerical Solution of Electric and Magnetic Fields*, John Wiley & Sons, N.Y., 1994.

[12] Salinas. E. "Using OPERA for passive and active shielding of 50 Hz Magnetic Fields", Vector Fields European User Meeting 2000, Proceedings, Lille, 2000.

8 PFMFs from Busbars

Busbars are the most efficient way to transport large amounts of electrical energy within a reduced space such as a secondary substation. They are usually made of copper or aluminium covered by copper. Depending on their specific design they can have different lengths, geometrical arrangements, and cross sections. Two typical arrangements are shown in figure 8.1. In this chapter a number of properties are deduced of PFMFs originating from busbars.

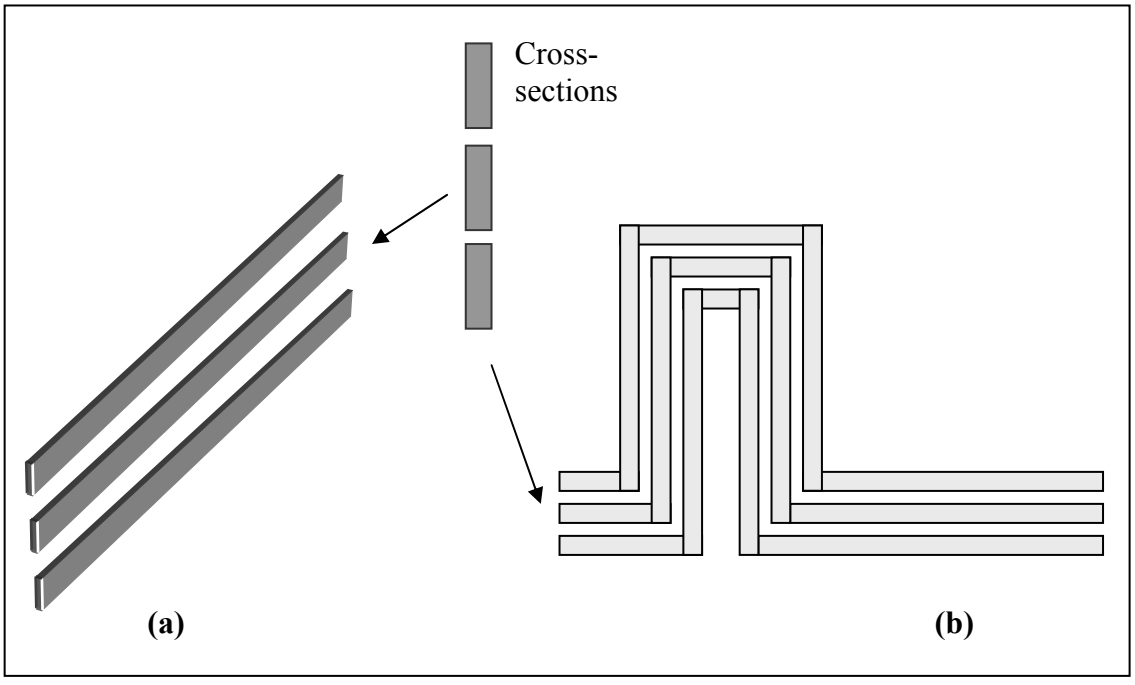

Fig. 8.1 Two different geometrical arrangements of busbars, (a) simple and (b) complex.

8.1 Equivalence of busbars to a set of thin wires

In order to calculate the magnetic field of a three-phase system of busbars it is useful to consider them as segments of infinitely thin conductors. This approximation holds well for distances larger than the dimensions of the system (i.e. x and y > *b*), which is given by the separation *b* between busbars. Fig. 8.2 shows the contour plots for a common type of a busbars system. It has the following parameters: cross-section of each bar = (0.1 m) x (0.01 m), current per phase I = 400 A (rms), separation between busbars b = 0.2 m, length L = 2m. The field was evaluated for three different scales corresponding to the value ranges: I) [500 μT- 1000 μT], II) [50 μT- 500 μT], and III) [0.5 μT- 5 μT]. There are differences in field values only in the first range. In the areas of interest, i.e. range III, the systems are equivalent (i.e. they differ in les than 1%). This fact makes the formulas presented in chapter 2 useful for evaluating the properties of the field from busbars.

8.2 Dependence on the length

In order to have a realistic approach, when studying the field from busbars systems, it is important to determine when to use 2-dimensional or 3-dimensional computational codes. For the specific case presented in the former section, the field is evaluated on the plane with vertical distance $Z = Z_1 = 4$m. Fig. 8.3 shows that 2D simulations can be applied accurately for long systems (L >> 10m). This is because the field

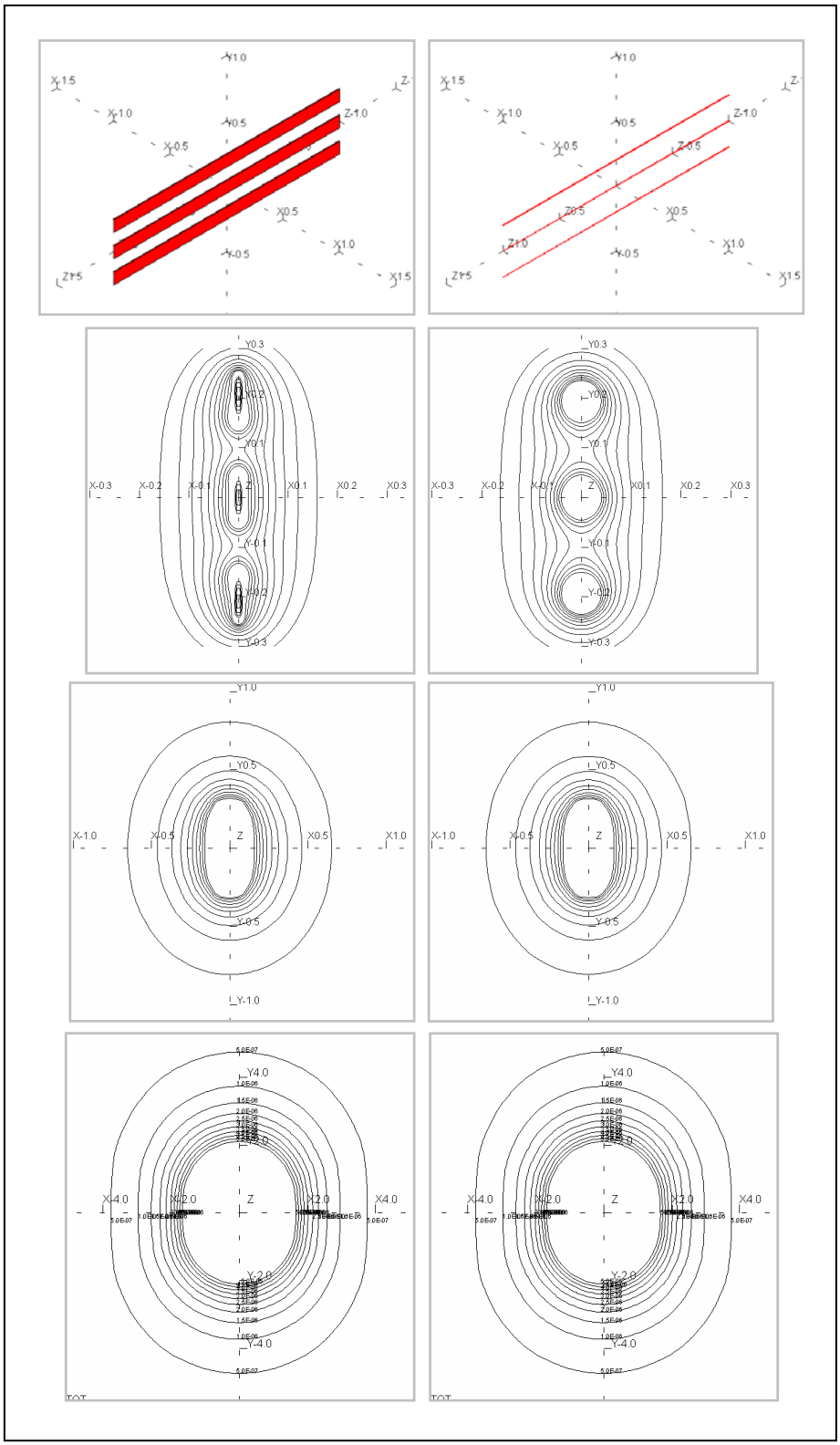

Fig. 8.2 Approximation of busbars by a infinitely thin conductors. The magnetic field can be considered equivalent for distances larger than the dimensions of the system, in the displayed case (I = 400 A per phase) the field values differ in less than 1% for: x, y >0.3 m.

becomes independent of the direction along the busbars. For shorter busbars, a 3D formulation should be used. This can also be observed in Fig. 8.4, where the values at the centre of symmetry (x = 0, y = 0) are plotted.

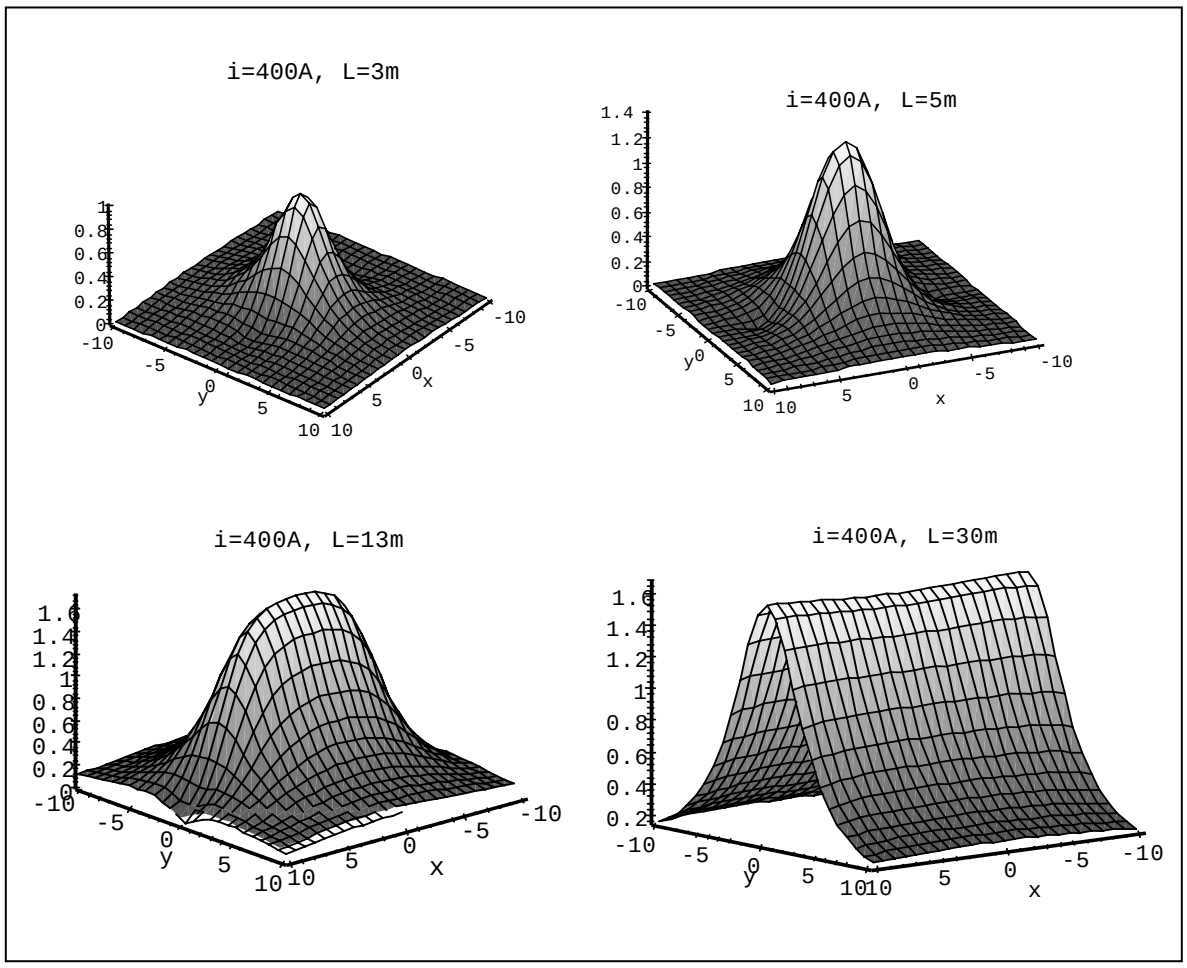

Fig 8.3 Magnetic field dependence on the length L of the busbars, evaluated at a vertical distance of 4 m

8.3 Variation of the field along the vertical distance

Fig. 8.5 shows the dependence of the magnetic field on the vertical distance Z to the observation plane for the particular current *I= 400A*.

The separation between busbars is $b = 0.2\ m$. This dependence is shown for various lengths of the busbars system.

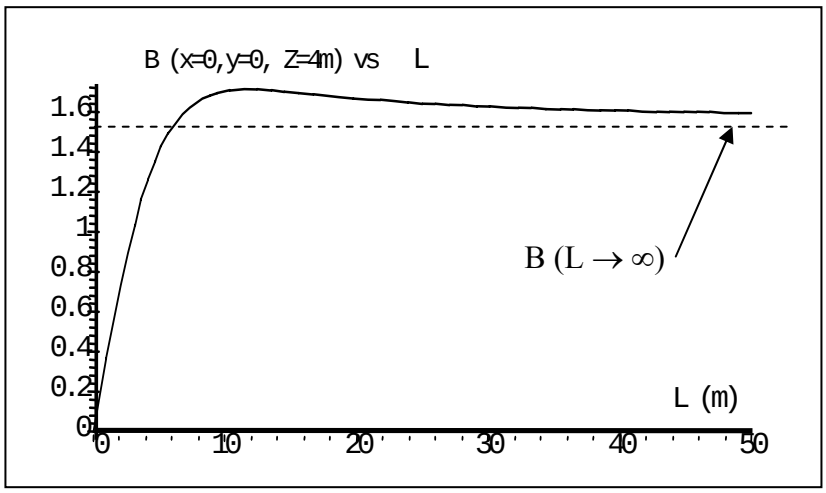

Fig. 8.4 Dependence on the length L .

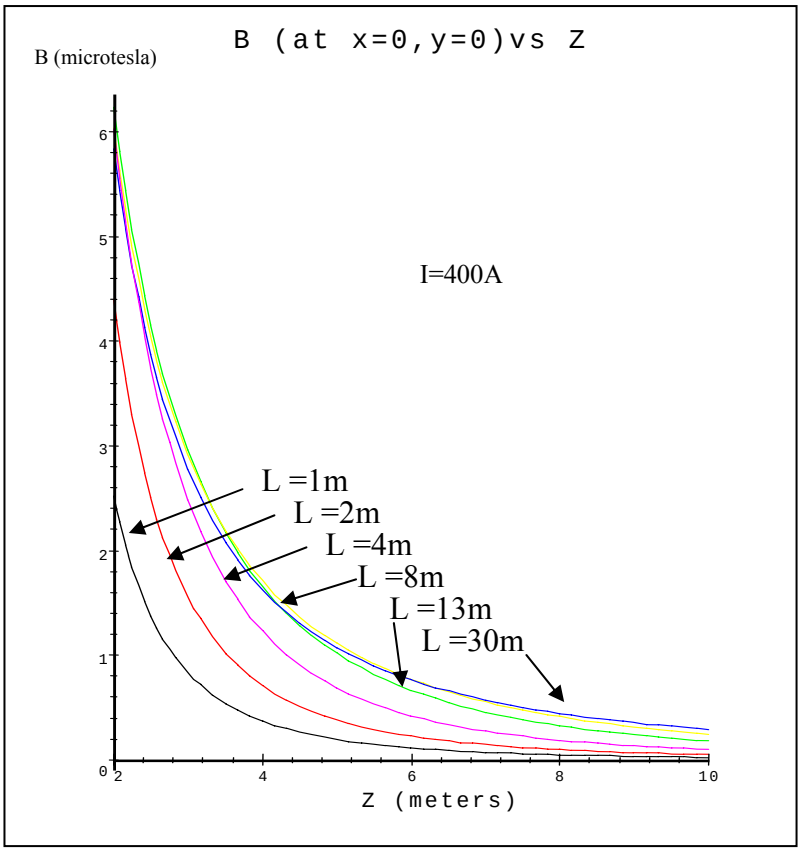

Fig. 8.5 Variation of the magnetic field as a function of the vertical distance from the busbars system to the measuring point.

8.4 Field variation with the distance between busbars

In a similar way as the study for bundles of several conductors in the former chapter, the distance (b) between busbars is very important; the larger it is, the higher the field will be (Fig. 8.6). When the distance is very small, the fields from the three phases tend to cancel each other.

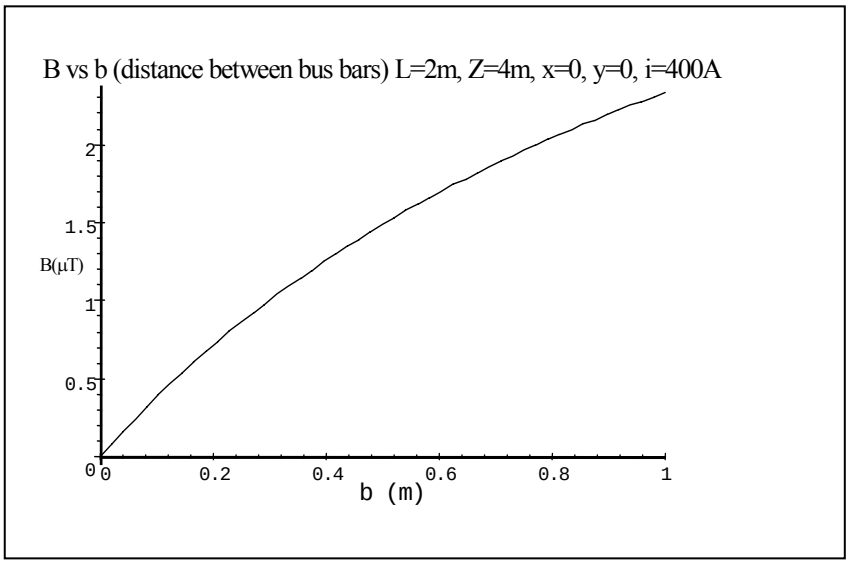

Fig. 8.6 Variation of the field as a function of the distance (b) between busbars.

It is often necessary to contrast shielding results with the case when the shield is not present. Results discussed here become relevant in that case.

References

[1] E. Salinas and L. Aspemyr, *Experimental Study of 50 Hz Magnetic Fields from 10/0.4 kV Substation Components.* Proceedings of the Fourth Latinamerican Congress on Electrical Genertion, Transmission and Distribution, Vinha del Mar, 2000.

[2] E. Salinas and L. Aspemyr, *Measurements and Reduction of 50 Hz Magnetic Fields from the New Substation at the Department of Electric Power Engineering,* Technical Report No. 14R, ISSN: 1401-6176, Chalmers University of Technology, Gothenburg, 1999.

9 Conductive and ferromagnetic shielding

For the reason of cost-effectiveness the main interest in shielding PFMFs is in *thin shields*. By *shield* we mean a finite metal layer (open, closed or semi-closed) that is placed around or near a device (or an affected area) whose magnetic field is aimed at mitigation. *Thin* refers to sub-centimetre thickness. Most of the results in this chapter are deduced for three-phase busbars systems. However, the method can be applied to various sources such as coils or cable arrangements carrying mono or multi-phase currents.

9.1 Shielding effectiveness at power frequencies

It is customary to discuss the performance of a shield in terms of a figure of merit named *shielding effectiveness* (*SE*). The shielding efficiency depends on the ratio of the field evaluated at the point (x,y,z) for two different circumstances and depends on the frequency. For quasi-static systems (e.g. power frequency regime) the electric and magnetic fields can be considered separately. For the magnetic field[1] it is defined in decibels (dB) as:

$$SE = 20\log_{10}\left[\frac{B_0(x,y,z)}{B_{Shielded}(x,y,z)}\right] \tag{9.1}$$

[1] A similar expression is given for the shielding efficiency of electric fields in the quasi-static regime: $SE = 20\log_{10}\left[E_0(x,y,z)/E_{Shielded}(x,y,z)\right]$. However at high frequencies E and B cannot be considered separately, thus S has to be defined by means of the electromagnetic power flow P(x,y,z) evaluated before and after placing the shield: $SE = 10\log_{10}\left[P_0(x,y,z)/P_{Shielded}(x,y,z)\right]$.

where B_0 is the magnetic field in the absence of the shield, and $B_{Shielded}$ is the magnetic field after placing the shield.

Unlike the case of high frequencies [1], where mitigation of several orders of magnitude can be rather common, a field reduction of an order of magnitude at power frequencies is often considered rather good. In this case the definition of the *attenuation factor A* given in chapter 6 can still be used in practical evaluations of shielding.

9.2 Penetration depth

When a harmonically varying magnetic field $B(x, \omega t)$ penetrates a metallic medium with conductivity σ, and permeability μ, the magnetic flux change produces an electromotive force (EMF), which induces eddy currents circulating in the conductor and opposing the incident field. As a result of this the net magnetic field is altered. This is a situation that can be solved exactly using Maxwell's equations for the quasi-static regime. In fact, the problem is fully 1-dimensional, even though three dimensions are involved! (i.e. the fields B and H have only one component along the vertical direction y, the eddy currents and the associated electric field propagate along z, yet these four quantities vary only in the direction x). In Fig. 9.1, since $\partial / \partial y = 0$, and $\partial / \partial z = 0$, the set of equations given in Eq. 7.1-(a)-(b) simplify. Thus Faraday's law that governs eddy currents becomes:

$$\frac{1}{\sigma}\frac{\partial J}{\partial x} = j\omega B \tag{9.2}$$

At the same time, these currents generate a magnetic field, this is described by Ampere's law

$$\frac{\partial H}{\partial x} = J \tag{9.3}$$

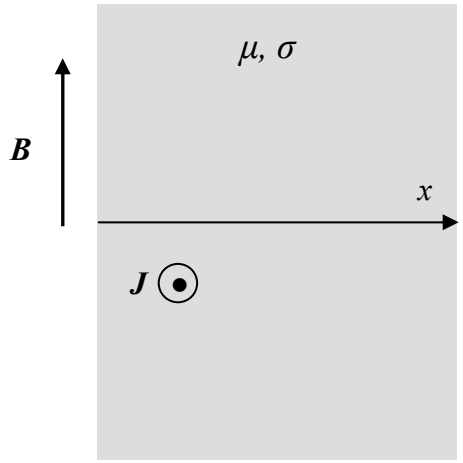

Fig. 9.1 Propagation of a magnetic field inside a semi-infinite medium.

These two equations, and the constitutive relation $B = \mu H$, give a second order differential equation:

$$\frac{\partial^2 B}{\partial x^2} - j\omega\mu\sigma B = 0 \tag{9.4}$$

to which the general solution is

$$B = C_1 \exp(\sqrt{j\omega\mu\sigma}\, x) + C_2 \exp(-\sqrt{j\omega\mu\sigma}\, x) \tag{9.5}$$

Applying the boundary condition $B(x \to \infty) = 0$ makes C_1 to vanish. Defining the field at the surface of the interface as $B(x = 0) = C_2 \equiv B_0$, and introducing the *penetration depth* (or *skin depth*) δ which is defined as

$$\delta = \sqrt{\frac{2}{\omega\mu\sigma}} \tag{9.6}$$

Then the solution becomes

$$B = B_0 e^{-(1+j)\frac{x}{\delta}} \tag{9.7}$$

Thus the magnetic field is both damped and phase shifted with distance inside the conductor. A similar behaviour is obtained for the current density *J*. Eq. (9.2) together with Eq. (9.7) gives

$$J = -B_0 \frac{(1+j)}{\mu\delta} e^{-(1+j)\frac{x}{\delta}} \tag{9.8}$$

Defining $J_0 = B_0(1+j)/\mu\delta$ as the current density at the surface,

$$J = J_0 e^{-(1+j)\frac{x}{\delta}} \tag{9.9}$$

Consequently the current density also decays inside the material in the same fashion than the magnetic flux density B.

Table 9.1 shows the penetration depth calculated for some common metals.

Table 9.1

	Penetration depth δ [mm]		
f (Hz)	Cu $\sigma = 5.99 \times 10^7 Sm^{-1}$	Al $\sigma = 3.77 \times 10^7 Sm^{-1}$	Fe $\mu_r = 200$
25	13.4	17.4	2.54
50	9.44	12.3	1.8
100	6.77	8.7	1.3
1 000	2.11	2.75	0.41
10 000	0.667	0.87	0.13
100 000	0.211	2.75	0.041
1 000 000	0.067	0.087	0.13

The penetration depth in iron is much smaller than that of aluminium or copper. Therefore, it is common [2] to regard conductive shielding with thin non-magnetic materials at power frequencies as inherently inefficient (since any practical shield would have thickness < δ), or, in any case not better than iron. However, the problem is not settled by the concept of penetration depth, since the model presented in this section contains various ideal assumptions. In the EMC literature [3], [4], other models for thin layers have been developed but it is still common to consider infinite dimensions in the direction perpendicular to the plate, which enables to study the model analytically. Another assumption is to develop the model for high frequencies where the electric and magnetic fields are coupled and form a plane wave, which is not the case of PFMFs

9.3 Modelling of finite and open shields

The complexity of shielding PFMFs with thin finite plates is shown in Fig 9.2 for a three-phase system of busbars. The incident field experiences reflection, penetration and diffraction around the borders of the shield. Moreover inside the shield reflection on the second surface becomes relevant when the shield is thin, in addition power absorption due to ohmic losses (which are temperature dependent) take place. As a result of this, an accurate study of *finite, open shields* by analytical methods is difficult and to obtain accurate numbers numerical modelling is required.

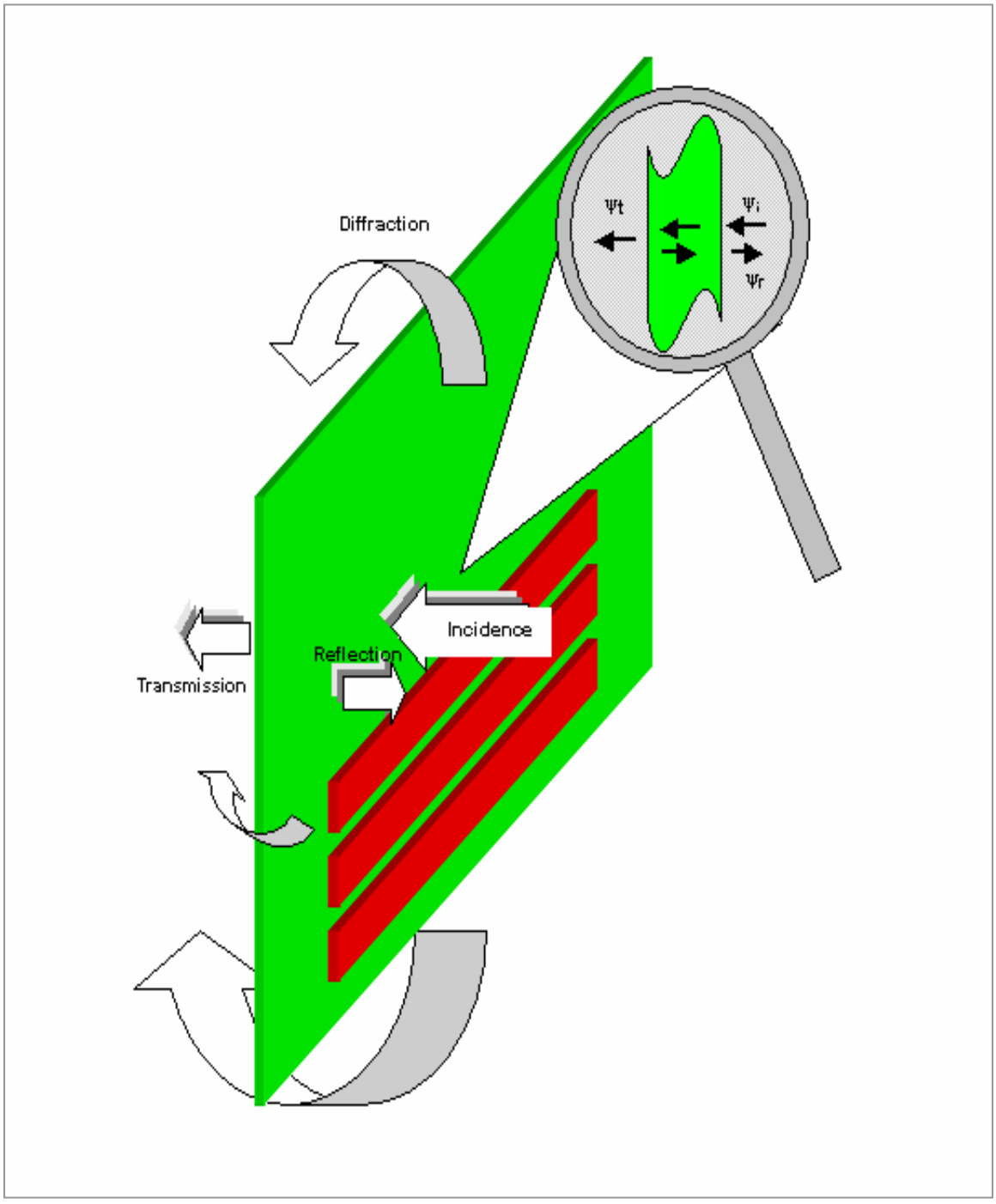

Fig. 9.2 Some of the complexities inherent to the use of finite and open shields.

Figures 9.3 and 9.4 show two examples of geometrical configuration for

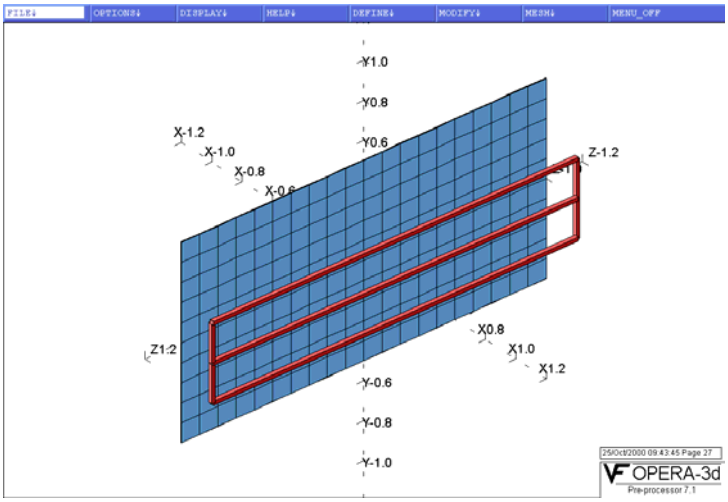

Fig. 9.3 Pre-processing geometrical configuration for the shielding of a 3-phase busbars system (L = 2m). The plate thickness is 3 mm and the distance *d* plate to busbars is 20 cm. The current in the busbars is 100 A per phase.

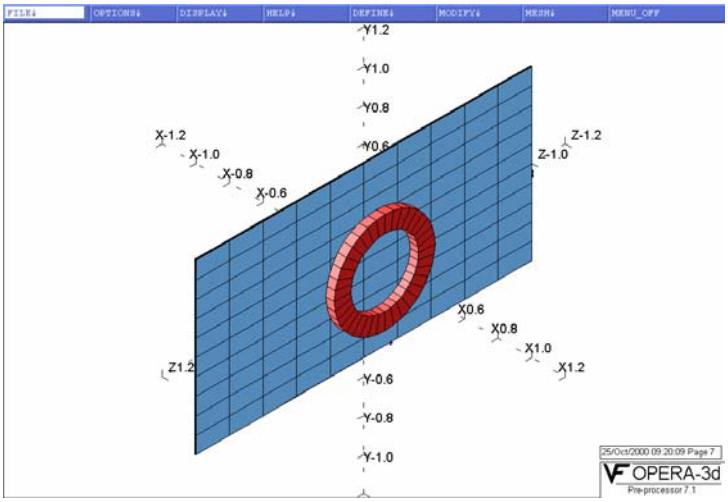

Fig 9.4 Shielding of the magnetic field of a coil. The size of the plate is 2 m wide, 1 m high, and 5 mm thick.

the OPERA-3d pre-processing of simulations with busbars and coils. Coils have different field patterns thus yield extra information to the shielding analysis. The shield with dimensions 2m x 1m is divided in

facets, next it is subdivided even further by allocating enough number of elements along the plate thickness to permit assessment of eddy currents (Fig. 9.5).

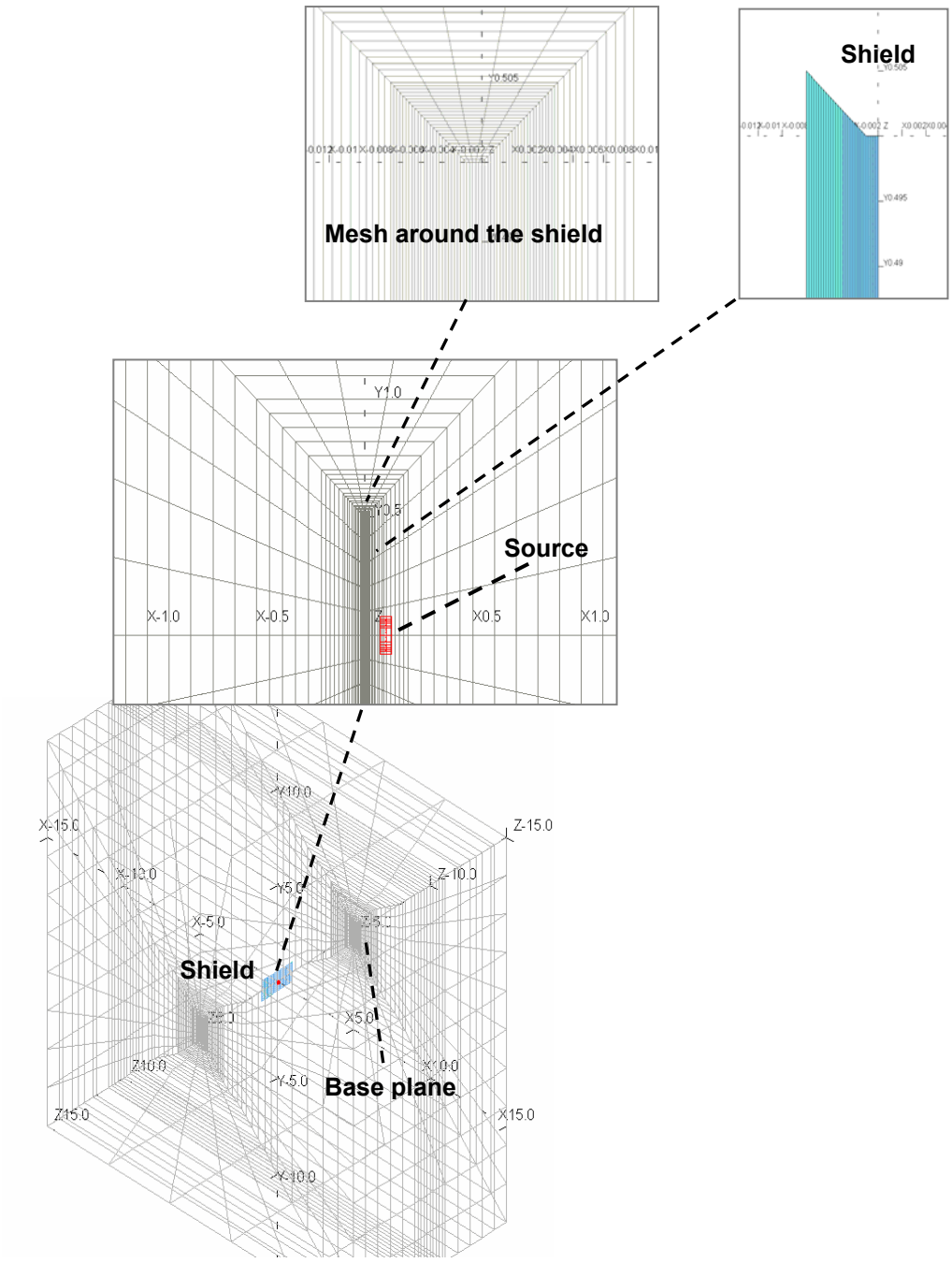

Fig. 9.5. Construction of a mesh for the shielding configurations described in Fig. 9.3, and 9.4.

The structure of the mesh in Fig. 9.5 contains 52 000 elements. and the bounding box has the dimensions 30 m x 30 m x 10 m.

Fig 9.6 illustrates the formation of eddy currents on the surface of a shielding plate made of aluminium. The busbars carry a current of 100 A per phase. The geometry was shown in Fig. 9.3.

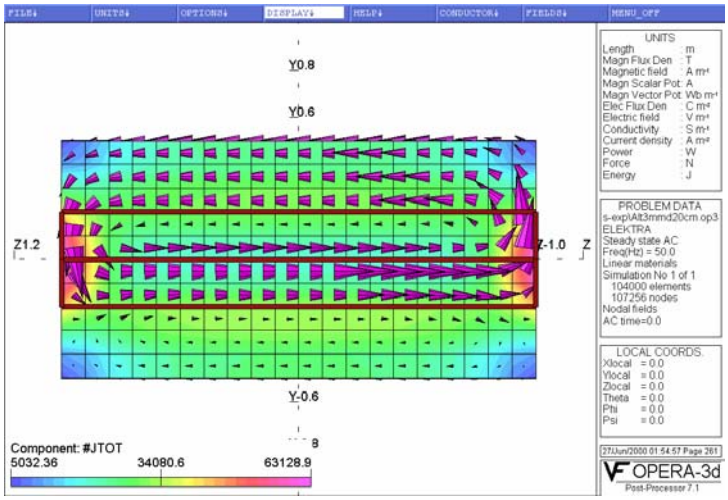

Fig. 9.6 Instantaneous view (at ωt = 0º) of eddy currents on the surface of a 3 mm-thick aluminium plate. The busbars carry a current of 100A per phase.

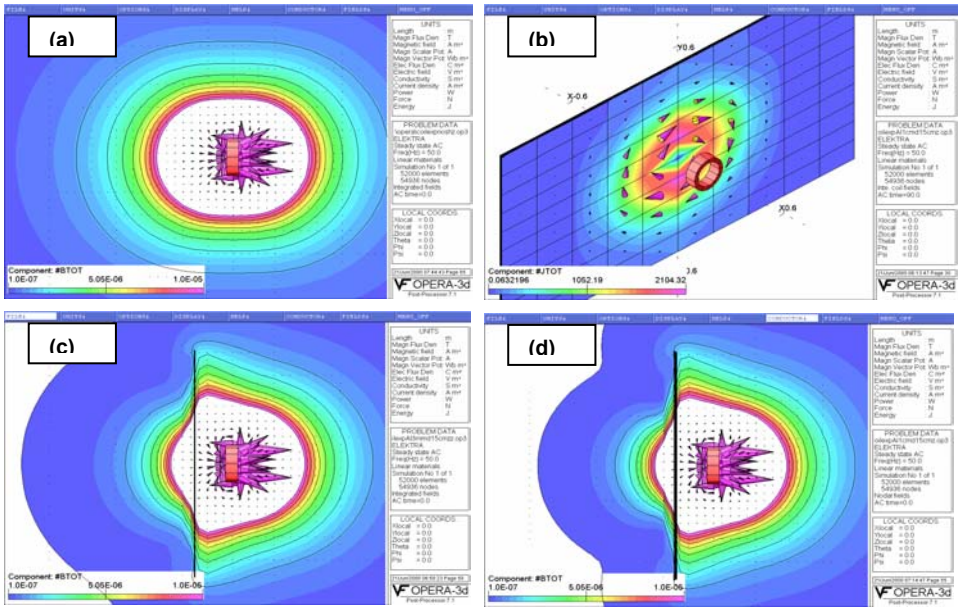

Fig. 9.7 (a) Field and contour lines of a coil (no shield) **(b)** eddy currents on an aluminium shield **(c)** 3 mm thick shield **(d)** 1 cm thick shield. Range: [0.1-10] microtesla.

9.4. Shielding Parameters

In this section we are interested in a formulation that represents shielding of a busbars system which is part of the geometry of a substation. For the purposes of shielding design it is useful to investigate the dependence of field mitigation on various parameters. To save computer time a long system of busbars was used and a 2D problem for finite shields was solved. Yet the 3D–Elektra code was used; an approach to a full three-dimensional solution was thereby possible using an extension of the same grid, as described in chapter 7. Fig. 9.8 shows the formulation of the

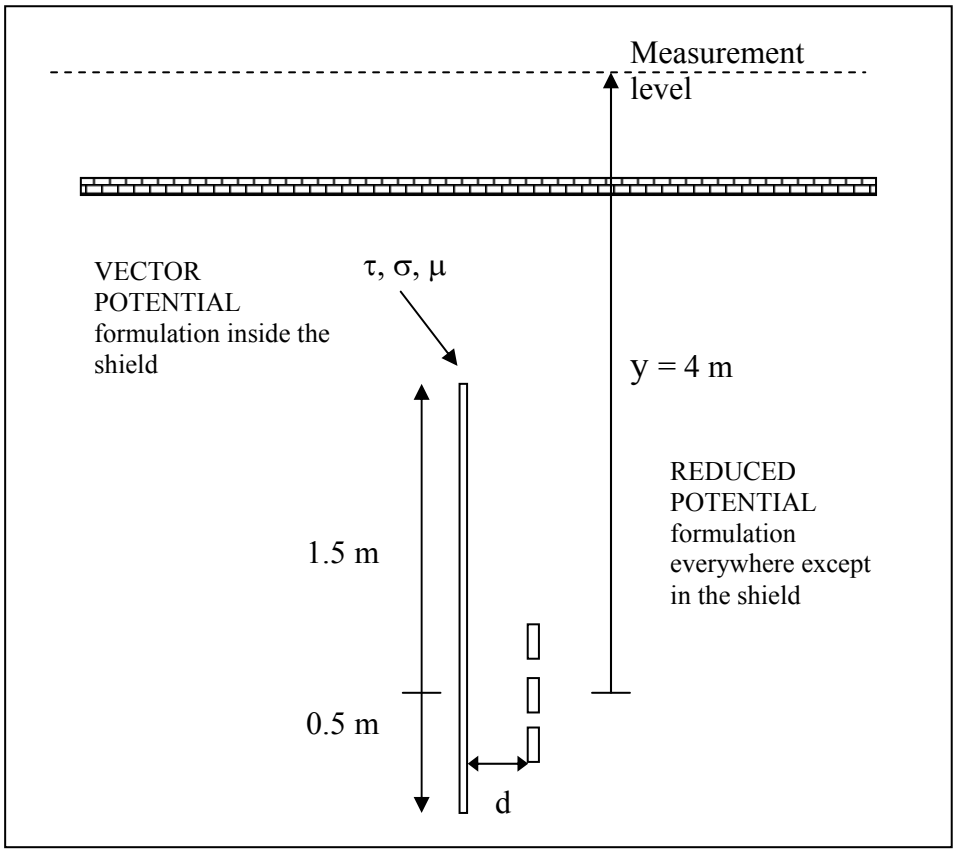

Fig. 9.8 Shielding configuration for a three-phase busbars system. The parameters to vary, and formulations of the potentials in different regions are also shown.

problem. The plate was placed asymmetrically along the vertical axis for a practical reason: the busbars are located not very high (0.5 m) above the floor. The results of the simulations in the case of conductive plates [5] are shown in figure 9. 9.

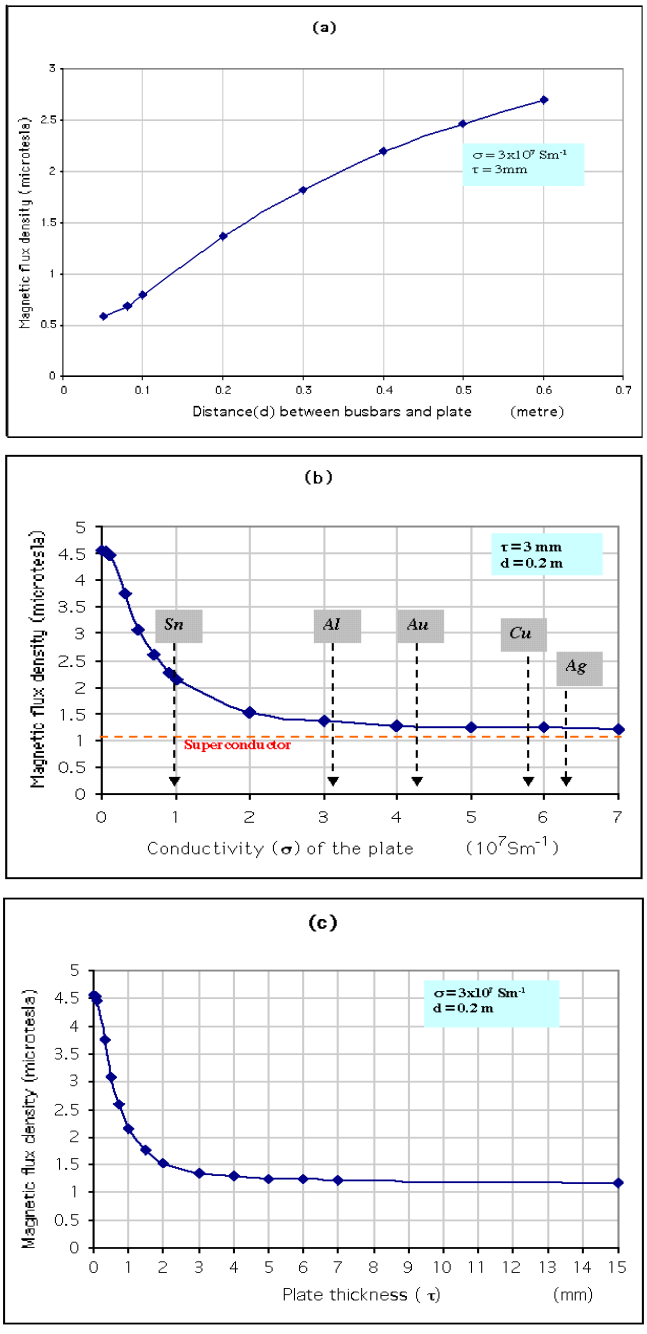

Fig. 9.9 Variation of the mitigated field (at y = 4 m) with **(a)** distance plate-busbars *d*, **(b)** conductivity σ and **(c)** plate thickness τ.

The current in the busbars was I = 1000A per phase and the field was evaluated at the level y = 4 m. Each point on the curves represents the maximum field value at that level after the shielding operation. A typical CPU time on a HP workstation for each point was about 4 hours.

Fig 9.9-(a) shows the dependence of the mitigated field on the distance between plate and the busbars. The field mitigation increases as the shield comes closer to the busbars. Contour plots of the fields in two contrasting cases are shown in Fig. 9.10. However at very close distances (d > 10 cm) there may be practical difficulties, such as heat generation by the high eddy currents values involved, risks of contact or brake down. Another related result is that the *averaged size of the eddy current loop* increases with increasing separation.

Fig. 9.9-(b) shows the mitigated field value as a function of the plate conductivity. However, there is no significant effect on mitigation when materials with conductivities higher than that of aluminium are used (for this reason simulations presented in figures 9.9-(a) and 9.9-(c) were performed for aluminium). In fact the field does not reach values under 1.1 microtesla, even when a superconductor is used as a shield. This is a direct consequence of the field diffraction around the plate, mostly under it.

It was also observed that the screening efficiency is maintained for values of thickness down to $\tau \sim 1/3 - 1/4$ of the skin depth before decaying rapidly (Fig 9.11). At this thickness ($\tau/\delta < 1$) the influence of the reflection at the second face of the screen becomes significant, as it

contributes to the attenuation of the incident field (appendix II), much as reflection of light by dielectric materials with high ε_r .

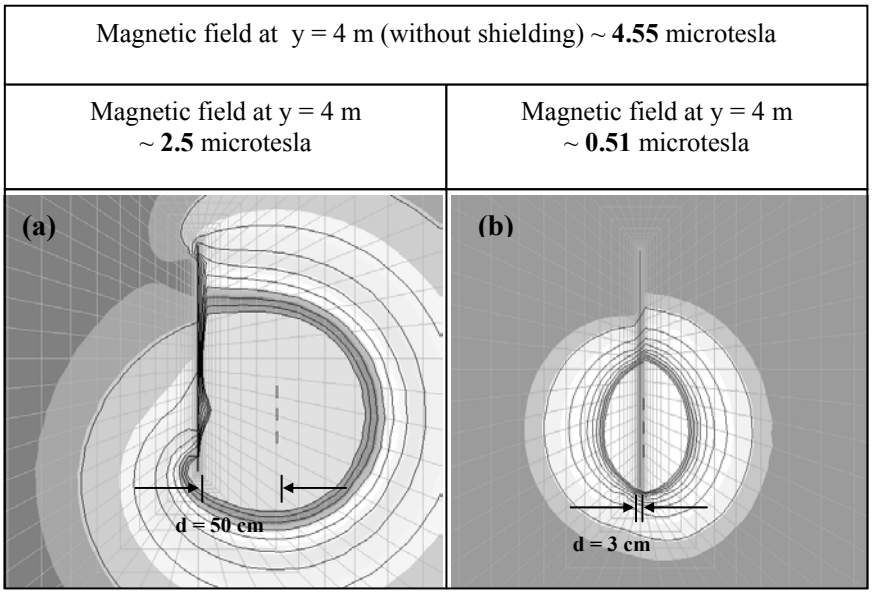

Fig. 9.10 Two examples of magnetic flux density reduction. In both cases the conductivity of the plate is $\sigma = 3x10^7$ S m^{-1} and its thickness is 3 mm. In **(a)** the shield is at d = 50 cm from the bus bars, while in **(b)** it is at d = 3 cm.

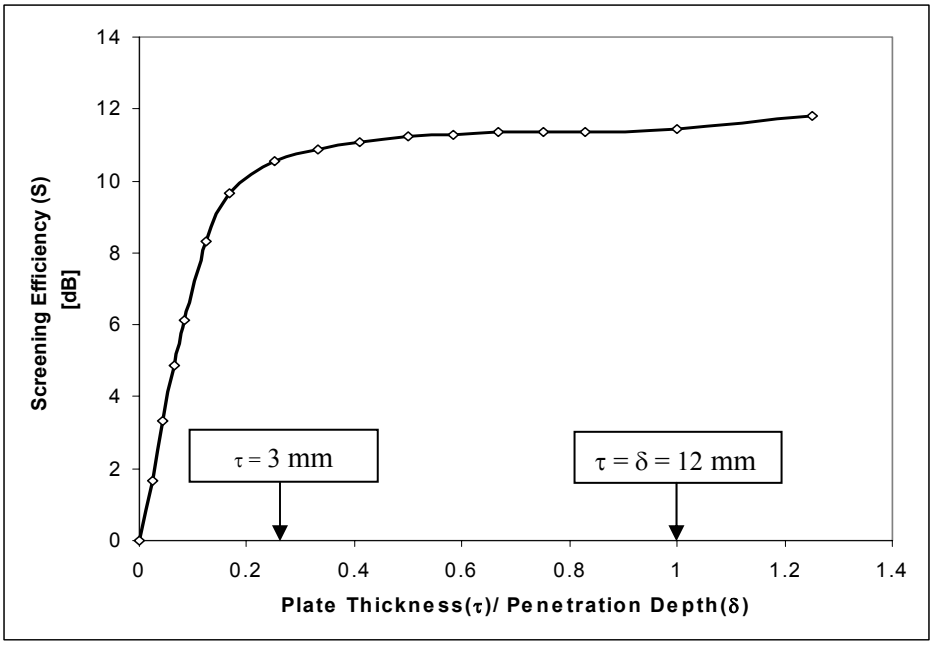

Fig. 9.11. Shielding efficiency of an aluminium plate at y = 4m as a function of τ/δ.

Diffraction of the field around the shield produces eddy currents on the other side of the plate. This effect is more evident as the separation between plate and busbars *d* increases, as can be observed in Fig. 9.12. In Fig. 9.8 the shielding plate was not located symmetrically with respect to the busbars system because the floor restricted the positioning of the

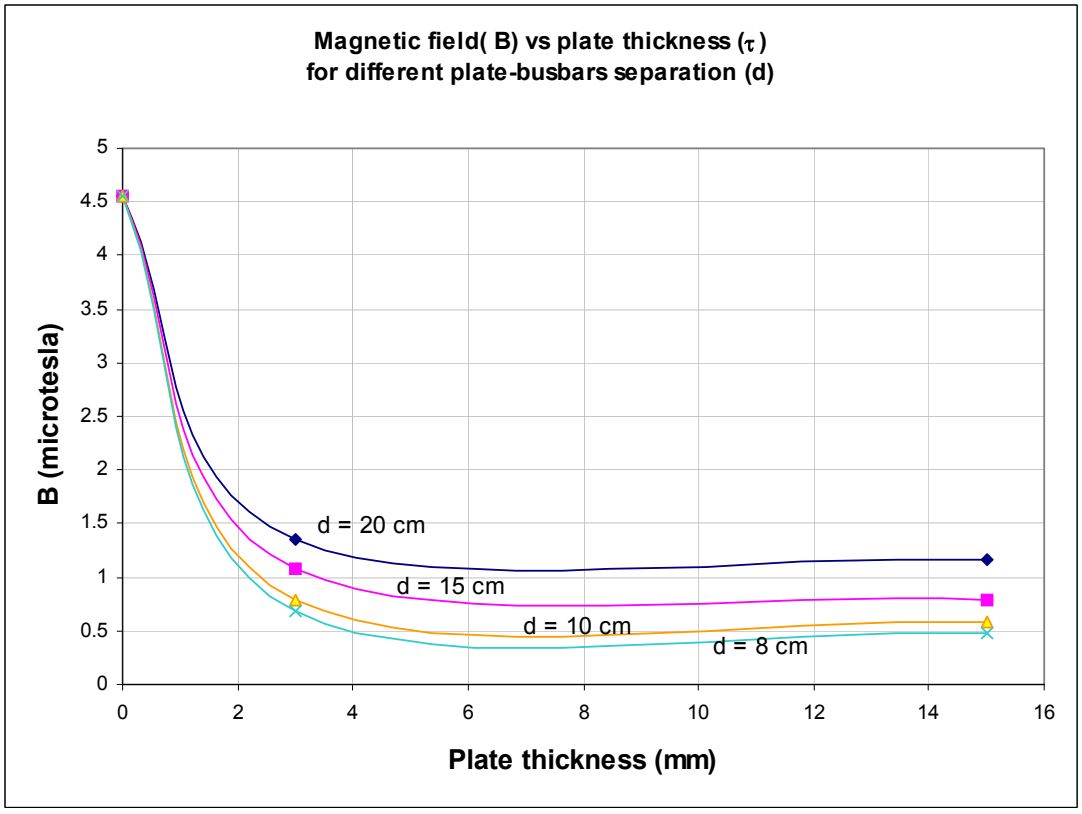

Fig. 9. 12 Influence of the positioning of the shielding plate on the diffraction of the field around the plate, y = 4m.

plate. This restriction, however, can be removed, for instance in the design of the substation or switchboard, allowing symmetrical positioning of the plate. Results of simulations for the symmetrical case shows that this operation improves the field mitigation (Fig. 9.13).

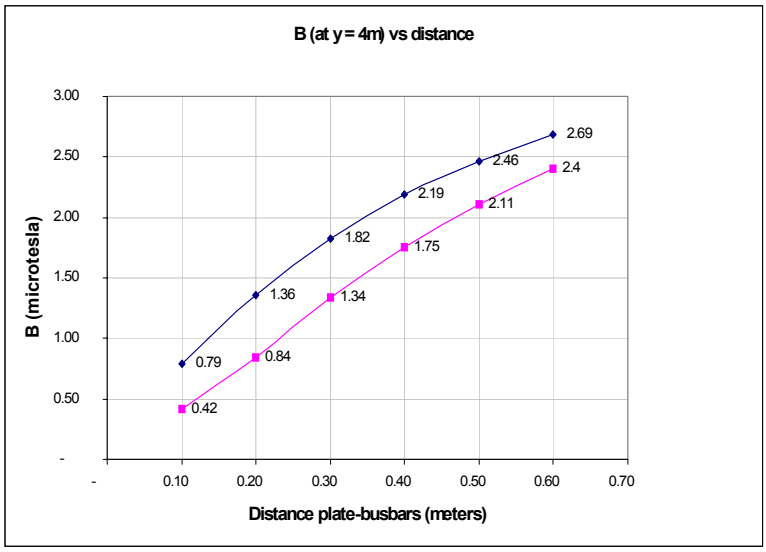

Fig. 9.13 Magnetic field in function of the distance for two different geometries. Except for the positioning of the aluminium plate all the parameters are the same as in Fig. 9.9-(a). The lower curve represents the case when the shield is symmetric with respect to the busbars.

9.5 Ferromagnetic shielding

The results in section 9.4 were obtained for the conductive shielding. However, the same formulation can be applied to ferromagnetic shielding. In fact, the new formulation should be a generalization of the conductive case since most of ferromagnetic materials considered in practical applications of shielding have a non-negligible conductivity. Results expressed as shielding efficiency (SE) considering a ferromagnetic plate are shown in Fig. 9.14. In all the simulations a linear relation between **B** and **H** was assumed.

Fig. 9.14 shows that a conductive material gives a more efficient screening than a ferromagnetic one [6]. This is in apparent contradiction with the concept of skin effect, which gives for iron ($\sigma = 1.07 \times 10^7$ Sm^{-1}, and $\mu_r = 250$) a skin depth $\delta = (\pi\, f\, \mu_0\, \mu_r\, \sigma)^{-1/2} \sim 0.14$cm, almost an order

of magnitude less than for aluminium – Hence better efficiency would be expected. The latter is correct right at the other side of the ferromagnetic screen, where a strong reduction is observed (Fig. 9.15). However, at 4 m over the system, the two properties of iron, conductivity and magnetic permeability, are in antagonism, as the first tries to cancel the field, the other tries to attract the field lines. In fact some of the field lines are pulled into the region where we want to mitigate the field.

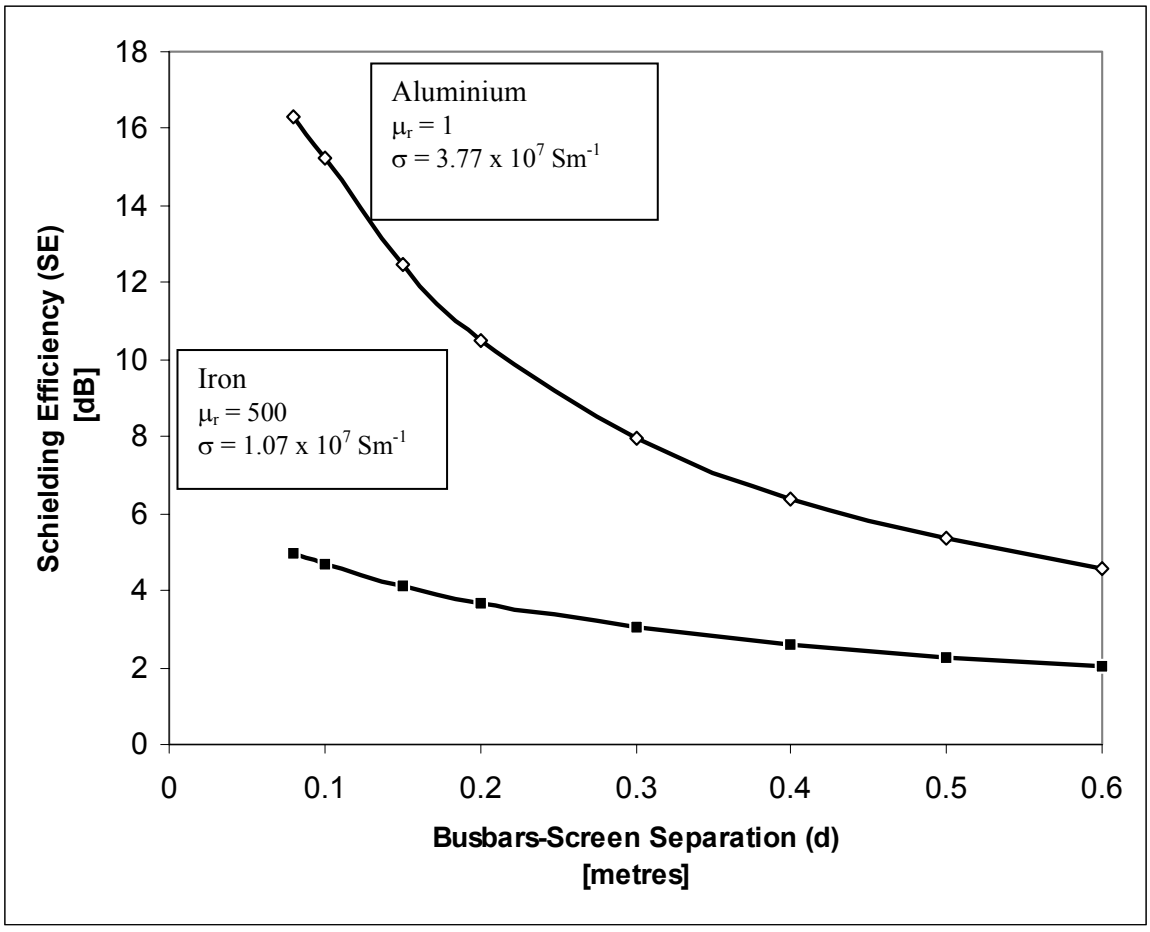

Fig. 9.14 Screening efficiency as a function of the distance between busbars and screen.

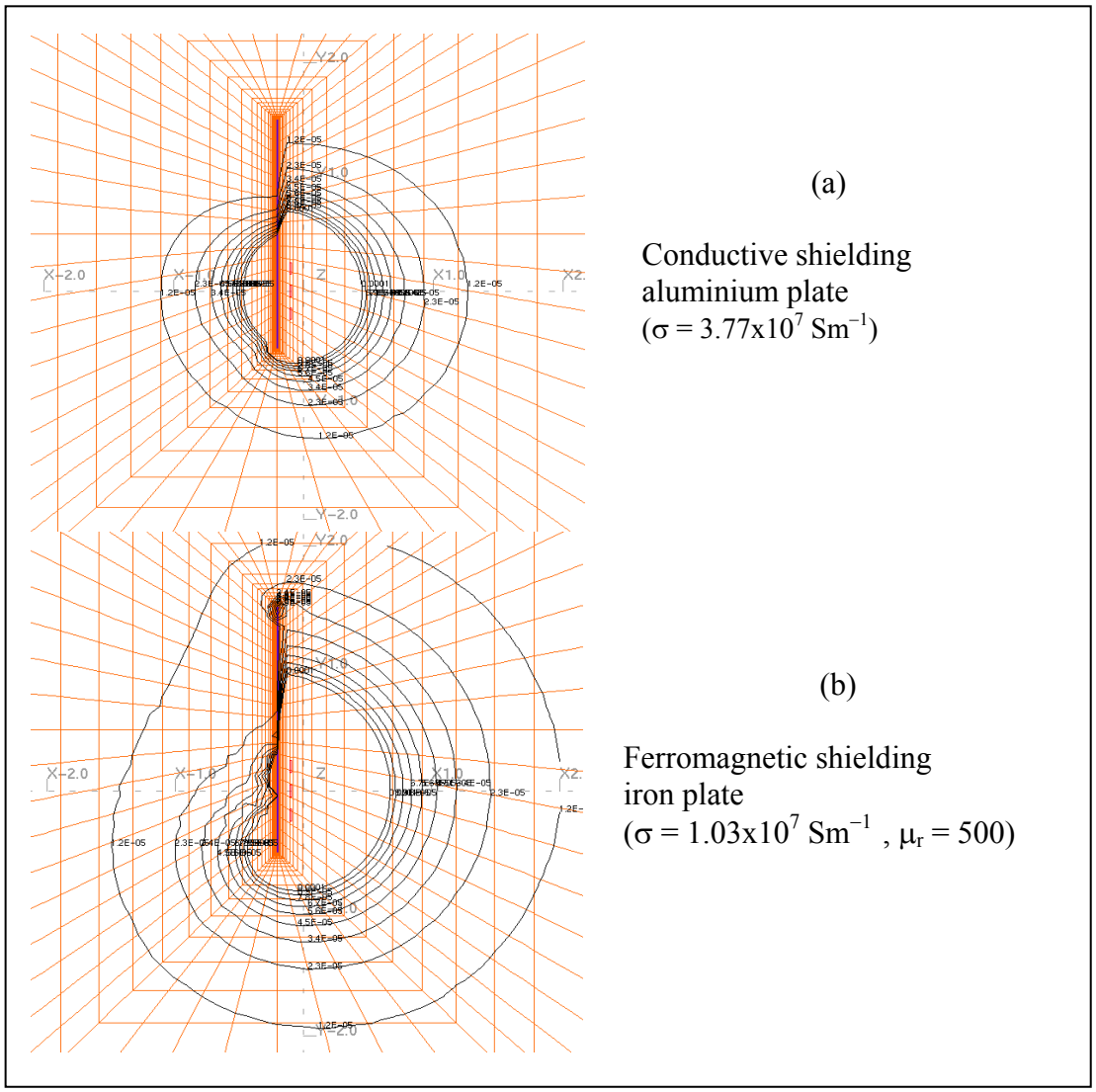

Fig. 9. 15. Contour lines of the magnetic field for two shielding configurations with the same geometry and current configuration. The only difference is that the two plates are made of different materials (a) aluminium, and (b) iron.

9.6 Recommendations

The results from the various simulations provide some suggestions for cost-effective mitigation of fields originated from busbar systems. The following practical criteria can be given:

- The plate should be made of a material with good conductivity, preferably aluminium. The improvement in shielding efficiency of copper with respect to the aluminium does not justify the higher cost of copper.
- The shield dimensions, height and width, should be larger than the dimensions of the system of busbars otherwise edge effects in the plate can diminish its effect as eddy currents tend to go to the borders when the plates are too small. A suggestion is to use similar dimensions than the switchboard. Moreover, it can be used as a support attaching the plate to the switchboard back wall.
- The plate can be thinner than the skin depth (e.g. 3 or 5 mm).
- The plate should be located facing the busbars system.
- The location of the shield should be as symmetrically as possible with respect to the busbars.
- The distance busbars-plate should be kept as short as possible without interfering with the safety regulations of the switchboard.
- The continuity of the plate is important for the formation of eddy currents. Slits, or holes should be avoided. In case of joining plates, it must be done by proper welding.

9.7 Remarks and discussion

In this chapter, field mitigation using the shielding method was applied for a system of busbars. Some results for thin shields have been obtained which were unexpected if one considers the attenuation of PFMFs in a semi-infinite medium. The shielding performance also depends on the

geometrical configuration of the arrangement of the source and shield. Moreover, due to the inherent characteristics of eddy currents, the shielding method can involve some counter-intuitive properties. For example, let us consider another configuration such as locating the shielding plate horizontally over the busbars. This configuration may look as an efficient shield because it seems to be "protecting" (as an umbrella under the rain) the area to be mitigated. However evaluation of the shielding efficiency shows that this arrangement hinders the flows of eddy currents that cancel the busbar's field in an efficient way in Fig16-(a). Out of the three geometries in Fig. 9.16 the most effective configuration is that in Fig. 9.16-(a).

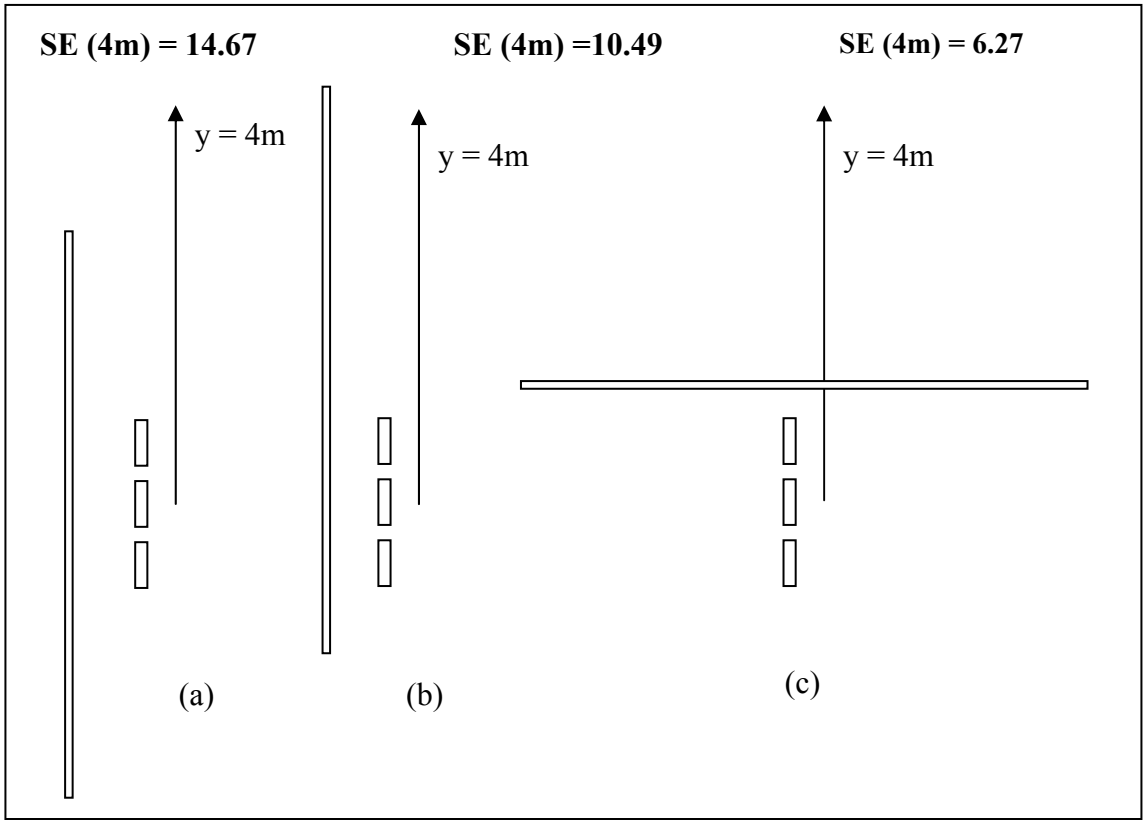

Figure 9.16 Different configurations of busbars and shielding plate evaluated for reduction of the magnetic field at y = 4 m. The material and currents are the same. The most effective configuration is (a).

A related effect is given in Fig. 9.17. Adding a bending to the upper part of the shield (attempting to create an "umbrella effect") is not very effective, since the currents formed in the bending are considerably small compared to the ones in the front part of the plate.

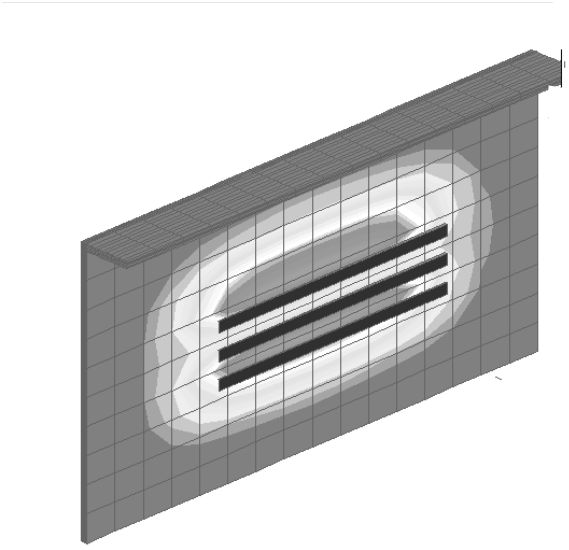

Fig. 9.17 Adding a bending to the upper part of a conductive shield. Eddy currents are much smaller in that part of this shield.

Double shielding also presents some interesting possibilities, Fig. 9.18 shows a comparison between the system ***Al-Fe-Source*** compared to the permutation ***Fe-Al-Source***. In both cases a coil of 20 cm diameter, carrying a current of 100 A (50 Hz) was used. The plate was (2 metres wide) x (1 metre high) x (3 + 3 mm) thick. The separation between plate and coil was 10 cm. Another interesting result is:

In double shielding, the closeness of the conductive plane to the source provides a better field mitigation.

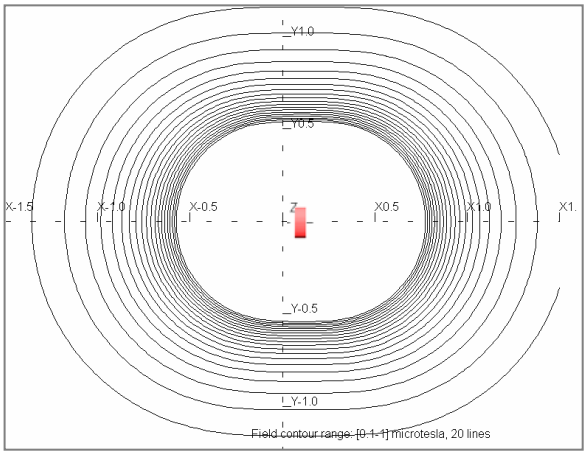

No Shield - Source

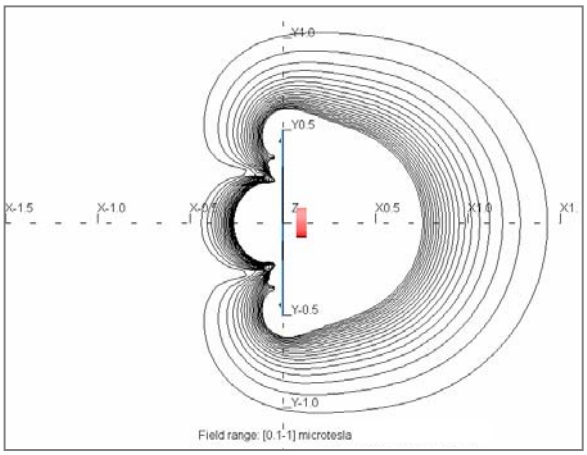

Aluminium - Iron - Source

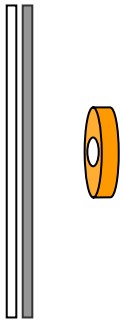

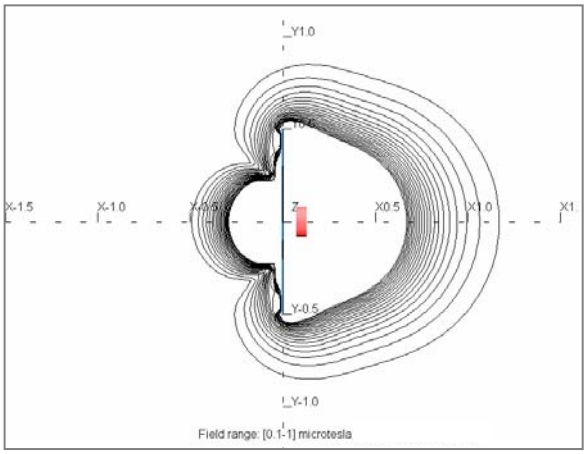

Iron - Aluminium - Source

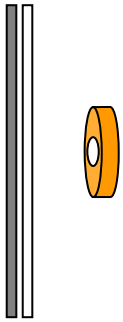

Fig 9.18 Mitigation by double shielding, comparison of the effect of permutation of aluminium and Iron. There is no actual separation between both plates.

Besides the double layer discussion, only the simplest solutions for the shielding problem were presented here because they involve low costs. However, further improvements of the method are possible. The use of multi-layer techniques (Appendix III), or different shielding shapes (Paper D) can provide more costly but also more efficient shielding.

References

[1] Clayton R. Paul, *Introduction to Electromagnetic Compatibility*, Wiley series in Microwave and Optical Engineering, john Wiley & Sons, Inc. N.Y. 1992.

[2] Welsby, V. G., *The Theory and Design of Inductance Coils*., Macdonald&Co. Publishers Ltd., London, 1960, p. 67.

[3] Schulz, R. B., "Shielding Theory and Practice", IEEE Transactions on Electromagnetic Compatibility, Vol. 30, No 3, 1988, pp. 187-201.

[4] Moser, R., "Low-Frequency Low Impedance Electromagnetic Shielding", IEEE Transactions on Electromagnetic Compatibility, Vol. 30, No 3, 1988, pp. 202-210.

[5] E. Salinas, L. Aspemyr, J. Daalder, Y. Hamnerius, and J. Luomi, *Power Frequency Magnetic Fields from In-house Secondary Substations.* CIRED'99, 15th Conference on Electricity Distribution, Technical Reports, session 2, pp. 161-164. University of Liège, Belgium, June 1999.

[6] E. Salinas, "Conductive and Ferromagnetic Screening of 50 Hz Magnetic Fields from a Three –Phase System of Busbars", Journal of Magnetic and Magnetic Materials, 2001, Vol. 226-0/2002, pp 1239-1241.

10 Active and passive compensation

The principle of active compensation was introduced in chapter 4. This principle uses the properties of naturally induced currents and imitates them by a designed electrical device. Passive compensation is also based on eddy currents but instead of plates (in the case of shielding) the paths of these currents are wires. In chapter 9, various properties of eddy currents have been described. Thus, it is possible to utilize these properties for elaborating compensating schemes.

10.1 Active compensation of busbars

Analysis of eddy currents in a conductive plate at different instants provides a hint of how to compensate the field of busbars. Fig. 10.1 shows the instantaneous configuration of eddy currents on a plate located in front of a system of busbars, which is 2m long, with 2cm x 2cm cross-sections, and carrying a current of 100A in each of the phases (R, S and T). The geometrical shapes of the paths of the eddy currents can be understood as the dynamics of two loops. This detail is more evident in the second frame of Fig 10.1. An “imitation” of these loops can be constructed with two coils carrying two different 1-phase currents, namely S and T, achieving in this way a 2-phase equivalent of a 3-phase system of busbars. These two loops are designed to generate a field similar but opposite to the field of busbars.

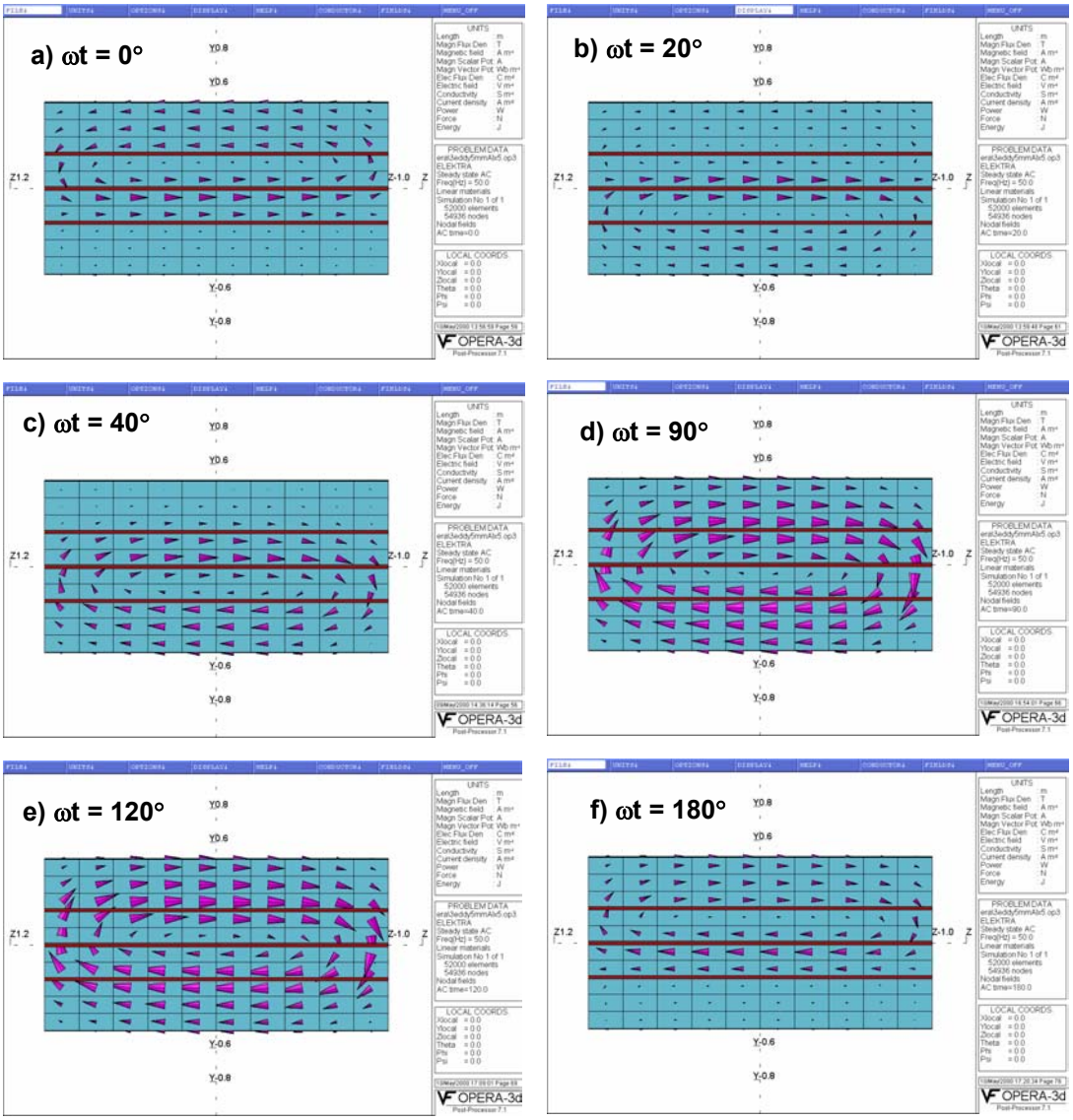

Fig. 10.1 Instantaneous configurations of the paths of eddy currents on the surface of a shielding aluminium plate for different angles ωt.

In order to obtain an equivalent current of 100A per loop and at the same time be able to connect the coils directly to the main feeding circuit the number of turns (N = 60), wire thickness and impedance was calculated. Thus the feeding current in each of the compensating coils was only 1.67A. The uppermost and lowermost sides of the

compensating coils then have opposite currents to the S and T branches of the busbars. The middle part of the coil arrangement yields an equivalent current with phase -S-T =-R, that will compensate the middle branch of the busbars (Fig. 10.2).

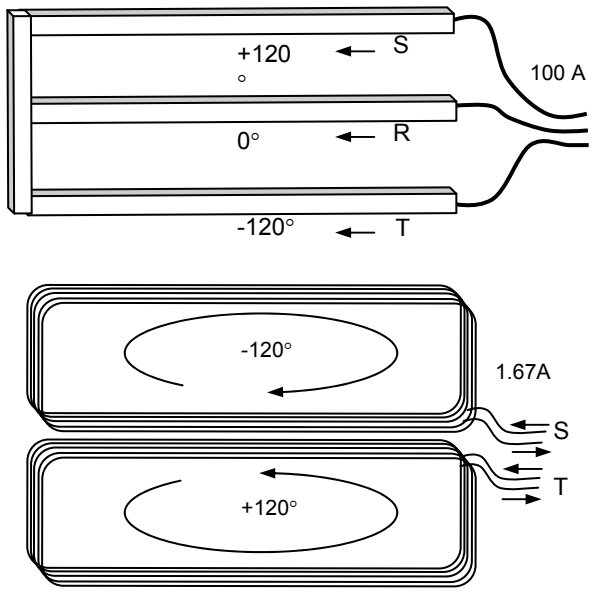

Fig. 10.2 Busbars (3-phase) and compensating coils (1-phase each). The coils are placed in front of the busbars.

The shielding efficiency at y = 1.5 m from the busbars was measured experimentally (Fig. 10.3) varying the parameter distance (d) busbars-coils. It varies from SE = 8.6 dB to SE = 15.4 dB, when the distance d between busbars and coil vary between d = 20 cm and 10 cm respectively. The efficiency gets higher for smaller values of d. However, influence on design rules and safety regulations (e.g. too high values of the mutual impedance, and appearance of induced forces when d < 10 cm) do not allow the placement of coils too close to the busbars.

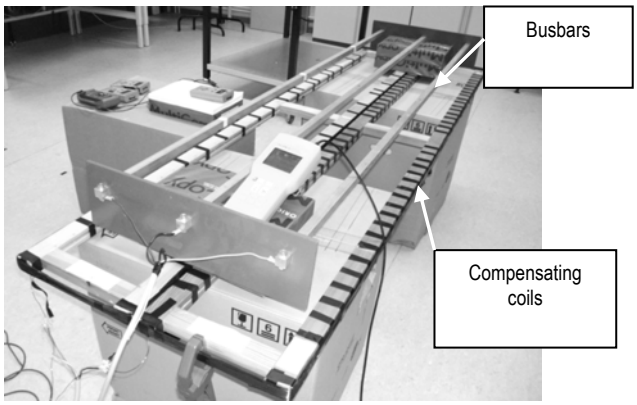

Fig. 10.3 Experimental implementation of active compensation. Each coil is 2m long and 0.25 m wide.

Fig. 10.4 shows the result of a FEM simulation for active compensation (presented in two contour plots shaded regions for initial conditions and shaded regions for the compensated case). The attenuation factor obtained was about 13 dB for the external values (B_0 = 0.1 μT).

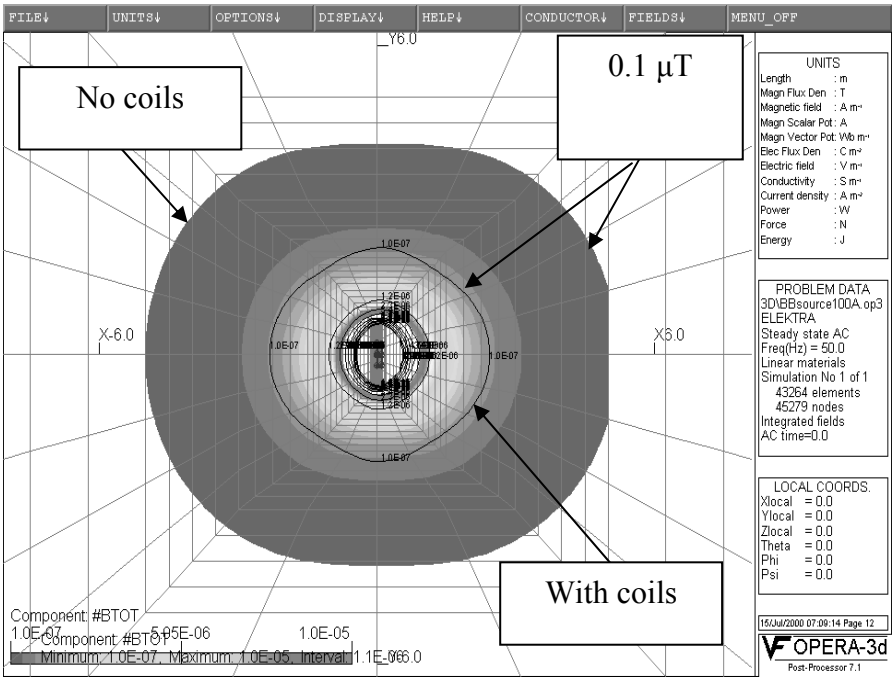

Fig. 10.4 Busbars: field after active compensation (lines) contrasted with the field without shielding (contour regions).

10.2. Active compensation of underground cables

Another application of active compensation is the field mitigation of an arrangement of long underground cables carrying a current of 200 A per phase (Fig. 10.5). For this geometry, active compensation technique (using I = 46 A in a triangular configuration of 40 cm each side) provides a mitigation of 18-20 dB. Shielding with flat or wedge shaped plates either ferromagnetic or conductive provides a maximum mitigation of 10.6 dB for realistic configurations. More details of this example will be presented in chapter 12.

10.3. Passive compensation

The equivalence of three phase systems to two dipoles makes it also possible to use conductive loops without introducing an external source of current other than the currents induced by the source field. The use of passive loops depends significantly on the kind of source. There have been suggestions and discussions about the use of passive loops in transmission lines [1]. But it seems that this technique has not been applied to busbars. We have tested a short circuit of coils in the experiment shown in Fig. 10.3 but the mitigation was negligible. In comparison with the conductive plates, where eddy currents are able to "choose" their optimal path on the surface, the coils represented an inefficient path. However, low-resistivity (copper), 1-turn, and thick (5 mm diameter) loop conductors presented only fair mitigation factors between 5 to 8 dB but only when they were located extremely close (a few millimetres) to the source (busbars). Low induced currents seem to be the major disadvantage of this method, which can be improved in a

future study by partially compensating the inductance by a series capacitor (Fig 10.6).

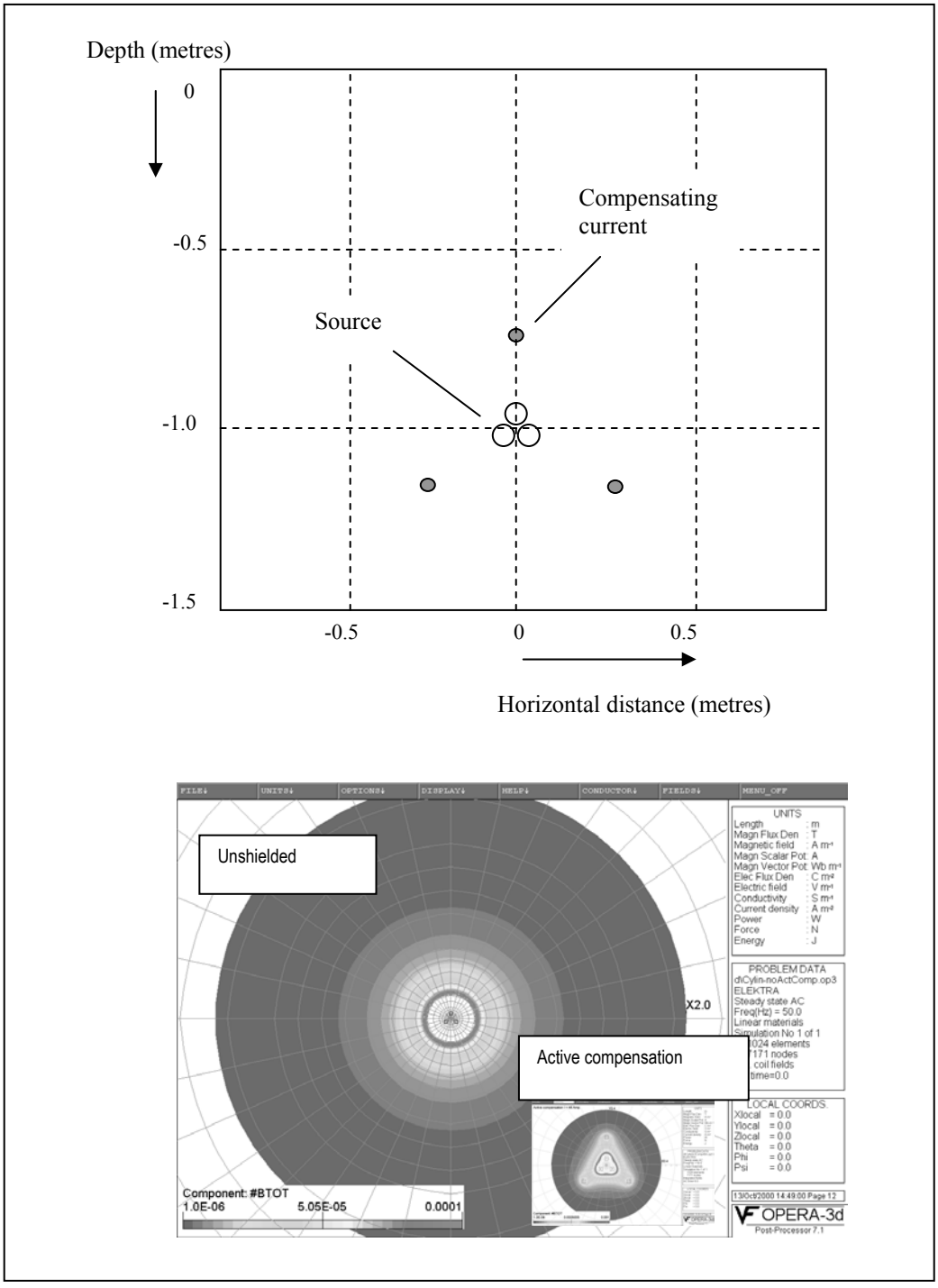

Fig. 10.5 Unshielded and active compensated configurations for a system of three-phase conductors (I = 200A per phase). The compensating current is 46 A.

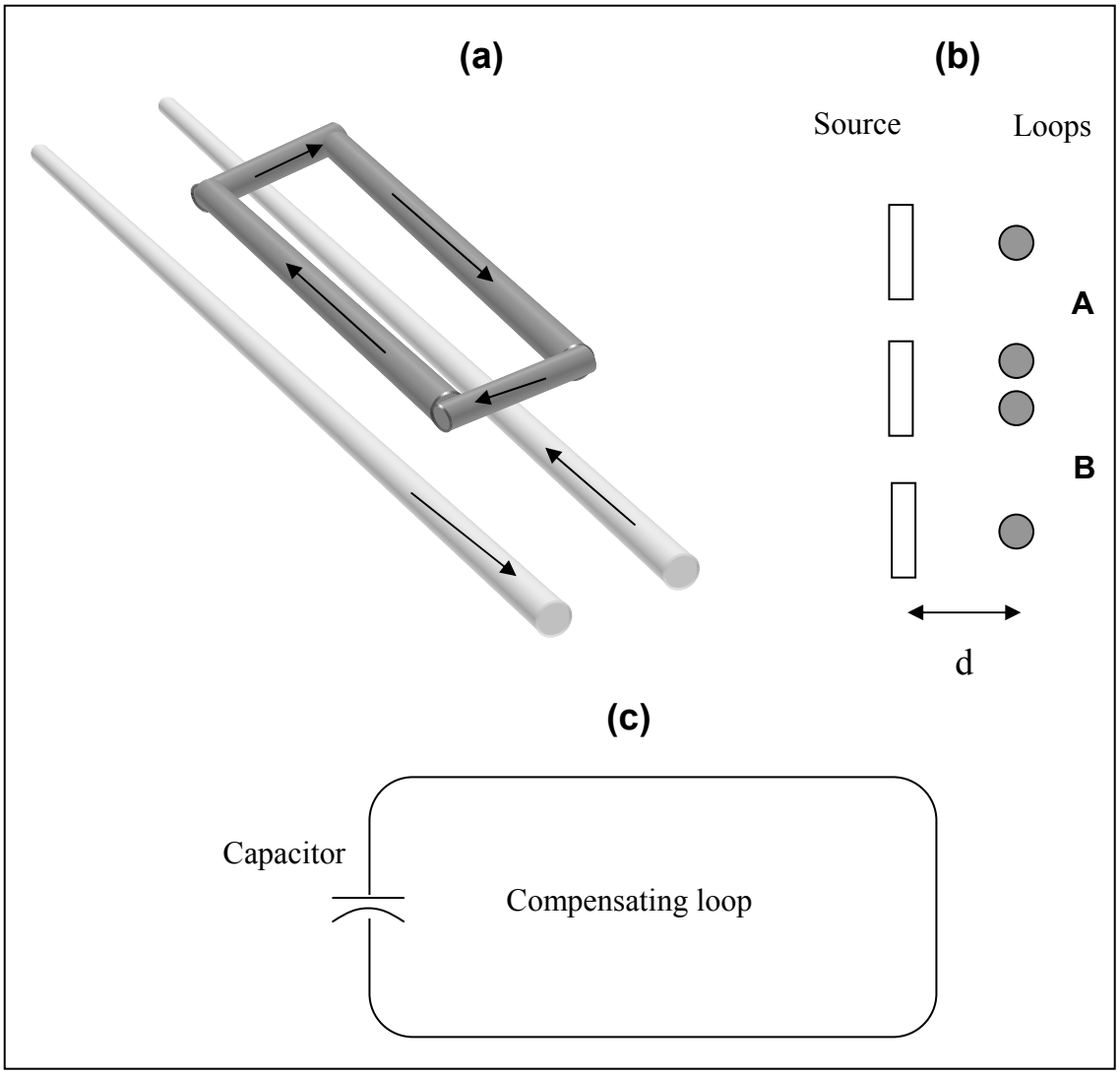

Fig 10.6 Passive compensation schemes.

References

[1] U. Johnsson, A. Larsson and J-O. Sjödin, "Optimized Reduction of magnetic field near Swedish 400 kV lines by advanced control of shield wirecurrents. Test results and economical evaluation", IEEE trans. Power Delivery, Vol. 9, April 1994, pp. 961-969.

[2] H. Olsson, Petersson, A. Eriksson, "Reduction of Transmission Line Magnetic Field-Possibilities and Constraints", CIGRE Report 36-101, 1990.

11 Mitigating the field of transformers

There are various kinds of distribution transformers. The most common type is the oil-insulated transformer; also dry transformers and epoxy-insulated transformers are used.

In liquid/oil-immersed units a sealed tank construction, made of steel, effectively contains the windings and active parts in an optimal environment, as the liquid substance is both an insulating and a cooling agent. Because of their design losses are minimised – in fact, these units are very efficient and can operate in an overload condition up to 30% for several hours. On the other hand, they are considered and handled as flammable items and as such less suitable for domestic or public places.

Dry transformers neither contain any cooling liquid nor are they inside sealed metal containers. Their coils have a varnish impregnation, are cast in epoxy resin, or surrounded by other insulating materials, which are capable of leading excessive heat away. These types of transformers are often highly fire resistant. Their use is most advantageous in high-risk places (e.g. oil refineries or nuclear plants), public buildings (e.g. hospitals, airports), or dense residential areas.

The magnetic field from transformers is rather complex and has various origins, such as the leakage field from the coils and ferromagnetic laminations, or the connections at the low/high voltage parts. To model the complete field emission from a transformer is rather a difficult task.

Attempts have been made to use numerical methods to deal with various parts of transformers [1], [2]. Because of this complexity, the shielding characteristics have to be obtained experimentally. Even though small-scale experiments can help to decide upon some suitable shielding features [3], they do not provide definitive answers since the magnitude of a transformer's magnetic field do not scale linearly with its size. Therefore actual-size experiments have to be performed.

11.1 Comparison between a shielded and an unshielded transformer

Two commercially available transformers were studied [4], one unshielded (TU) (Fig. 11.1), and the other shielded (Fig. 11.2) with a 5 mm aluminium box cover (TS). Fig. 11.3 shows a comparison of the field from these transformers and other substation components. Although the transformers TU and TS have different manufacturers and different designs (both of them are dry, but TS is varnished and TU is epoxy cast), they have various similarities. Both are 800 kVA, three-phase, and were connected to the same feeding transformer in similar configurations as to provide a comparison. The comparison showed that the shielding cover was the most relevant differentiating factor between the two transformers. Design of both transformers involved secondary connections situated at the bottom of the transformer and tests were made with optimal cable connections (Fig. 11.2).

The shielding efficiency (SE) of the shield of TS relative to TU, showed values that were about 15 dB in average in an area 4m x 4m above the

transformer, at h = 3 m over the floor of the substation. The field from internal connections (on the transformer's secondary side) of TS and the stray field from coils and core were mitigated via eddy currents by the aluminium box. In addition, it was demonstrated that the emission from TS was about 50% lower compared with the averaged values of the field from the switchboard, which was part of the experimental set ups.

Fig. 11.1 Epoxy insulated dry transformer, unshielded (TU).

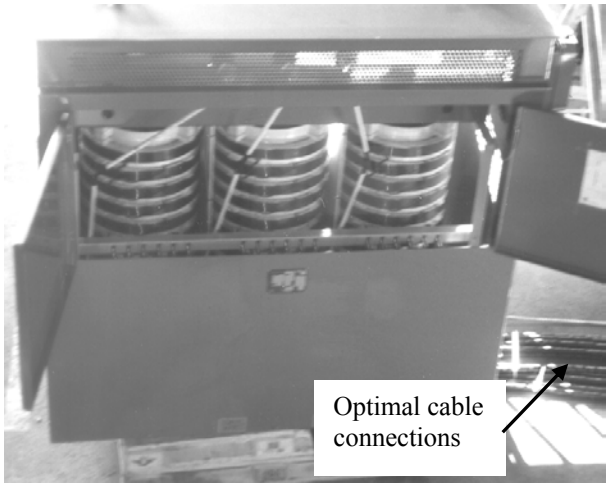

Fig. 11.2 Varnish coated dry transformer, shielded (TS).

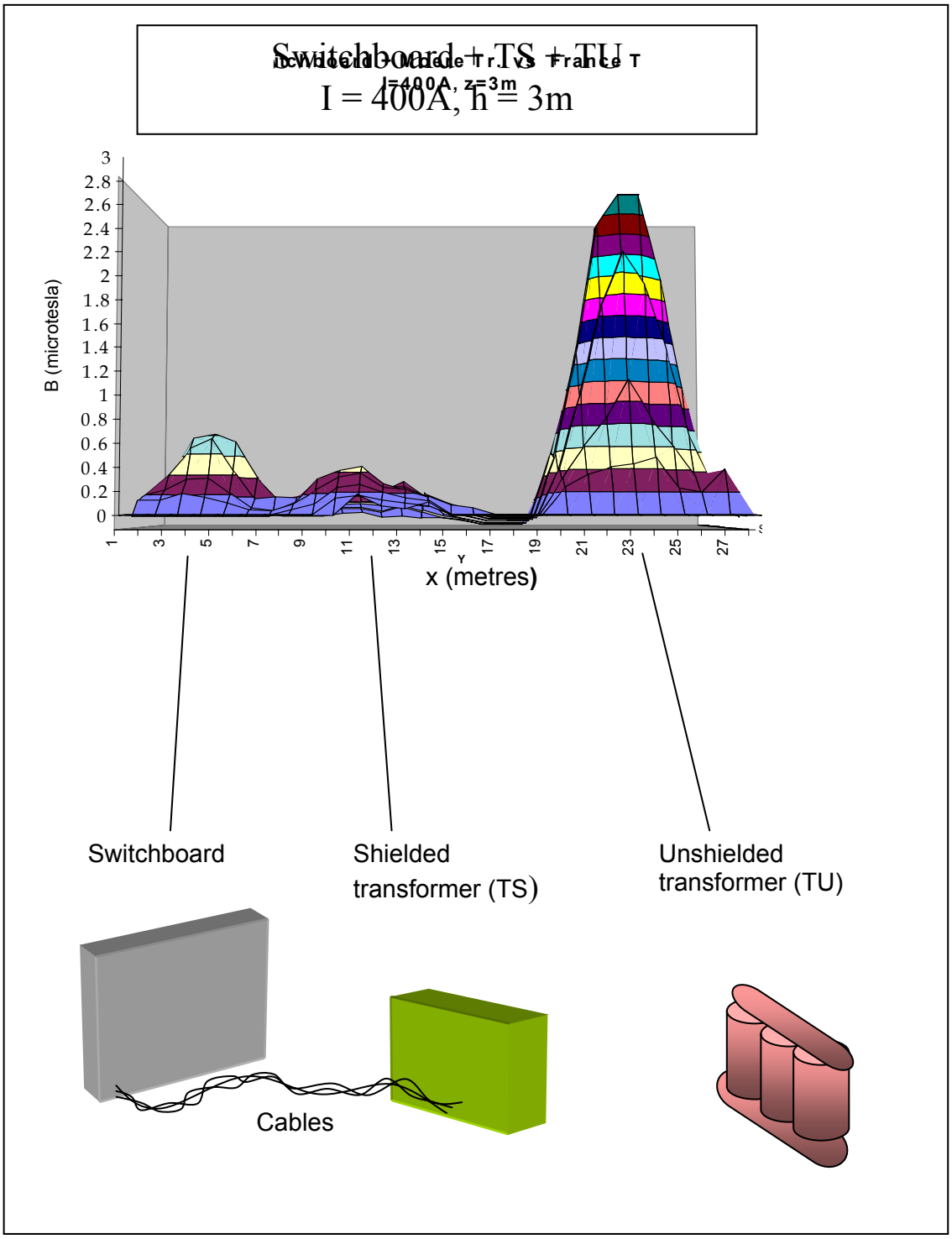

Fig. 11.3 The field from various components of a secondary substation. The shielded transformer gives a field emission that is significantly lower as compared with the unshielded one.

11.2 The largest contribution to the field of the transformers

In the former section, the secondary connections were located at the lower side of the two transformers. In addition, these connections were optimised by phase grouping. However, in functioning substations, which were not designed for low field emission, this is not necessarily the case, as is presented in the following example.

The substation (10/0.4 kV, 800 kVA) located at *Haga* (in central Gothenburg) was studied. The contour plots of the magnetic field, at the floor above the substation, are given in Fig. 11.4. The analysis of the highest field values and its gradient along the vertical direction provided a negative reply to the conjecture that these values may be originating directly (i.e. coils or core) from the transformer T1. The field values at 1 metre above the floor means about 4 metres above the floor of the substation, therefore much lower fields are expected from T1 than the ones read in Fig. 11.4-(b). In fact, the source seems to be much closer to the ceiling and decaying in a different way than a transformer's field [4].

A simple internal inspection established that the large separation between phases (R, S and T) was responsible for the high field values (Fig. 11.6-a). Moreover, the low voltage connections followed a long path rather close to the ceiling of the substation (Fig. 11.5 and 11.6-b). However the cables along this path were well packed allowing for field self cancellation. Large phase separation was not observed at the other transformer (T2) since the connections were rather direct (Fig. 11.6-c) and following a short distance path to the low-voltage switchboard.

To approach this problem, a modification in phase configuration is suggested (Fig. 11.7). The cables should be kept packed all the way to the very end at the secondary side of T1, where they can be reconnected to the transformer individual phases. 3D-simulations for obtaining the magnetic field of the total cable arrangement were performed. The comparison between the two arrangements (Fig. 11.8) gave a good field mitigation expressed in a mitigation efficiency of about 18 dB at the locations of maximum values. Since the resulting values can still be considered high, an improved solution is suggested (Fig. 11.9), which consists of various stages: (i) upside down positioning of the transformer, (ii) phase rearrangement, (iii) connections to the low voltage side at the floor level or, if possible, by the cellar of the substation, and (iv) eventual shielding of the transformer. Future implementation of these measures is expected to mitigate the field to values at the sub-microtesla level.

References

[1] J. Turowski and A. Pelikant, *IEE. Proc.- Electr. Power Appl*., Vol. 144, No. 6, 1997, pp. 435-440.

[2] J. Shen, Z. Andrelic and B. Schaub, *IEE Trans. on Magn. Vol. 34. No 5*, 1998, pp. 2636-2639.

[3] T. Zhong. "Field mitigation from power transformers", Master thesis (in preparation), Chalmers University of Technology, 2001.

[4] E. Salinas and L. Aspemyr, *Experimental Study of 50 Hz Magnetic Fields from 10/0.4 kV Substation Components.* Proceedings of the Fourth Latinamerican Congress on Electrical Generation, Transmission and Distribution, Vinha del Mar, Chile, November 2000.

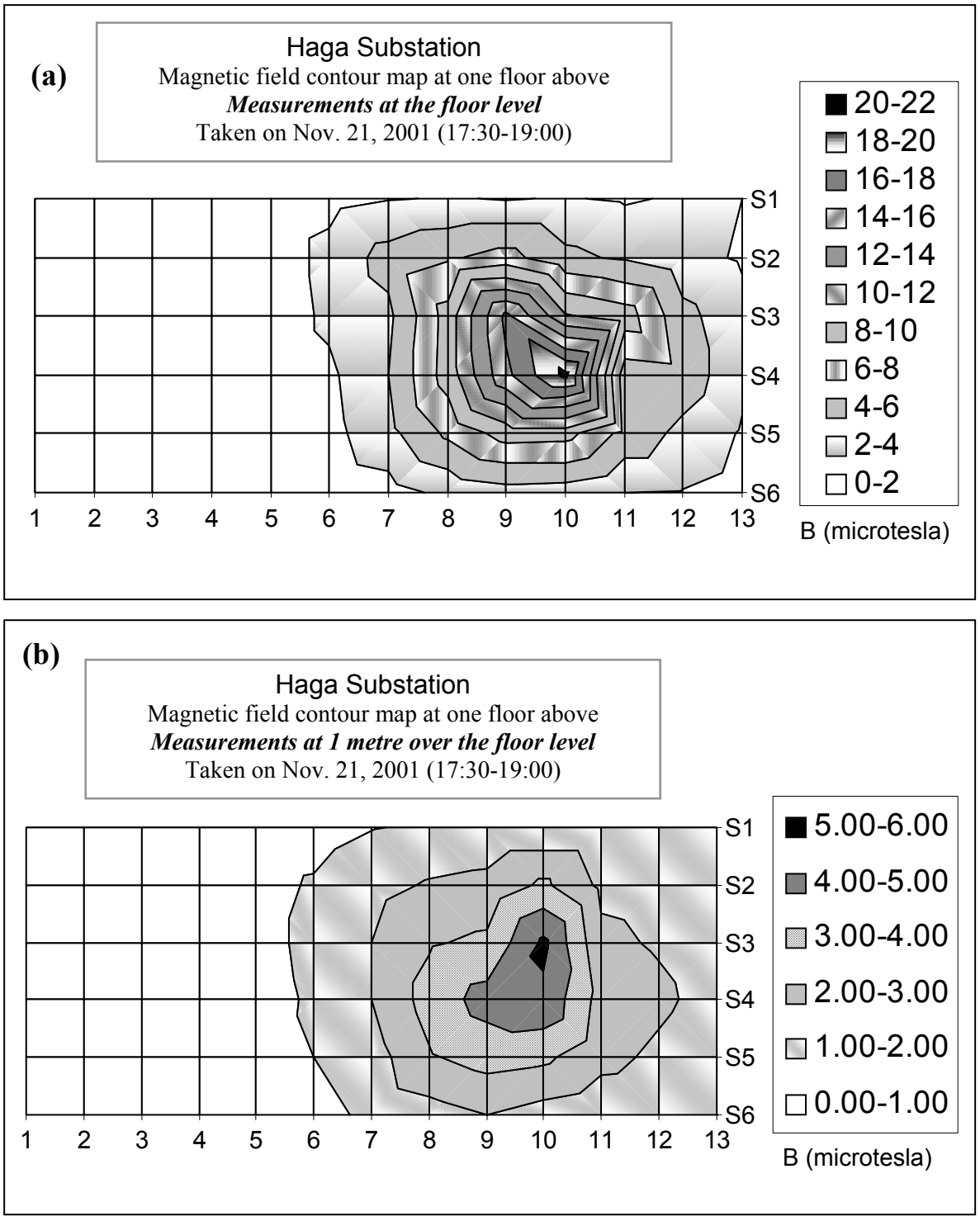

Fig. 11.4 Contour plot of the magnetic field one floor above Haga substation.

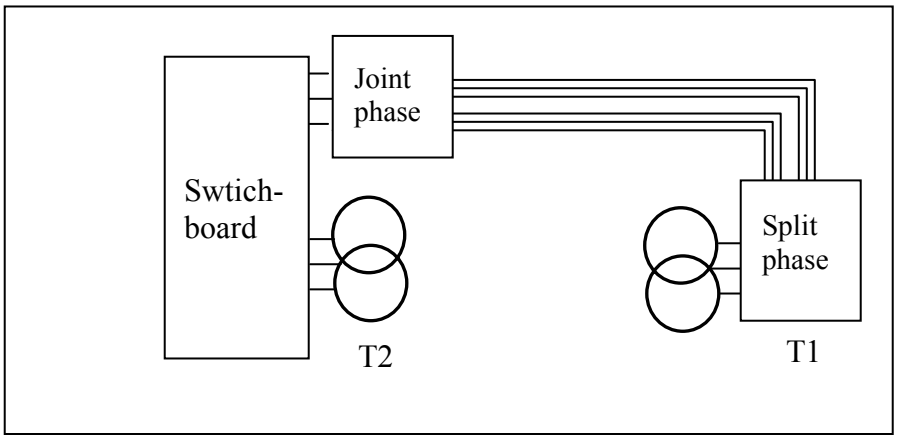

Fig 11. 5 Configuration of Haga substation. T1 has a split-phase/joint operation, while T2 is directly connected to the low voltage switchboard.

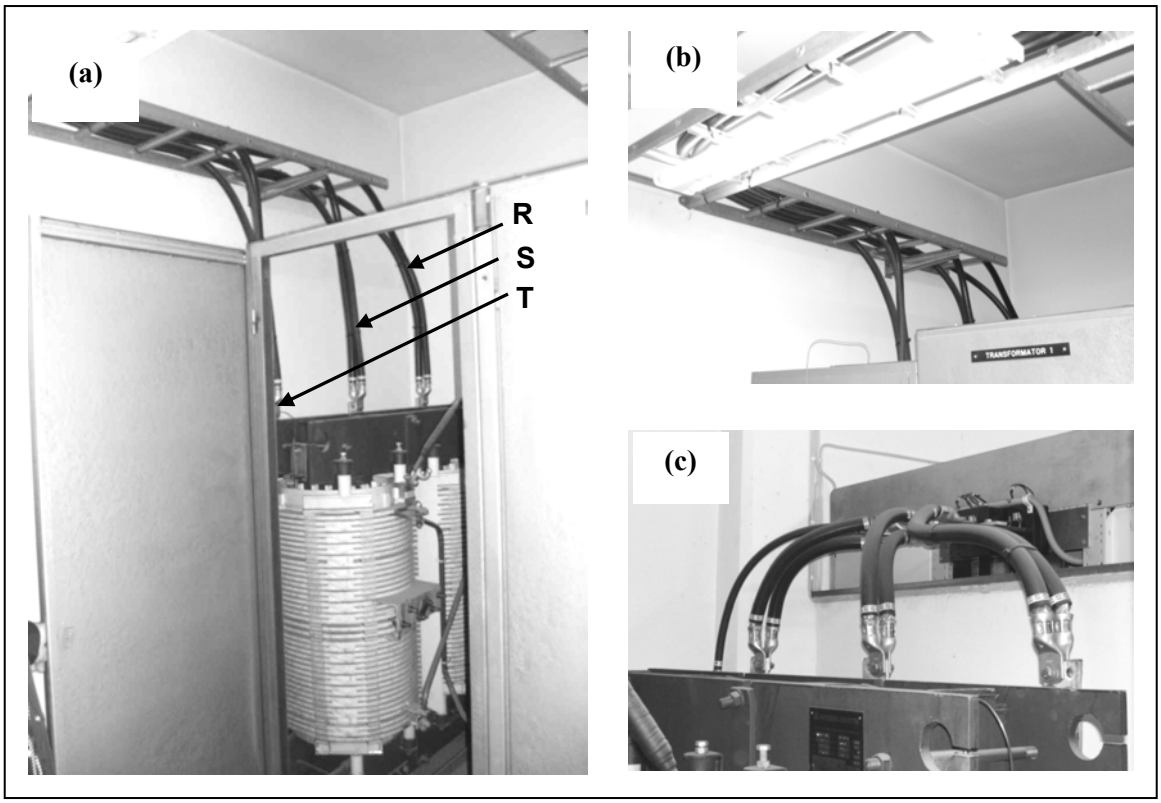

Fig 11.6 Interior of Haga substation. The responsible for the high fields on the floor above the substation is the large separation between phases (a) in transformer T1. The cables from the secondary side of T1 follow an upper trajectory (b) to the low voltage switchboard. The connection of transformer T2 is more suitable for low field emission.

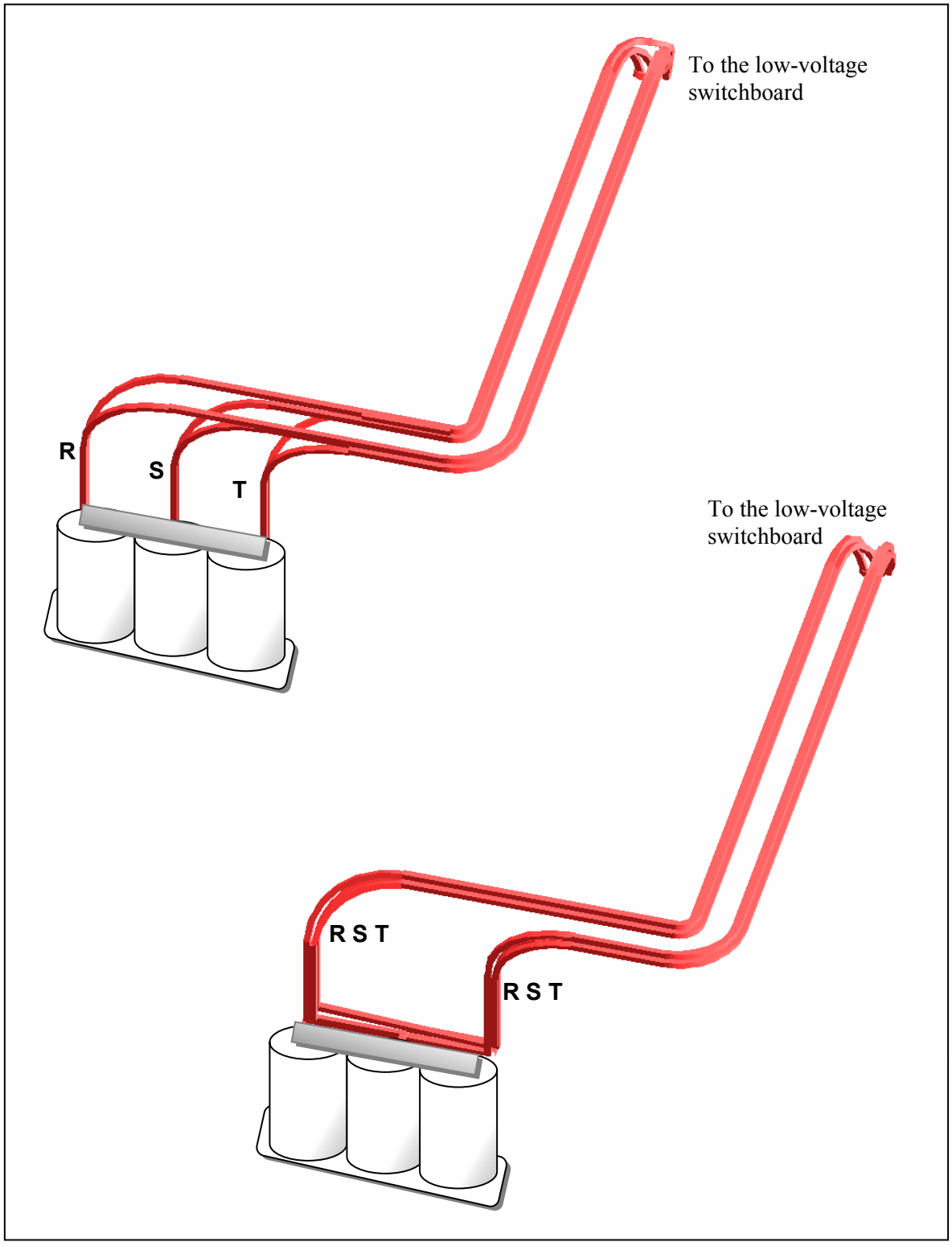

Fig. 11.7 phase split and phase reconfiguration at the connections of transformer T1.

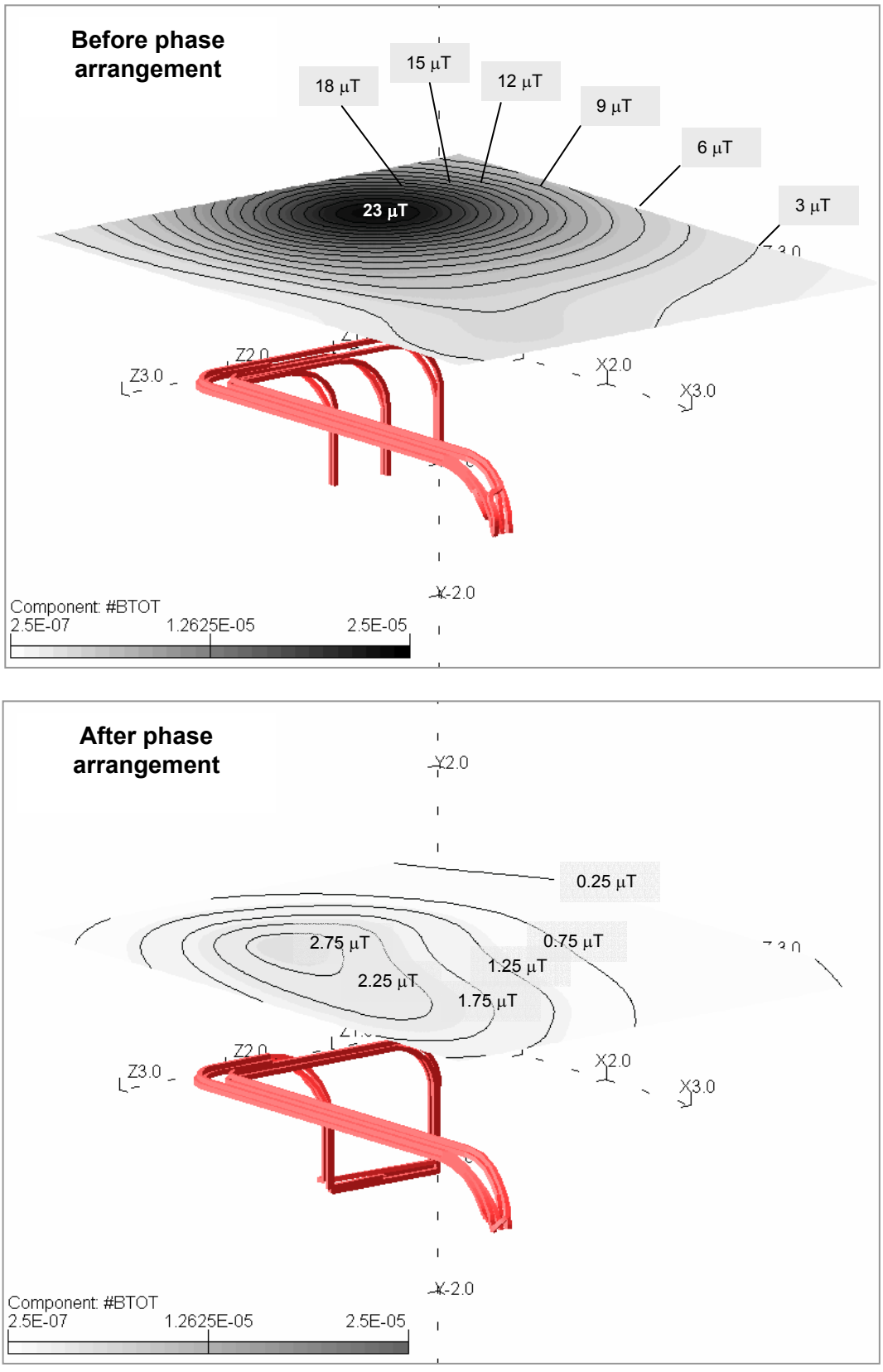

Fig. 11.8 Contour plot at the floor level before and after phase rearrangements.

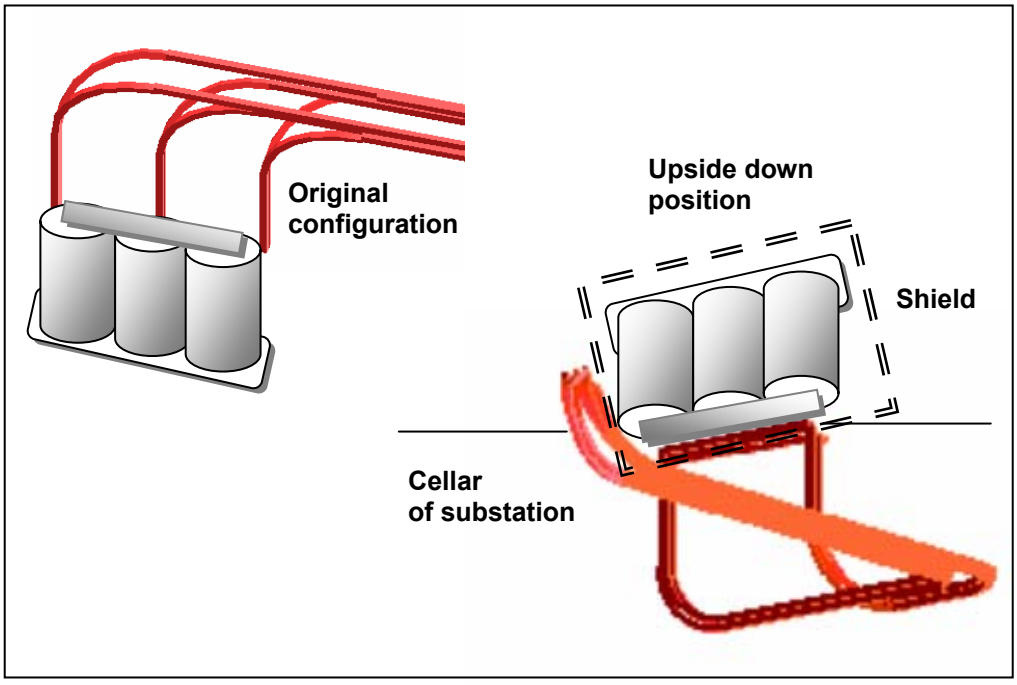

Fig. 11.9 The optimal solution for minimizing the field of Haga substation is: (i) upside down positioning of the transformer, (ii) phase rearrangement, (iii) connections to the low voltage side by the cellar of the substation and (iv) eventual shielding of the transformer.

12 Examples of field mitigation

Some of the techniques developed in this report can be applied to actual cases where the measured values of the magnetic field are considered as problematic. One example was already described in section 11. 2, and a few more are presented in this chapter. These examples also helped to develop mitigation techniques, since the most adequate method was often not known in advance. Sometimes the cases yielded unexpected results, as in the case of stray currents (sections 12.2-12.3).
A course of action frequently used was: (i) measurement of the field, (ii) analysis of the data and modelling, which provided hints for the choice of mitigation techniques, (iii) implementation of the mitigation proposals, and iv) measurement of the field after mitigation. However, sometimes the issue required the application of mitigation schemes before the installations became operative, i.e. already at the design level, to ensure low field emission. In that case, modelling was more relevant.

12.1 Measurement of PFMFs

In order to measure magnetic fields, various devices have been designed. They are known under various names: gaussmeter, magnetic field meter, magnetic field dosimeter, magnetic field logger, and for the particular frequency of interest in this work: power frequency magnetic flux density meter, or simply magnetometer. Most of them are based on the same principle that was used for conductive shielding and passive

compensation i.e. *the induction principle*. The magnetic field generates a voltage signal in a coil with a large number of turns. This signal has to be amplified and electronically processed before it is displayed. The necessary components of these instruments are: detection coils, integration circuits, time-averaging devices, filters and amplifiers (Fig. 12.1). Measured quantities are given in rms (root mean square) values.

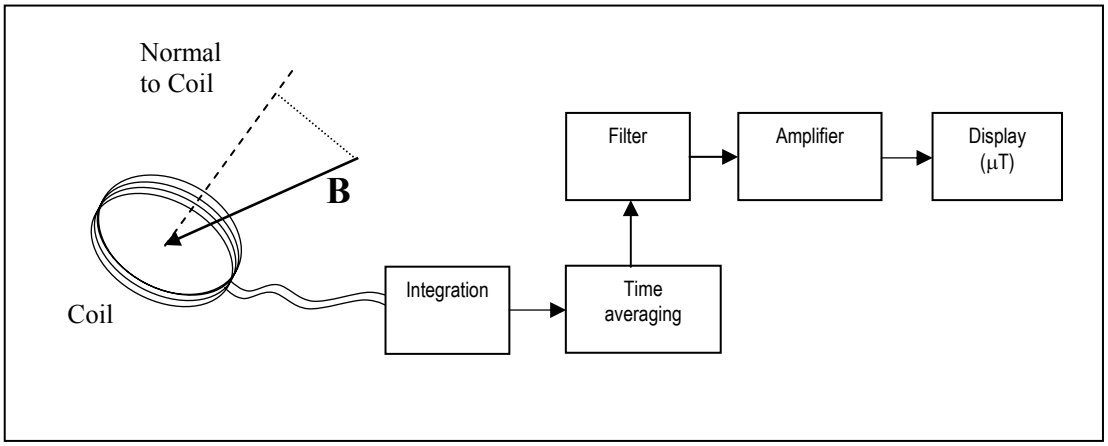

Fig. 12.1 Structure of a typical magnetometer.

There are two kinds of field meters: single-axis magnetometers and three-axis magnetometers. The first one measures the magnitude of the magnetic field along the axis perpendicular to the detection coil. The second contains three perpendicular coils. To measure single-phase fields the first instrument is rather useful since it can even determine the direction of the field. In a three-phase system, the magnetic field is elliptically polarized, therefore quite difficult to determine its rms-value by a single-coil instrument. In that case, the second type of magnetometer is needed. The magnitude of the magnetic field is in this case determined by:

$$B_{rms} = \sqrt{\left(B_{x,rms}\right)^2 + \left(B_{y,rms}\right)^2 + \left(B_{z,rms}\right)^2} \qquad (12.1)$$

The instrument most frequently used in this project is a magnetic field logger[1]. This instrument belongs to the second type and can register the rms-value of the magnitude (but not the direction) of the magnetic field, which can be seen directly on the display. The values are displayed in microtesla. The range of frequencies (bandwidth) this instrument can detect is between 30 Hz and 2000 Hz.

12.2 The fields at the Gothenburg City Library

Here a study is presented of magnetic fields originating from a secondary substation located in the cellar of the Gothenburg City Library (Göteborgs stadsbibliotek). This public library (Fig. 12.2) is located in the centre of Gothenburg and is surrounded by other public and urban buildings. About 190 persons work in this building and around 3,000 visit each day.

The electricity supply to the library and nearby public buildings consists of a secondary 10/0.4 kV substation (two 800 kVA, three phase transformers). The configuration of the components is shown in Fig. 12.3-(a).

[1] EnviroMentor ML-1

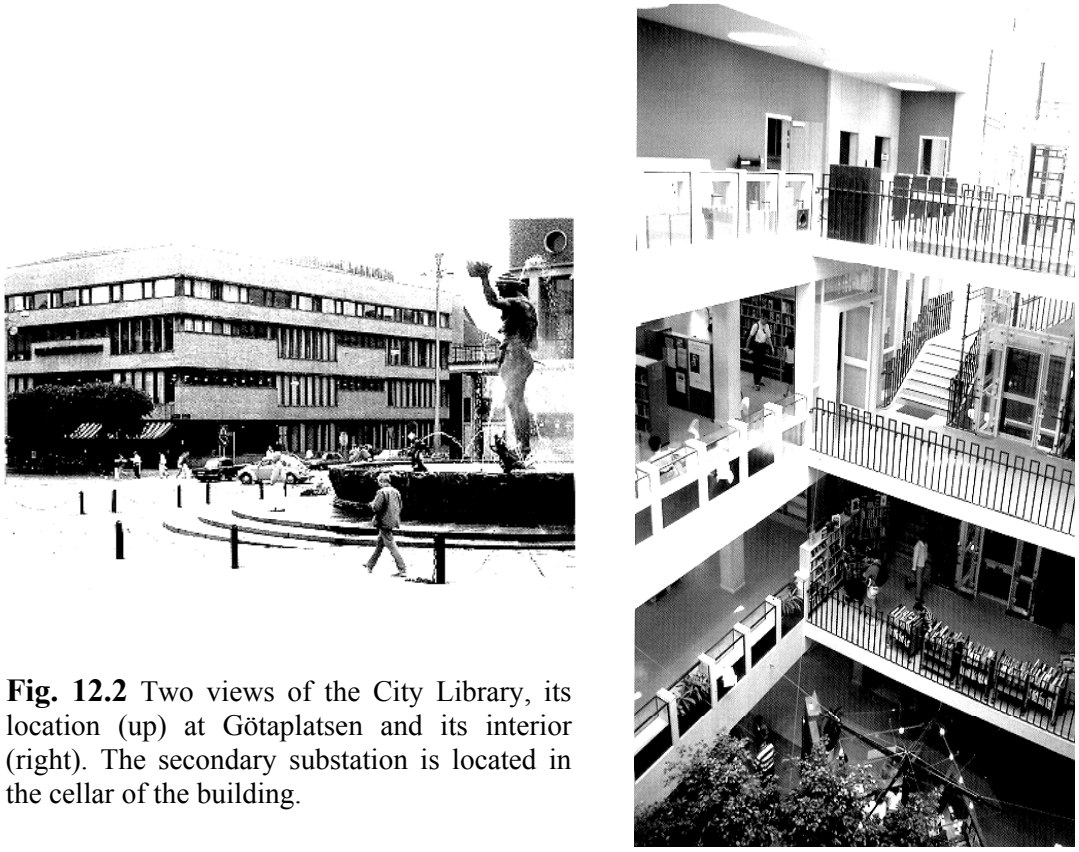

Fig. 12.2 Two views of the City Library, its location (up) at Götaplatsen and its interior (right). The secondary substation is located in the cellar of the building.

Extensive measurements were made [1] of the 50 Hz magnetic field at the floor above the substation. Figure 12.4-(a) shows the distribution of the magnetic field. Field values of around 1-4 microtesla were registered in areas right above the location of the substation. Values up to 6 microtesla were measured in areas under which there were no substation parts. Moreover, the field contour curves corresponding to these values followed a diagonal across the room. Thus the presence of stray currents (see next section) was suspected. Using analytical calculations [1] it was possible to determine the equivalent value (10-15 amperes) and the

location of these currents (0.5-0.75 meters under the floor of the reading room).

Various modifications were proposed, not only by installing new substation components, but also altering their geometrical disposition in the room of the substation, as shown in figure 12.3-(b). The main modifications were:

- Replacement of the unshielded transformers with new low emission transformers with an aluminium cover.
- A shielding of aluminium (5mm-thick plate) welded to the back of the low voltage switchboard. Additionally a 5mm welded aluminium shield lined the ceiling and the back of the low-voltage switchboards of the substation.
- The cable connections between components were positioned under the floor. Prior to the renovation some cables were positioned over the floor, some even close to the ceiling.
- A modern high voltage switchboard with low magnetic field emission characteristics replaced the previous one.

After the modification of the substation a series of measurements were again performed in the same area. The contour plot of these values is shown in figure 12.4-(b). Most of the values registered on the region right above the substation were well under 1 microtesla and had an average value of 0.5 microtesla. It can be noted that there is a peak value (in a very small region) of 1.1 microtesla. Additional measurements of

this value along the vertical distance gave a rapid decay according to $1/(\text{distance})^3$, thus it was suspected that the origin of this maximum was not the substation components but a local source. The source was later found to be the motor of a cooling fan installed at the ceiling of the substation.

In the same figure it can be observed that the values of the field due to stray currents, though still high, have an appreciable different distribution than before the renovation. This is due to the fact that stray currents have a broad variation in time.

The last part consisted in reducing the field due to stray currents. There are two methods to achieve this; one is to install a five conductors system; the other is to install magnetic field reducers. The first solution is very costly and the second option was adopted. The stray current is a problem that is not the domain of the utilities but of the customer. Therefore the field reduction procedures were decided and carried out by the owners of the building. Ferromagnetic cores were installed, which surround the cable forming a booster transformer, thus forcing the net current in the cable to be reduced. The result after installing the reducers is shown in figure 12.4-(c). The average field on the area above the substation has also diminished.

If one takes into account that a former alternative was to relocate the substation, which represented a difficult and costly option, the decision to modify the substation produced significant cost reductions to the utility.

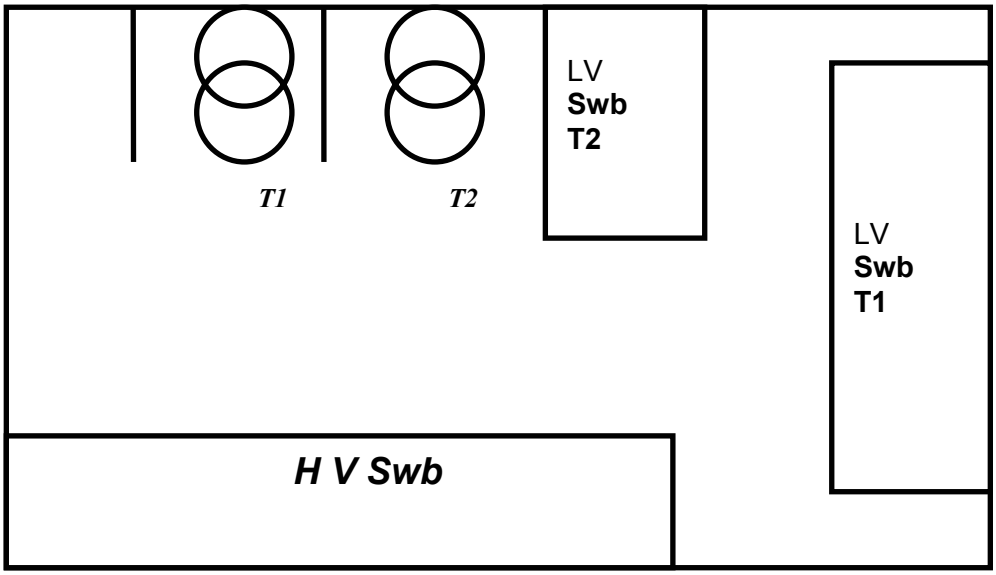

(a) ***Substation before renovation***

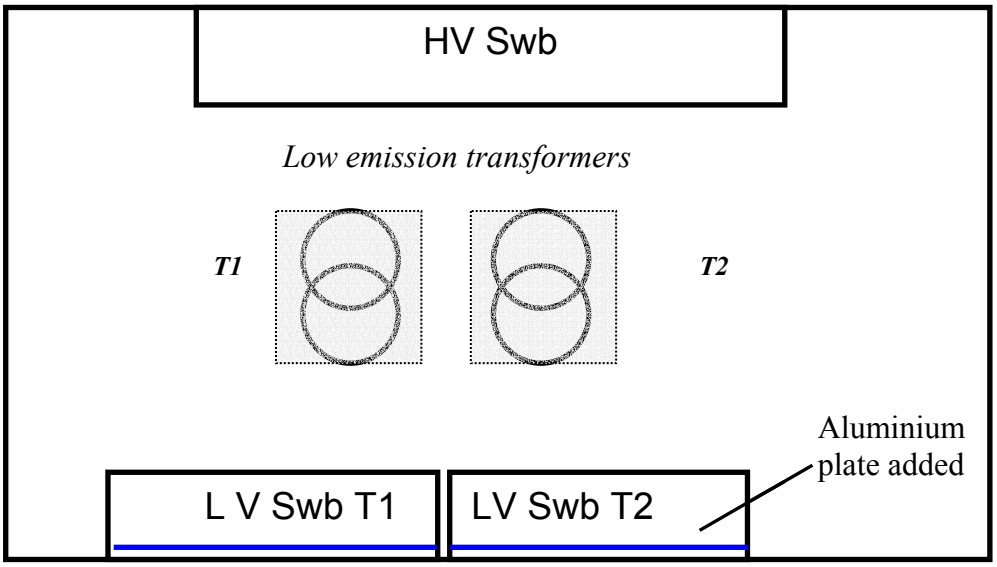

(b) ***Substation after renovation***

Fig. 12.3 Secondary substation located in the cellar of the library. **(a)** Configuration before the renovation: there are two transformers T1 and T2; and high voltage (HV) and low voltage (LV) switchboards (Swb). **(b)** Renovated substation at the cellar of the library. The new transformers are shielded; the cables in and out from the transformers go under the floor level; a 5mm welded aluminium shield lined the ceiling and the back of the low-voltage switchboards of the substation.

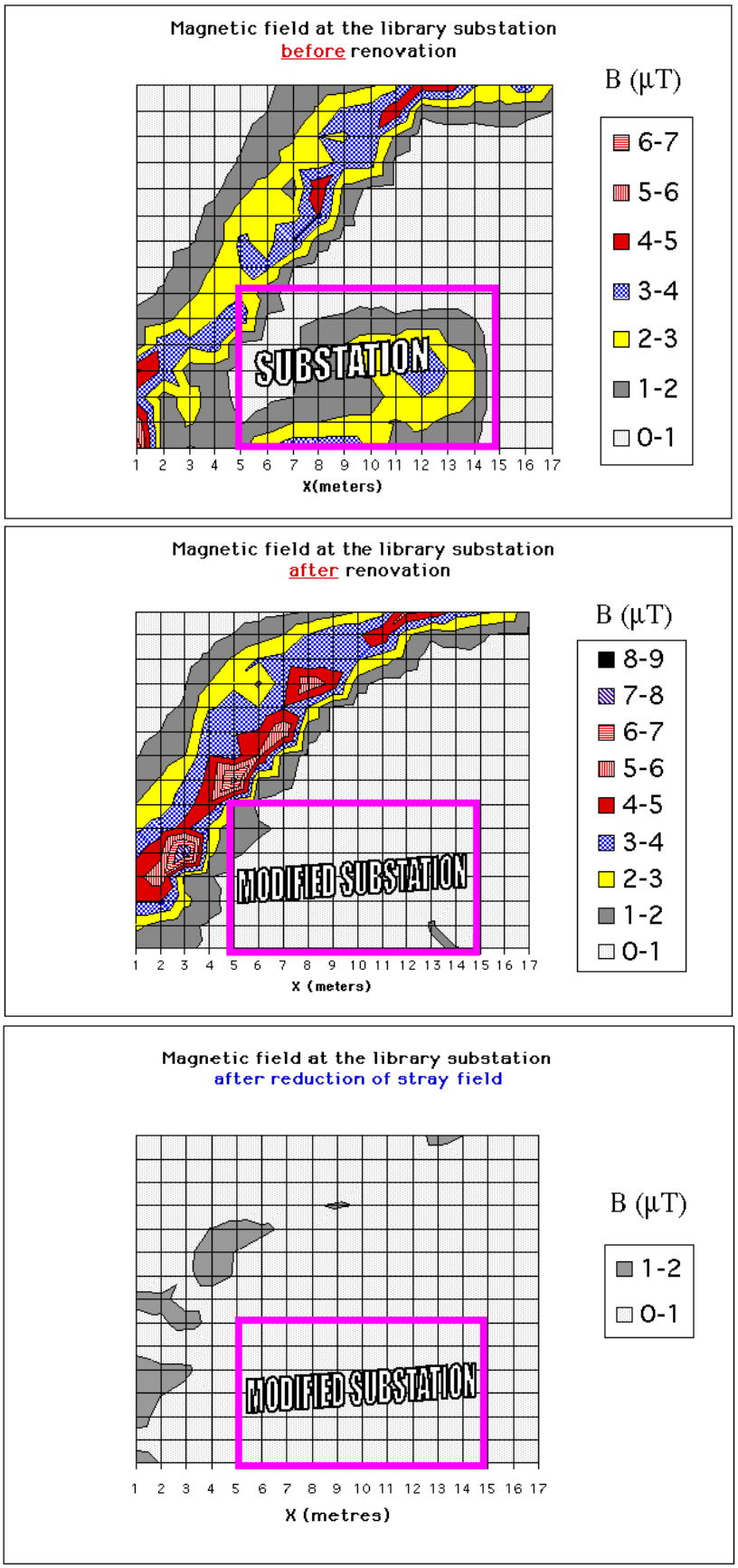

Fig. 12. 4 The magnetic field one floor above the library and its reduction at different stages.

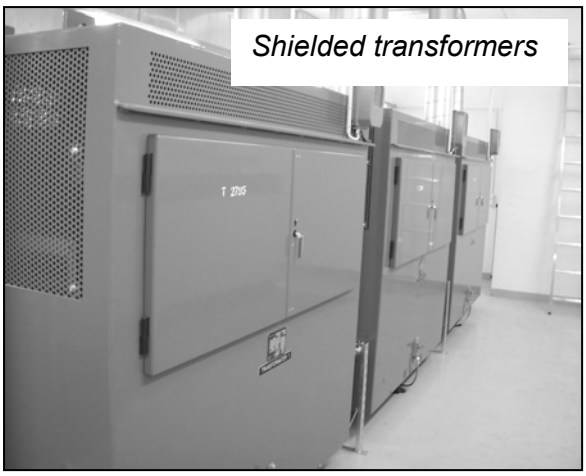

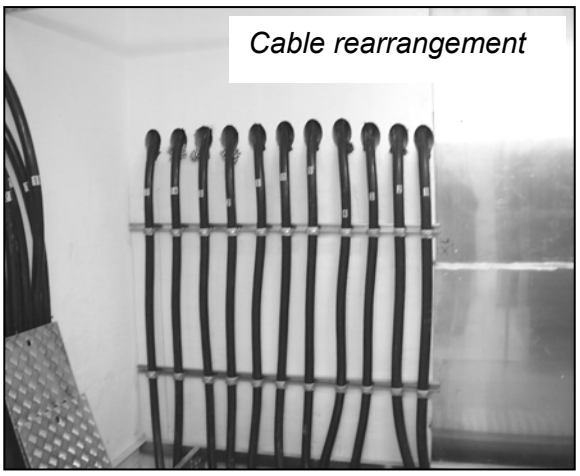

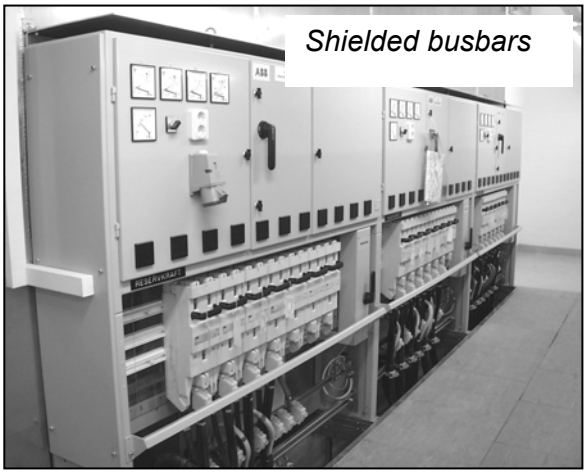

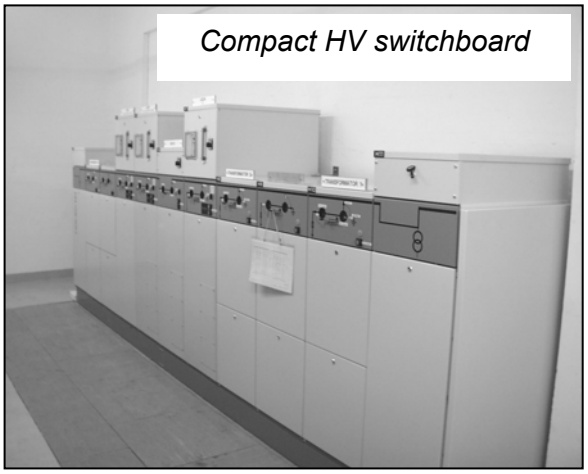

Magnetic field reducers

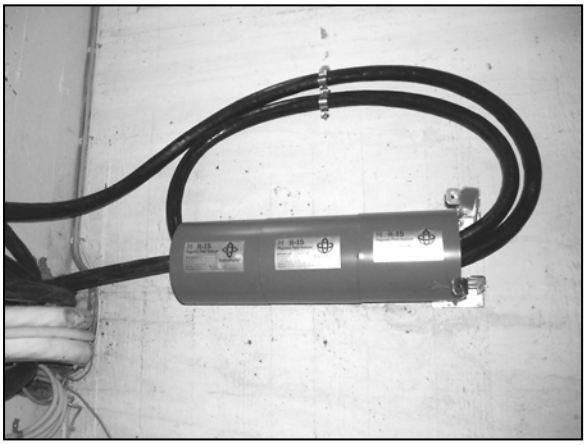

Fig 12. 5 Measures taken to mitigate the field from the substation at the Gothenburgs City Library.

12. 3 Stray currents

The most common type of cable configurations installed in houses and connected to electrical appliances contains two parallel conductors carrying opposite currents. These conductors are close to each other and the total magnetic field, in principle, nearly cancels (a similar statement is valid for a larger number of cables).

Stray currents are one of the most common sources of magnetic fields in Sweden (and other countries that have similar cable connections systems); these are currents that escape from an intended electric circuit and return. Such currents may run along pipes, and spread to neighbouring houses, instead of staying along the neutral conductor, which is intended to carry the current back to the feeding system.

This problem is common in a four-conductor system. Fig. 12.6 shows the principle of stray currents; a simplified diagram of a four-conductor system shows the division of a load current (I) into the return (I_n) and a stray current (I_w) running along metallic water pipes.

An interesting characteristic of stray currents is that they are not possible to mitigate using conductive shielding, since induced currents need a returning path. Neither can they be passive or actively compensated for similar reasons.

A solution to it is to add an extra cable (five-conductor system), which will give the current a direct return path to the ground of the feeding system, without dividing or spreading (Fig. 12.7). Another solution is to use magnetic field reducers (see section 12.2), which are connected along the line carrying stray currents. The former solution is economically

suitable in the initial stages of an electrical installation. The latter is convenient when the problem is detected afterwards.

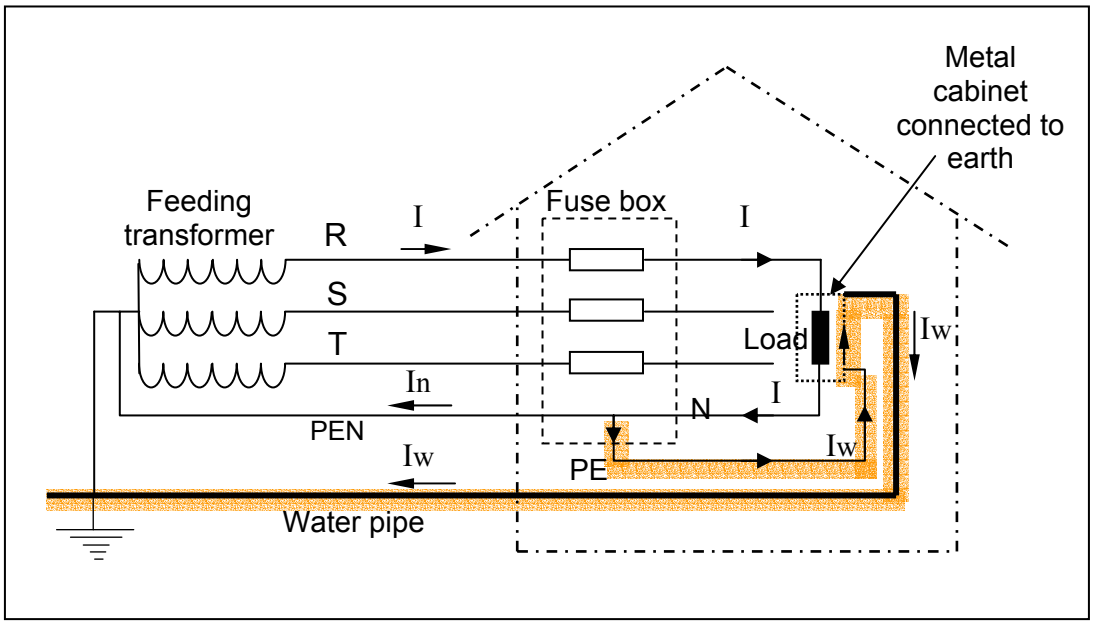

Fig. 12.6 Stray currents in a four-conductor system.

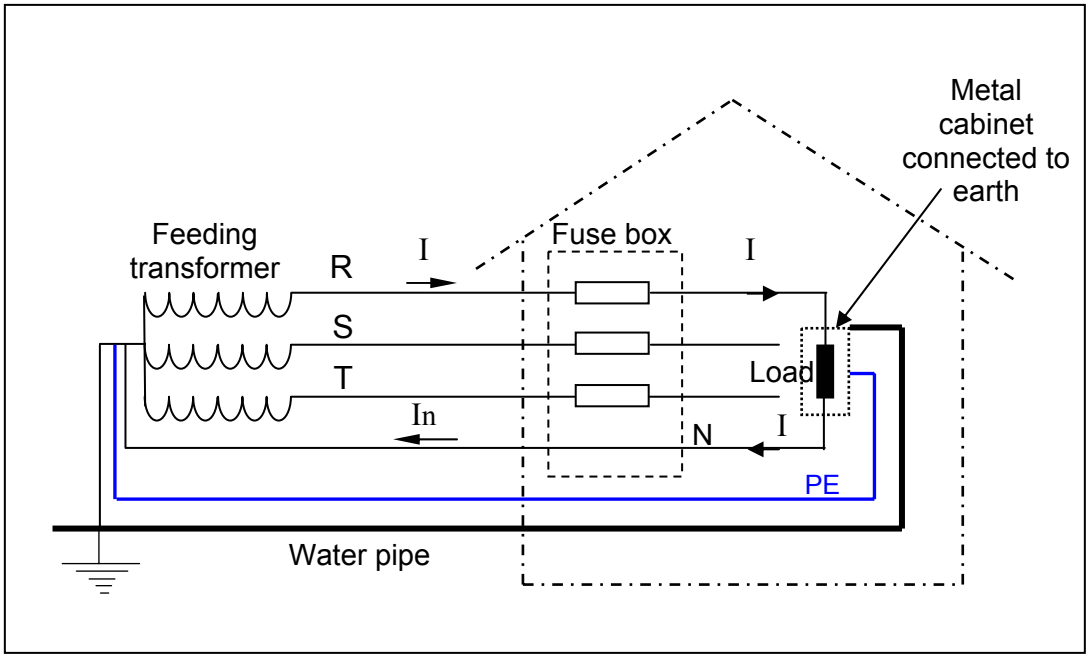

Fig. 12.7 Five-conductor system.

12. 4 Magnetic fields at the renovated Electrical Power Engineering building

Another case in which it was possible to test some of the tools developed for mitigation of PFMFs was the renovation of the Electrical Power Engineering (Institutionen för Elteknik) building at Chalmers. The study and reduction of the fields were executed as the same time as the renovation of the secondary substation took place; thus the project was bounded in time, therefore results were to be obtained in a form readily to be applied. For details see reference [2]

Figure 12.9 shows the distribution of the main components of the substation (10/0.4 kV, 2 x 800 kVA). The magnetic field was measured on the floor above the substation (a conference and IT room was going to be located on that floor), particularly at the level of 3 and 4 meters above the busbar system. A realistic configuration and maximum values of currents were assumed; usually the currents involved are much smaller. The values of the field registered before reduction operations are shown in figure 12.9-(a). In order to study the magnetic field emitted by the substation, analytical calculations and numerical simulations (using the 2D-FEM program ACE) were performed. It was found that a plate of aluminium a few millimetres thick was enough to bring down magnetic field values to levels recommended by the Swedish building board [3]. An aluminium plate (3 mm thick, 13 m wide and 2 m high) was welded to the back of the switchboard. The measured values after the reduction of the magnetic field are shown in figure 12.9-(b). At the present time the values at the studied areas are below the recommended levels, even under high load conditions.

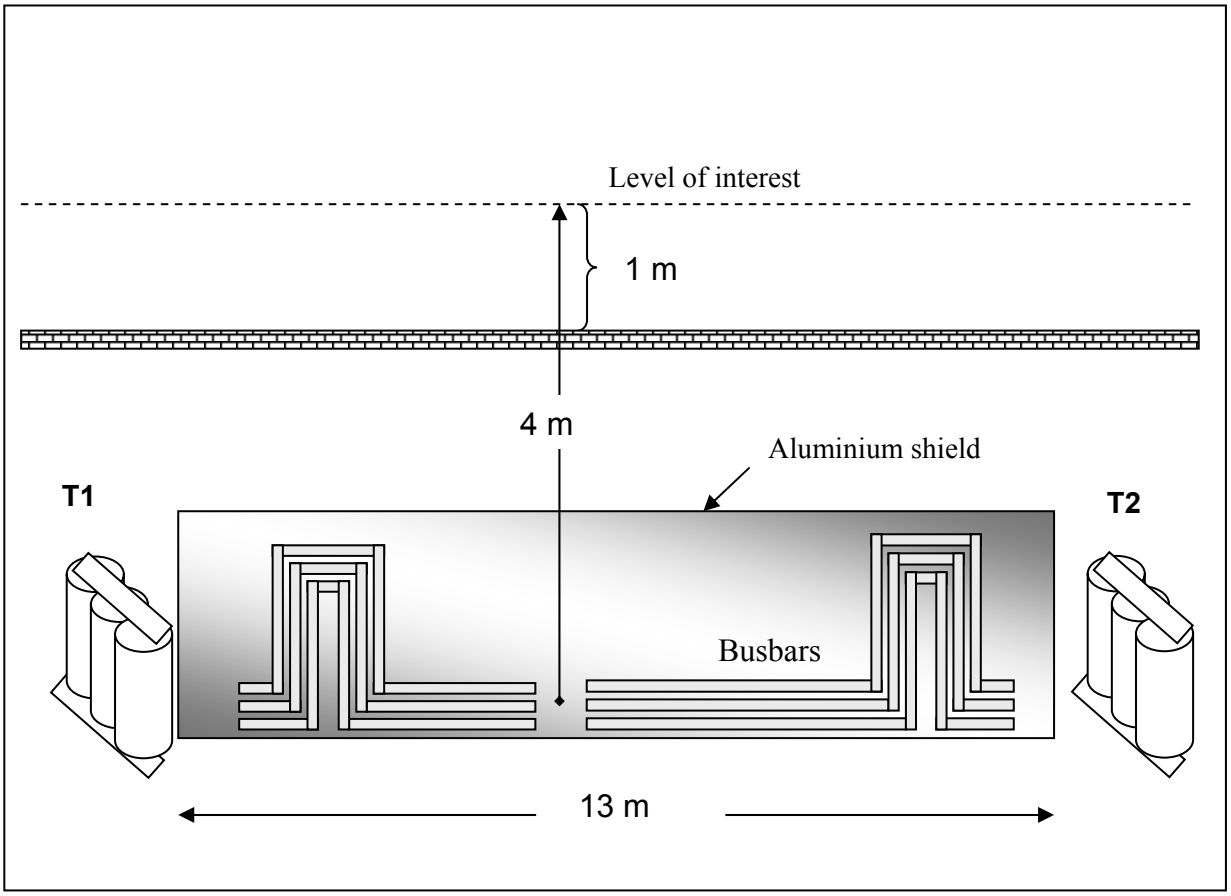

Fig. 12.8 Representation (not in scale) of some of the major components of the substation at Elteknik. The busbars are inside a switchboard made of steel. Only one of the transformers is connected at the time. The Aluminium shield is 3mm thick, 13m wide and 2m high.

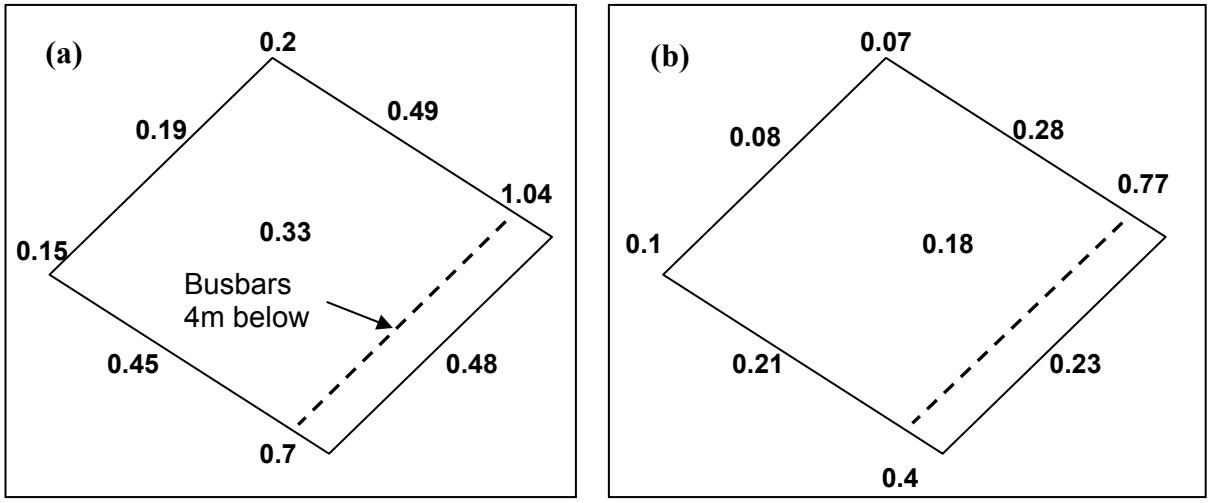

Fig. 12. 9 Magnetic field values before (a) and after (b) the field reduction operation. The values were taken at the plane located 4m above the busbar configuration.

12.5 Shielding of underground cables

Shielding of PFMFs from power lines by using metal plates is difficult because of the lack of support for metal settings. In the case of underground cables, the shielding option exists, as the soil provides a natural support for arrangements of metal plates.

Here, the case of a three-phase 130 kV system of underground cables is analysed (Fig 12.10). The system consists of 200 m long cables located at 1 m under the ground. They carry a nominal current of 200A/phase, having each cable a cross section with outer diameter of 83 mm, and inner conductor diameter of 26.4 mm.

The cables are placed in a triangular configuration. It can be assumed that the ground has $\mu = 1$, $\sigma = 0$ and does not have any relevance in the field computations. It does, however, define the area of interest 10m x 2m, and sets economical restrictions to the choice of mitigation method, as digging and installation costs are involved.

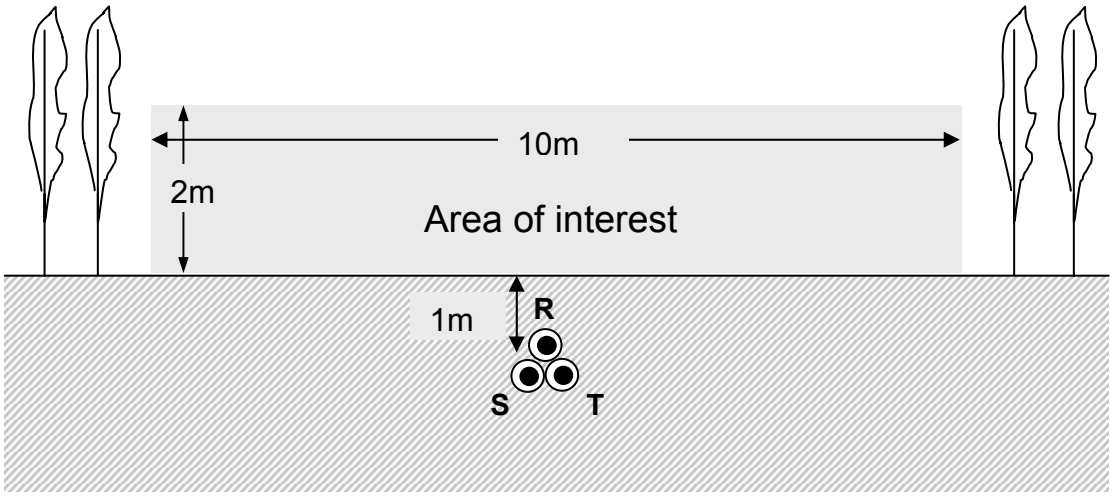

Fig. 12.10 Three-phase underground cables below an area of interest. e.g. a children's playground.

Four different configurations were modelled in two dimensions using Opera and compared with the initial field (no-shield) case. In all cases the length of the shields (or compensating cables) were as long as the cable length.

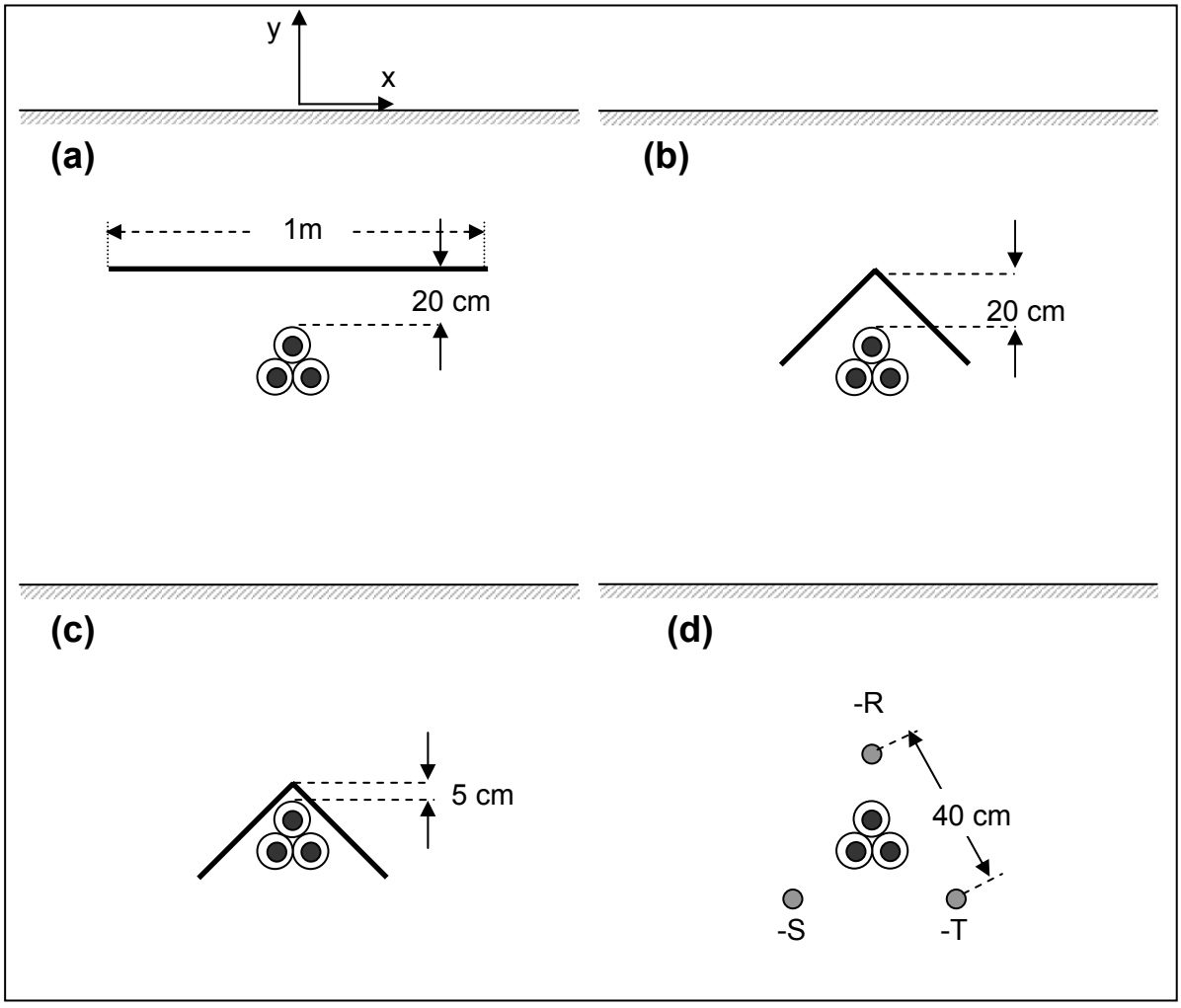

Fig. 12. 11 Different shielding configurations for the magnetic field of underground cables (a) 1 m plate, (b) - (c) continuous wedge 90 cm wide and bent 90°. Active compensation was also considered (d).

Case (a): A flat metal plate, 1 metre wide and 5 mm thick, is located d = 20 cm above the cables.

Case (b) - (c): A wedge-shaped metal plate, 90 cm wide, 5 mm thick and 90° bent, is located at (b) d = 20 cm, and (c) d = 5 cm respectively, above the cables.

Case (d): Active compensation by a three-phase system of cables, forming an external triangle of 40 cm per side and carrying a current I = 46 A per phase. (Fig. 12.11-c) The phases on the external triangle are opposite (-R, -S, -T) to the ones in the interior triangle.

In the cases of shielding with metal plates, the following materials were used:

Table 12.1 Materials

Material	Conductivity, Sm^{-1}	Relative permeability (μ_r)
Aluminium	3.77×10^7	1
Iron	1.03×10^7	250, 500, 1000, 1500, 2000

Fig 12.12 shows an example of a FEM simulation in Opera. The complexity of the field around a shielding configuration is evident.

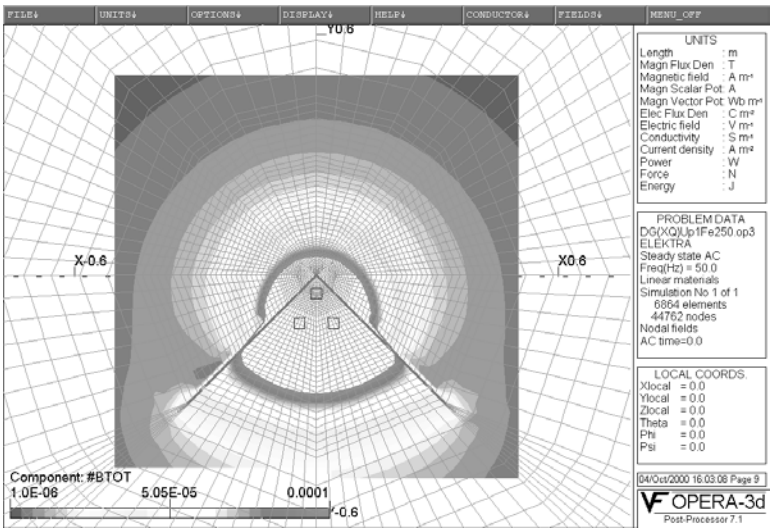

Fig. 12.12. Field around a shielding configuration, wedge-shaped iron plate, $\mu_r = 250$, d = 5 cm.

The simulations for the cases of shielding and compensation give, for different vertical distances, the following magnetic field values:

Table 12.2 Case a: Flat shield (d = 20 cm)

	B (microtesla)		
	y = 1m	y = 2m	y = 3m
No shield (B_0)	*4.06 μT*	*1.02 μT*	*0.455 μT*
Al	*2.43 μT*	*0.69 μT*	*0.312 μT*
Fe 250	*2.36 μT*	*0.65 μT*	*0.296 μT*
Fe 500	*2.35 μT*	*0.65 μT*	*0.294 μT*
Fe 1000	*2.29 μT*	*0.66 μT*	*0.287 μT*
Fe 1500	*2.26 μT*	*0.63 μT*	*0.284 μT*
Fe 2000	*2.24 μT*	*0.62 μT*	*0.282 μT*

Table 12.3 Case b: Wedge shield (d = 20 cm)

	B (microtesla)		
	y = 1m	*y = 2m*	*y = 3m*
No shield (B_0)	*4.06 μT*	*1.02 μT*	*0.455 μT*
Al	*1.85 μT*	*0.49 μT*	*0.210 μT*
Fe 250	*2.03 μT*	*0.52 μT*	*0.233 μT*
Fe 500	*2.05 μT*	*0.52 μT*	*0.235 μT*
Fe 1000	*2.01 μT*	*0.51 μT*	*0.229 μT*
Fe 1500	*1.98 μT*	*0.50 μT*	*0.225 μT*
Wedge-Fe 2000	*1.95 μT*	*0.49 μT*	*0.222 μT*

Table 12.4 Case c: Wedge shield (d = 5 cm)

	B (microtesla)		
	y =1m	y = 2m	y = 3m
No shield (B_0)	*4.06 μT*	*1.02 μT*	*0.455 μT*
Al	*1.19 μT*	*0.30 μT*	*0.141 μT*
Fe 250	*1.94 μT*	*0.56 μT*	*0.335 μT*
Fe 2000	*2.23 μT*	*0.63 μT*	*0.285 μT*

Table 12.5 Case d: Active compensation, Extras: Double-layer shielding

	B (microtesla)		
	y = 1m	y = 2m	y = 3m
No shield (B_0)	*4.06 μT*	*1.02 μT*	*0.455 μT*
Active compensation	*0.78μT*	*0.13μT*	*0.05μT*
Wedge Al (d = 10 cm)	*1.2 μT*	*0.36 μT*	*0.170 μT*
Wedge (d=10cm)-Double-Fe-Al	*1.8 μT*	*0.47 μT*	*0.216 μT*

Evaluation of the shielding efficiency yields the following results (for the different methods according to the best mitigation factors obtained in each case)

Table 12.6 Average shielding efficiency

	METHOD			
	Flat shield (d=20cm)	Wedge shield (d =20cm)	Wedge shield (d = 5cm)	Active Compensation
Average Shielding Efficiency (SE)	*4.6 dB*	*6.3 dB*	*10.5 dB*	*17.5 dB*

Consequently, the mitigation method that gives maximum field attenuation -for this particular case of underground cables- is active compensation. Fig. 12.13 shows the global mitigation effect of the compensating cables.

Maximum filed attenuation not necessarily means a cost-effective method. Cost-efficiency should additionally take into consideration:

i) Cost of energy supply on the compensation cables.

ii) Maintenance cost.

Remark: It is interesting to notice that, as in section 6.1, the mitigation factors for active compensation evaluated from table 12.5 give an increase of the shielding efficiency (SE) with the distance:

SE (1m) = 14.3 db, SE (2m) = 17.9 dB, SE (3m) = 19. 5 dB.

Is this a general characteristic of efficient mitigation techniques? Certainly it deserves more study. This behaviour is not necessarily present in other -less efficient- methods (e.g. shielding with Al and Fe [mu=2000] in case a, table 12.2).

Another remark is that, at the design stage, i.e. before starting cable installation, the possibility of applying phase-split may be considered (e.g. section 6,

Fig 6.4). This method is cost effective only when is performed at the initial stages.

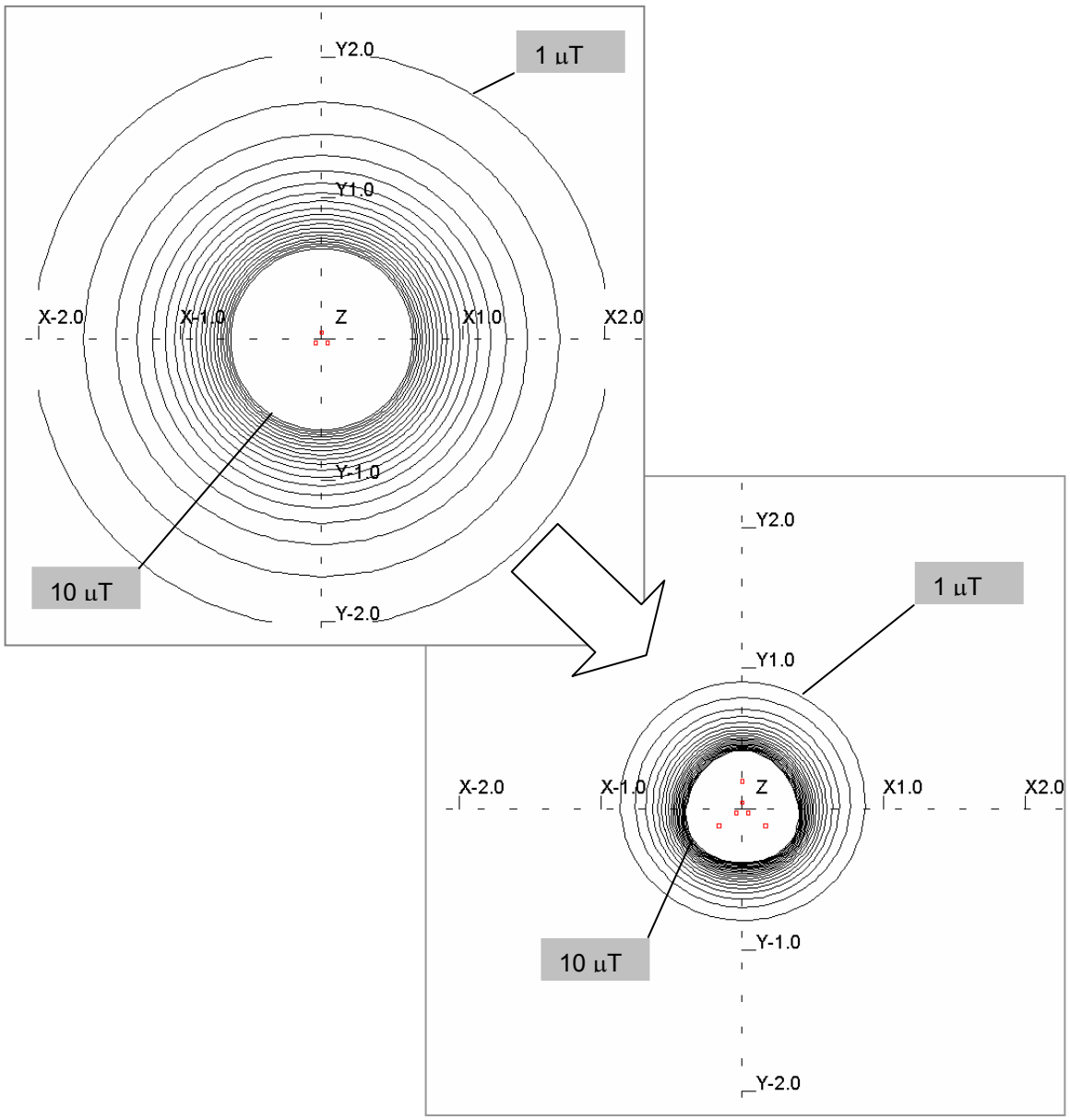

Fig. 12.13 Mitigation by active compensation.

12.6 Mitigation from electrical service rooms

Distribution panels and other electrical installations in small rooms are complementary to substations. It is not unusual to find them in different floors of buildings. Sometimes they can emit high values of PFMFs since they contain small busbars and several conductors.

Here, the shielding of an electrical room with dimensions of a rectangular box, 3.5 m x 2.0 m per side, was modelled in two dimensions using opera. A semi-open shield was used (Fig. 12.14).

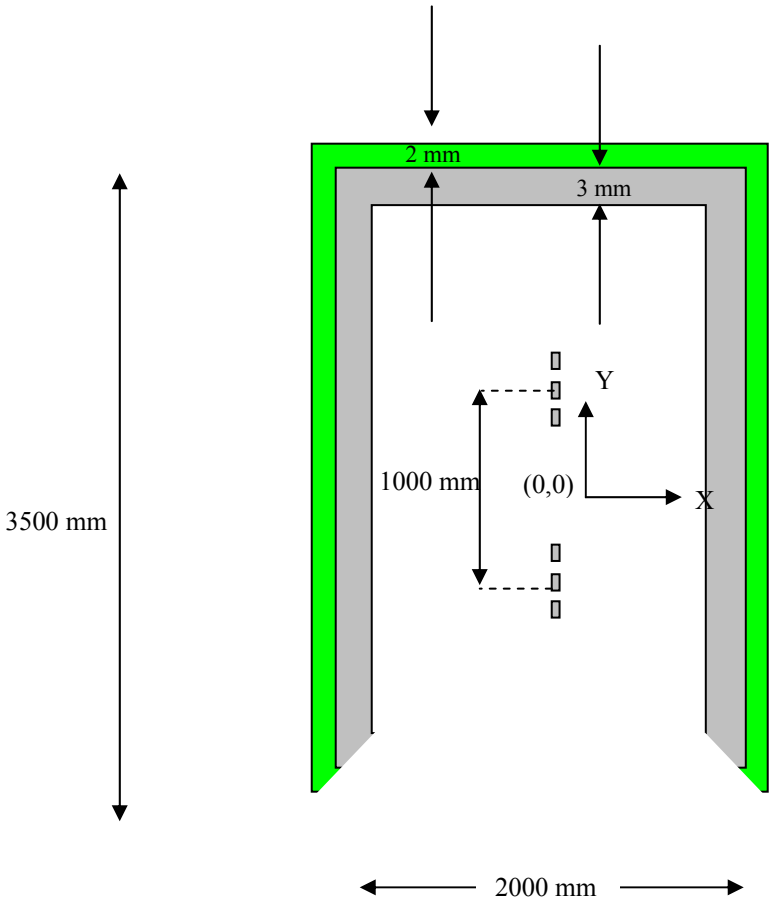

Fig. 12.14 Shielding of a small electric service room using a semi-open shield.

Test source:

The sources were: two sets 3-phase busbars; cross section: 4 mm x 2 mm; separation between busbars: 10 cm.

Current I = 100 A (rms).

Materials tested:

- Aluminium: conductivity = 3.77 x 10^7 S/m, relative permeability = 1
- Transformer steel (96% Fe + 4% Si): conductivity = 0.18 x 10^7 S/m, average linear relative permeability = 1000.

Results:

Fig. 12.15 and 12.16 show the FEM meshing and the field from the sources in the absence of a shield.

Fig. 12.17 shows the field (in the range: 0.05 < B < 2 microtesla) using a shield of iron, 5 mm thick.

Fig. 12.18 shows the field (in the range: 0.05 < B < 2 microtesla) using a shield of aluminium, 5 mm thick.

Fig. 12.19 shows the comparison of the field in an interesting region, between y =3m and y =5 m.

Conclusions

A semi-closed shield made of 5 mm aluminium yielded the best field attenuation (over 20 dB). However a cover of 3 mm is suggested as a possible cost-effective solution (Fig 12.19).

Cost-effective solutions choosing closed, or semi-closed shields covering the walls and ceiling of a room are feasible only for small rooms, for larger ones it is advisable to consider shielding of the sources.

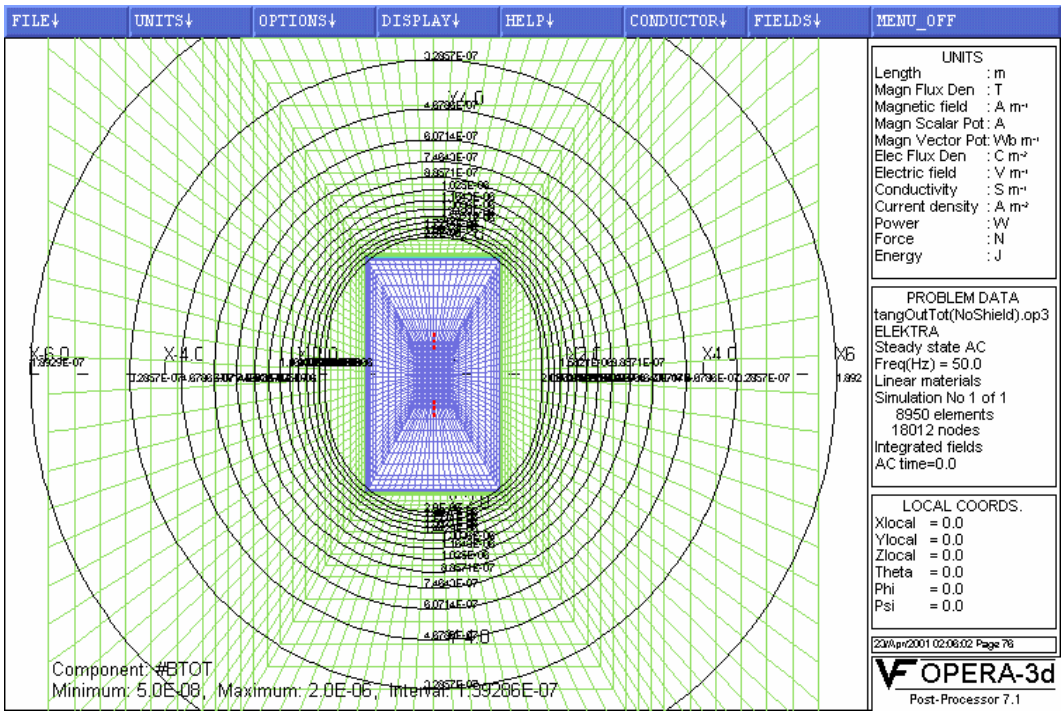

Fig. 12.15 Fields originating in an electrical service room. Range: 0.05 μT < B < 2μT.

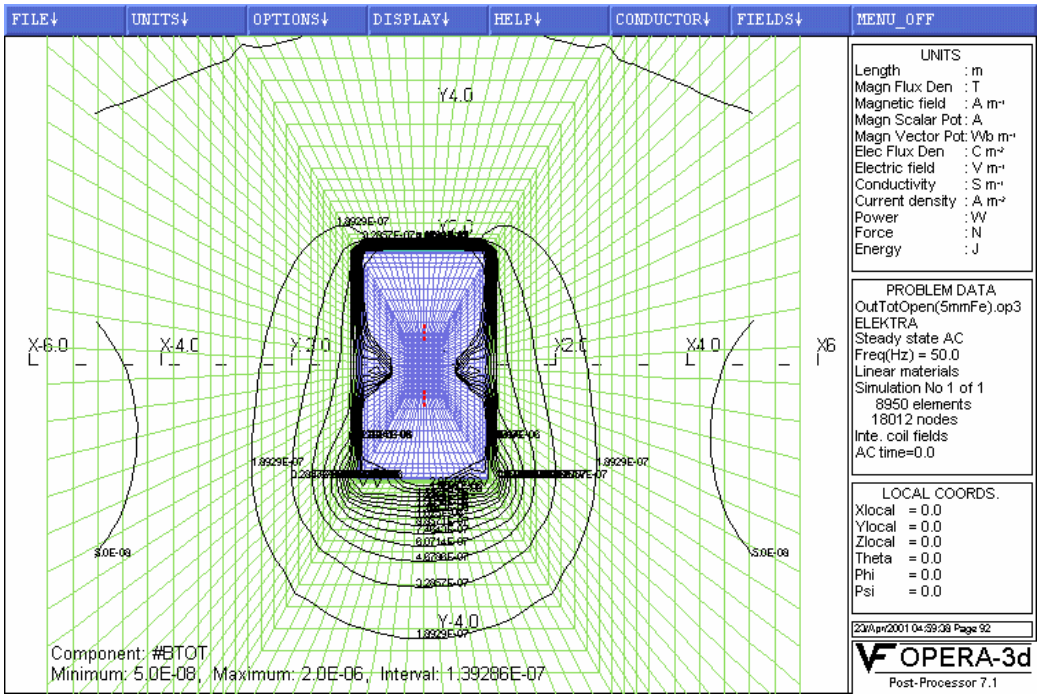

Fig. 12.16 Shielding with a semi-close shield made of 5 mm iron. Range: 0.05 μT < B < 2μT.

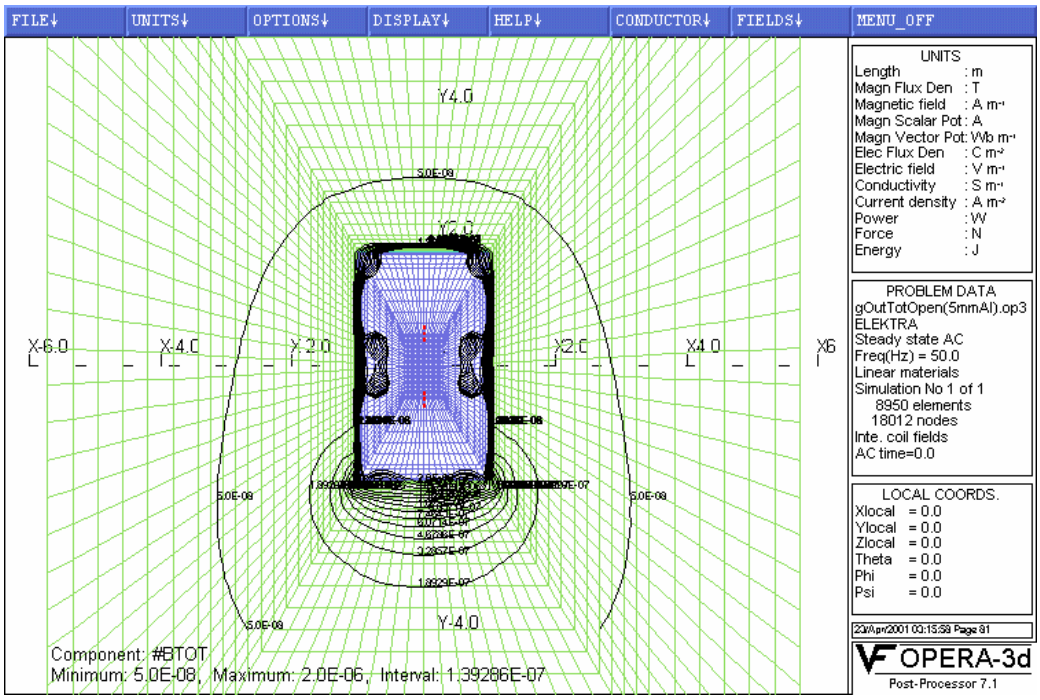

Fig. 12.17 Shielding with 5 mm aluminium semi-closed shield. Range: 0.05 μT < B < 2μT.

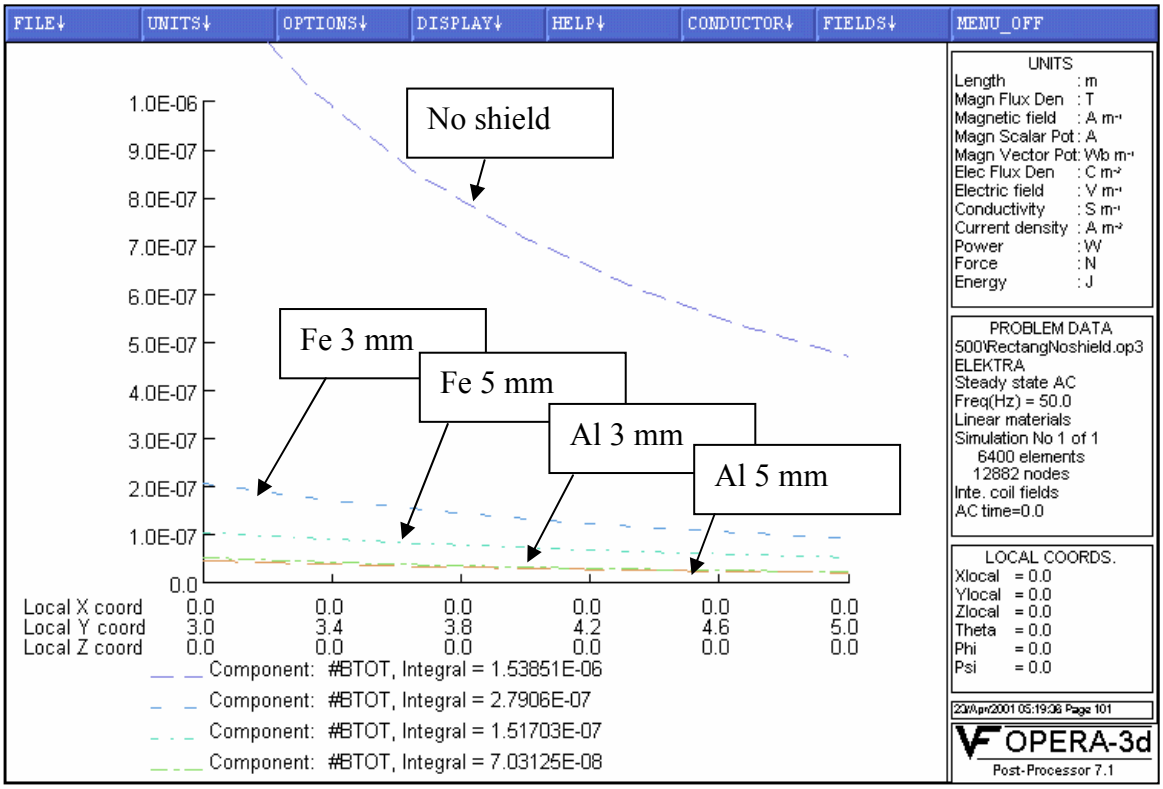

Fig. 12.18 Comparison between different shields for a vertical distance: 3m < y < 5m.

12.7 Summary of Mitigation methods

Table 12.7 shows several methods that were applied or discussed in this work. The study of these strategies by application to actual cases may bring improvements to our knowledge on mitigation of PFMFs.

Table 12.7

Source	Field mitigation strategy	Design method
Busbars, long (> 5m)	• *Shielding* • *Active compensation*	• 2D-FEM • Analytical
Busbars, short (< 5m)	• *Shielding* • *Active compensation* • *Compact design*	• 3D-FEM • Experimental
3-phase transformers	• *Shielding* • *Placing connections by the lower side*	• Experimental • 3D-FEM
Cables, connections	• *Phase rearrangement* • *Relocation of cable paths.*	• Analytical
High voltage transmission lines (aerial)	• *Phase-split* • *Active compensation* • *Passive compensation*	• Analytical • Experimental
Underground cables	• *Shielding,* • *Active compensation* • *Phase-split*	• 2D-FEM • Analytical
Small Electrical service rooms	• *Semi-closed shields* • *Shielding of components*	• 2D/3D-FEM

References

[1] E. Salinas, L. Aspemyr, J. Daalder, Y. Hamnerius, and J. Luomi, "Power Frequency Magnetic Fields from In-house Secondary Substations", CIRED'99, 15th Conference on Electricity Distribution, Technical Reports, session 2, pp. 161-164. University of Liège, Belgium, June 1999.

[2] E. Salinas and L. Aspemyr, *Measurements and Reduction of 50 Hz Magnetic Fields from the New Substation at the Department of Electric Power Engineering.* Technical Report No. 14R, ISSN: 1401-6176, Department of Electric Power engineering, Chalmers University of Technology, Gothenburg, 1999.

[3] The Swedish: National Board of Occupational Safety and Health, National Board of Housing, Building and Planning, National Electrical Safety Board, National Board of Health and Welfare, Radiation Protection Institute, Low-Frequency Electrical and Magnetic Fields: *The Precautionary Principle for National Authorities*, Solna, Sweden, 1996.

13 Extensions of this work

As in any other study not all the possibilities have been exhausted here. There are indeed interesting issues regarding mitigation techniques that can still be explored.

The variation of mitigation schemes as a function of the frequency involves suggestive topics to investigate. An example is shown in Fig 13. 1 for the case of busbars analysed in section 9.4 where the shielding efficiency improves with the increase in frequency.

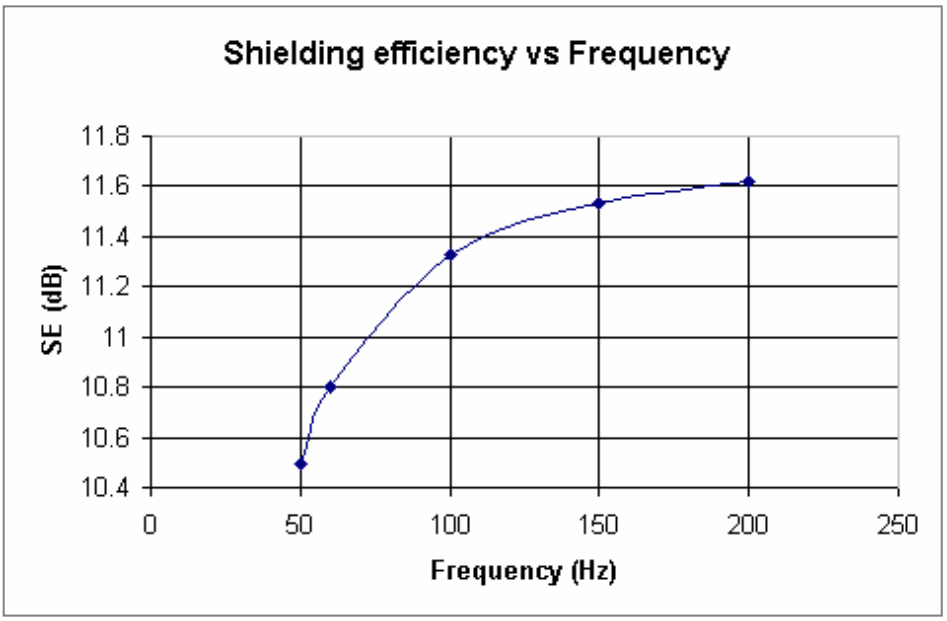

Fig. 13.1 Shielding efficiency improves with the increase in frequency, for the busbar system analysed in section 9.4.

In power electronic equipment, it is common to use non-linear devices. These devices produce non-sinusoidal currents, consequently non-sinusoidal magnetic fields. These fields can be analysed as a

superposition of the fundamental frequency (50 Hz) and their *harmonics.* Usually, but not always, the most relevant harmonics in a power system are the 3rd (150 Hz), the 5th (250 Hz) and the 7th (350 Hz). A distinctive problem caused by harmonic distortion are the high currents that may appear in the neutral conductor. As in the case of stray currents (section 12.3), a current in the neutral conductor is difficult to mitigate. Consequently, a systematic study of the effects of harmonics on the mitigation schemes is needed.

More experimentation is also needed. On the one hand, precise testing of some of the mitigation techniques can verify some of the results of this study. Small-scale experimentation can clearly save costs and time. Thus transformations of the parameters involved in mitigation schemes –in order to obtain scale-invariant results– need to be developed. On the other hand, more case studies are also needed in order to apply and improve the strategies developed in this study.

Active and passive compensation need further studies and improvements. Even though this study aimed at the search for simple and cost-effective solutions for mitigating PFMFs, combination of techniques such as active compensation and shielding may represent improved solutions for mitigation.

Some of the modeling methods used here can certainly be extrapolated to deal with problems in some other areas of engineering or science in which modeling of electromagnetic fields represents a valuable tool.

14 Conclusions

This thesis has investigated various schemes to mitigate power-frequency magnetic fields. It has focused on secondary substations, which represent the end points of the electrical distribution network and are located in the surroundings of residential buildings and highly populated areas. For this reason the magnetic fields emitted by these installations should be considered as important as the –much debated– fields from power lines. Electromagnetic compatibility and the increasing concern for health related issues were the motivations for the initiation of this project.

The transformer is the heart of a substation (and cables and busbars are its arteries and veins!). Therefore one may think that the magnetic field of the transformer represents a major contribution to the total field of a substation. This study, however, has shown that busbars and the ill self-cancelling fields of connections at the low voltage part of the substation are frequently the main contributors. Moreover, the field in the surroundings of a substation can have other origins such as stray currents. This type of source produces a field that decays slowly with the distance. In fact, this problem is rather common in Sweden due to its 4-conductor system.

This thesis showed that it is possible to achieve cost-effective mitigation of PFMFs down to sub-microtesla levels. Cables can be optimally

grouped and positioned in order to give maximum field cancellation. Stray fields from coils and the iron core of a dry transformer can be reduced by an aluminium box. The field of busbars can be shielded by a thin aluminium plate, symmetrically located and at a short distance.

These techniques are simple and not very costly to implement in comparison to the shielding of extensive areas. The methods developed were applied to study cases as strategies rather than a precise medium for testing each of the techniques. In fact, some of these cases were worked out at the same time that mitigation techniques were being developed.

Some of the techniques developed in this study can readily be applied to operative substations, while others can only be applied during the design stages. In addition, some of the strategies developed in this work are also valid for other parts of the electric network.

As the XXI century takes form, more technology is inevitable, consequently an increase of PFMFs is expected. At the same time development of sustainable societies is in growing demand. If we consider the electromagnetic field as part of such an environment, hopefully the methods developed in this study may contribute to the mitigation of unwanted magnetic field emissions in those societies.

Appendices

Appendix I: The field from a differential segment of current

To solve the apparent contradiction presented in chapter 2, one can assume the following argument, which is a "thought experiment": let's imagine an experimental set up (Fig. 1) in which the piece of wire representing the small element of current is covered by a tubular electrical insulator and immersed in a large container with a mercury bath

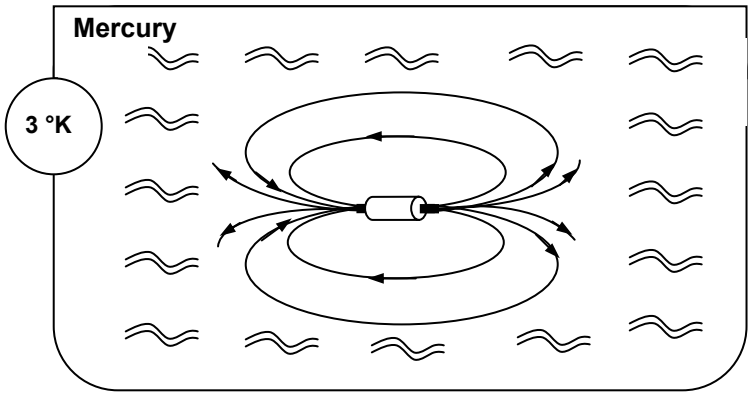

Fig. 1 Experimental set up to solve the contradiction of charge conservation.

at very low temperature to enhance its conductivity. Say, at 3 °K, since at 4 °K the resistance of mercury drops dramatically. The edges of the current element are not insulated thus the current is free to spread, which it does in all directions, hence it is possible to add end to end myriads of these insulated current elements as to form closed circuits filling the lines shown in Fig. 1. Once this is done the conducting fluid is drained away and would not contribute to any of the calculations. This spreading is symmetric on each edge, thus at a distance r the magnetic field $\boldsymbol{B}$ will be

distributed on a circle, as is shown in Fig. 2. In order to calculate $\boldsymbol{B}$ the flow of current though the spherical cap of radius r_c is evaluated and then obtained by the application of the Ampere circuital law.

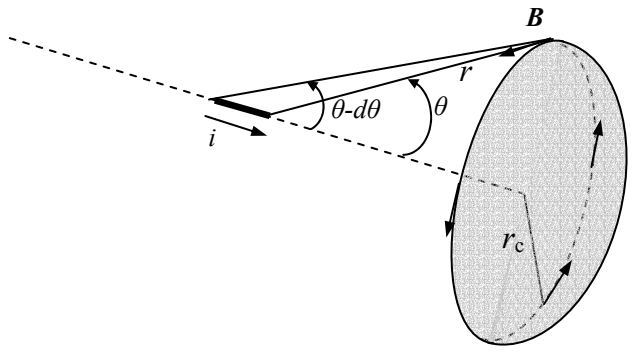

Fig. 2 Evaluation of the magnetic field $\boldsymbol{B}$ from a current element.

The current outflow through the spherical cap is given by

$$i_c = \textit{current density} \times \textit{area of the cap}$$

$$i_c = \frac{i}{4\pi r^2} \times 2\pi r^2 (1-\cos\theta) = \frac{i}{2}(1-\cos\theta)$$

Similarly, the current inflow through the cap is

$$i'_c = \frac{i}{2}[1-\cos(\theta - d\theta)]$$

Thus the total flow is the subtraction of inflow to outflow

$$i_c - i'_c = \frac{i}{2}[\cos(\theta - d\theta) - \cos\theta] = \frac{i}{2}\sin\theta \; d\theta$$

Applying the Ampere law to the circuit at the border of the cap

$$\oint \boldsymbol{B} \bullet d\boldsymbol{l} = \mu_0 (i_c - i'_c)$$

we obtain

$$2\pi r_c B = \mu_0 \frac{i}{2} \sin\theta \, d\theta$$

From Fig. 2, $r_c = r \sin\theta$, and $r\, d\theta = dl \sin\theta$, consequently

$$B = \frac{\mu_0 i dl}{4\pi r^2} \sin\theta \qquad (1)$$

In vector form this equation reconstructs the formula Eq. 2.1 (chapter 2). It is important to observe that the frequency of the current has not been specified. Therefore this formula is valid for 50 Hz (AC) which is the interest of this work, but even for continuous current (DC).

However for AC currents is possible another approach to the solution of the physical contradiction, namely to consider that the element of current consist of a charge attached to a harmonic oscillator, e.g. a spring (Fig 3).

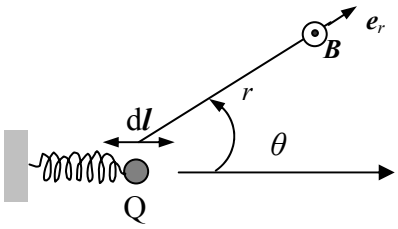

Fig. 3 An oscillating charge as model for the element of current.

The frequency of oscillation being 50 Hz, the current is $i(t) = dQ/dt = I \cos \omega t = \mathscr{R}e\,[I\, e^{j\omega t}]$. The direction of the oscillation is assumed to be along z. To determine the magnetic field of the system one can use the retarded vector potential [1].

$$\boldsymbol{A} = \frac{\mu_0 I\, dl}{4\pi} \left(\frac{e^{-j\beta r}}{r} \right) \mathbf{e}_z$$

where $\beta = \omega/c$. In spherical coordinates $\mathbf{e}_z = \mathbf{e}_r \cos\theta - \mathbf{e}_\theta \sin\theta$, thus the magnetic field is obtained from the expression $\boldsymbol{B} = (1/\mu_0)$ curl $\boldsymbol{A}$, giving

$$\boldsymbol{B} = -\frac{Idl}{4\pi}\beta^2 \sin\theta\left[\frac{1}{j\beta r} + \frac{1}{(j\beta r)^2}\right]e^{-j\beta r}\mathbf{e}_\phi$$

When $\omega = 2\pi f = 100\pi$, the region is in the near zone, (extremely low frequency) hence $\beta r = 2\pi r/\lambda << 1$. Therefore the magnitude of field in this approximation becomes

$$B = \frac{\mu_0 Idl}{4\pi r^2}\sin\theta \qquad (2)$$

Which again in vector notation represents Eq. 1, or Eq. 2.1 in chapter 2. Once the physical contradiction has been solved, Eq. 1 can be used to evaluate the field from specific sources.

Appendix II : Penetration depth for thin screens

For a magnetic field with two components B_x and B_y we assume propagation along the x-direction through a thin layer with conductivity σ and thickness h and infinite in y-z plane. Applying Maxwell's equations at power frequencies to this model gives

$$\nabla \times \mathbf{B} = \mu_0 \sigma \mathbf{E} \tag{1}$$

$$\nabla \times \mathbf{E} = -j\omega \mathbf{B} \tag{2}$$

From these two equations

$$\nabla \times \nabla \times \mathbf{B} = -j\omega\mu_0 \sigma \mathbf{B} \tag{3}$$

But $\nabla \times \nabla \times \mathbf{B} \equiv \nabla\nabla \cdot \mathbf{B} - \nabla^2 B$, and $\nabla \cdot \mathbf{B} = 0$, therefore

$$\nabla^2 \mathbf{B} = j\omega\mu_0 \sigma \mathbf{B} \tag{4}$$

With y-dependence proportional to e^{jky}, the x-dependence must be $e^{\pm\kappa x}$ where

$$\kappa^2 - k^2 = j\omega\mu_0 \sigma \tag{5}$$

Then we have the following formulation

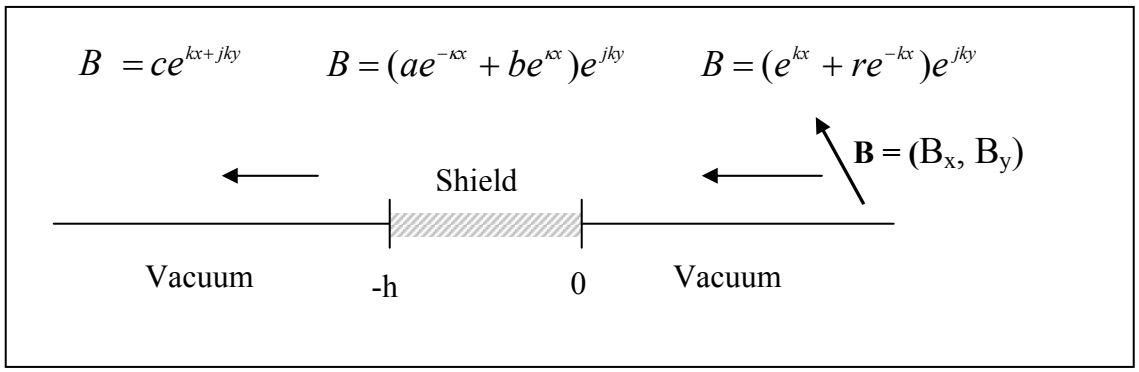

Applying continuity of B_x and B_y (which because of $\nabla \cdot \mathbf{B} = 0$, is the same than continuity for B_x and dB_x/dx) and Boundary conditions at x = 0 and x = -h, we obtain that

$$c = \frac{e^{kh}}{f} \tag{6}$$

where

$$f = \frac{1}{4k\kappa}\left[(\kappa + k)^2 e^{\kappa h} - (\kappa - k)^2 e^{-\kappa h}\right] = \cosh \kappa h + \frac{k^2 + \kappa^2}{2k\kappa} \sinh \kappa h \tag{7}$$

is the complex screening factor.

From Eq. 5

$$\kappa^2 \cong j\omega\mu_0\sigma = j\frac{2}{\delta^2} \tag{8}$$

then

$$\kappa = \frac{1+j}{\sqrt{2}}\sqrt{\omega\mu_0\sigma} = \frac{1+j}{\delta} \tag{9}$$

The penetration depth is

$$\delta = \sqrt{\frac{2}{\omega\mu_0\sigma}} \tag{10}$$

and in interesting cases $|\kappa| >> k$. Under this condition, an approximation of f that holds for h << δ is

$$f \cong 1 + \frac{\kappa^2}{2k}h = 1 + j\frac{h}{k\delta^2} \tag{11}$$

Note that since kδ << 1 if $|\kappa| >> k$, $|f|$ can be >>1 even if h < δ.

Therefore a screen that is thinner than the skin depth can give significant shielding. Also note that this effect is more significant for fields with long wavelength (small k) transverse to the screen.

Appendix III : Shielding of coils

A series of 3D simulations were performed with the coil described in section 9.3 in front of an open shield. Single, conductive and ferromagnetic; double, triple, and active shielding were simulated. Parameters such as distance to the shield and thickness were varied. Experimental verification was also carried out (e.g. Fig. 1 and Fig. 2). Some relevant information is given by the external shape (size) of the figures. It suggests a global comparison between all the cases (Fig. 3).

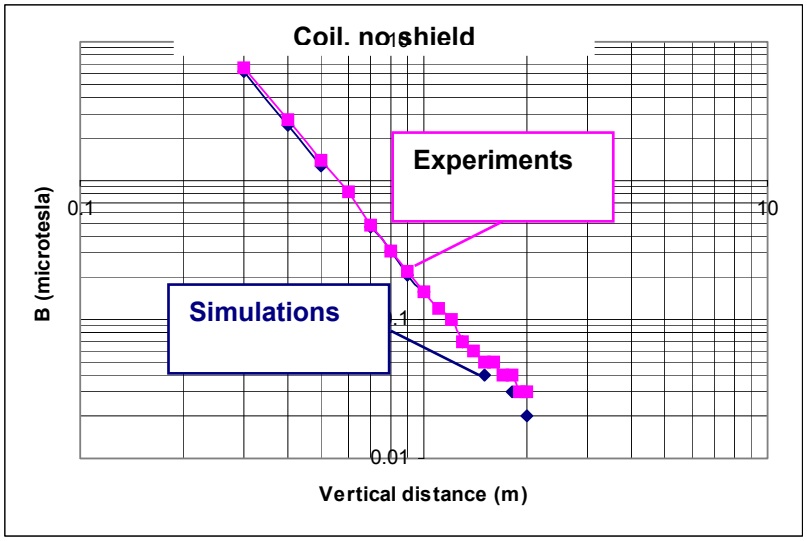

Fig. 1 Simulation vs. experiments, of the field from a coil, when no shield is placed.

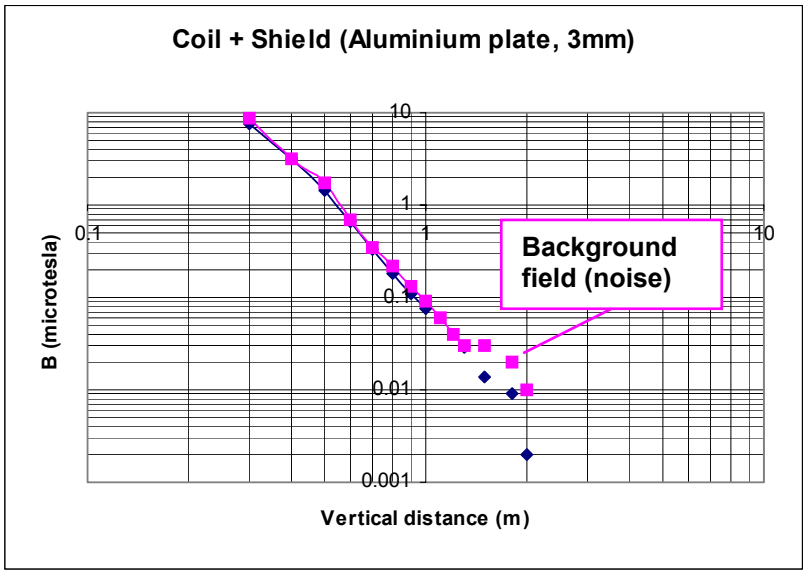

Fig. 2 Simulation vs. experiments, of the field of a coil, when a 3 mm aluminium plate is placed, at 15 cm from the coil. At distances larger than 1.5 metres, the magnetic background of the laboratory produces interference.

Fig. 3 Result from 3D-simulations: screening of 50 Hz magnetic field from coils, J = 100A/cross section. Range: 0.1-10 microtesla

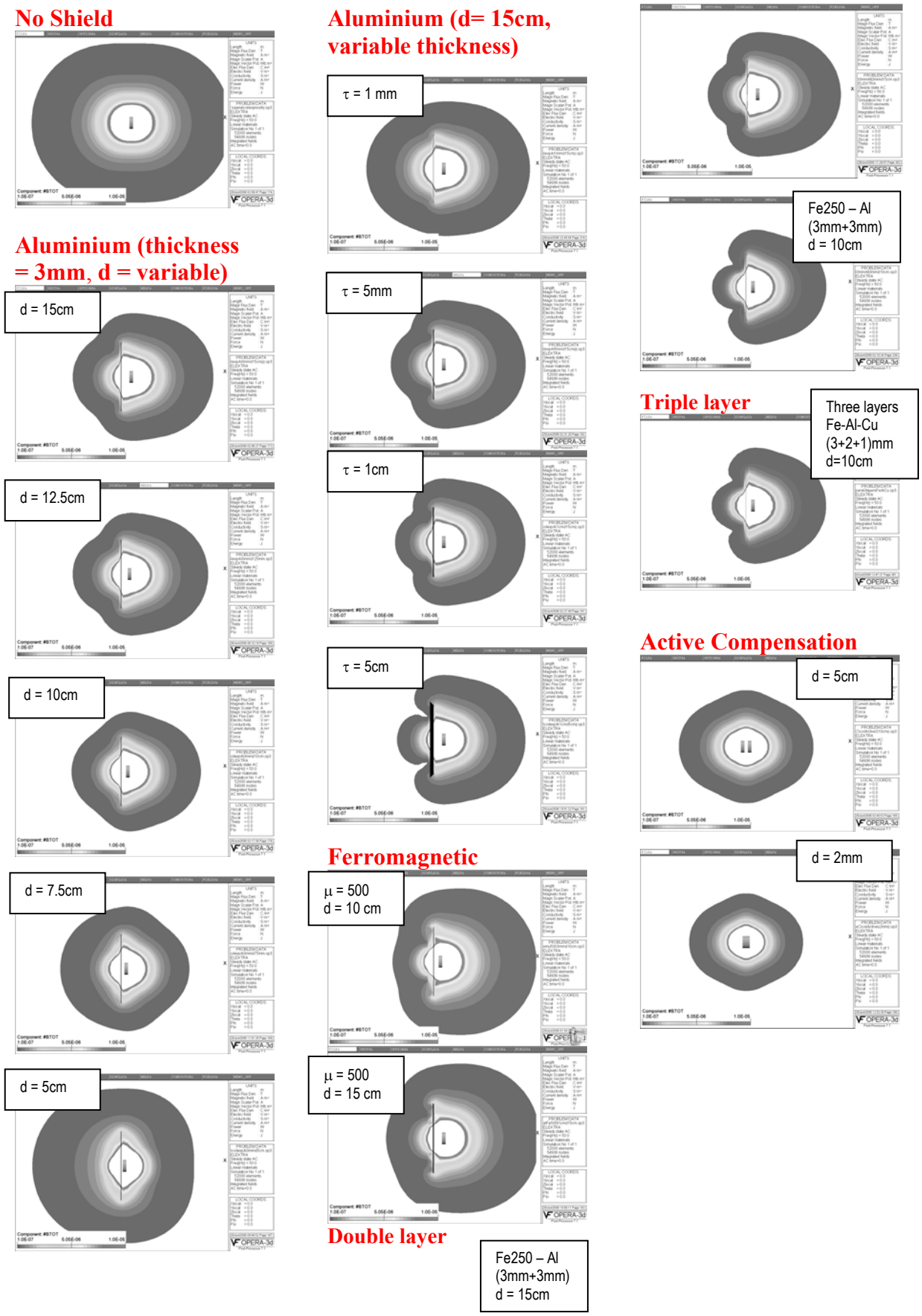

List of Articles

Paper A
E. Salinas, L. Aspemyr, J. Daalder, Y. Hamnerius, and J. Luomi, *Power Frequency Magnetic Fields from In-house Secondary Substations.*
Published at CIRED'99, 15th Conference on Electricity Distribution, Technical Reports, session 2, pp. 161-164. University of Liège, Belgium, June 1999.

Paper B
E. Salinas and A. Bondeson, *Shielding of Power Frequency Magnetic Fields from a Three-Phase System of Busbars.*
Published at IEEE-ANDESCON'99, International Conference of the IEEE Andean Region, Proceedings paper No. I031, Universidad Simon Bolívar, Caracas, Venezuela, September 1999.

Paper C
E. Salinas and L. Aspemyr, *Experimental Study of 50 Hz Magnetic Fields from 10/0.4 kV Substation Components.*
Published in the Proceedings of the Fourth Latinamerican Congress on Electrical Generation, Transmission and Distribution, Vinha del Mar, Chile, November 2000.

Paper D
E. Salinas and L. Aspemyr, *Measurements and Reduction of 50 Hz Magnetic Fields from the New Substation at the Department of Electric Power Engineering.*
Technical Report No. 14R, ISSN: 1401-6176, Department of Electric Power engineering, Chalmers University of Technology, Gothenburg, Sweden, August 1999.

Paper E
E. Salinas, A. Bondeson, J. Daalder and Y. Hamnerius
Towards a Global Strategy to Mitigate Power Frequency Magnetic Fields from Secondary Substations.
Published in proceedings of CIRED'2001, 16th Conference on Electricity Distribution, IEE Conference Publication No 482, Technical Theme 2, Paper 2.5, Amsterdam, 2001.

Paper F
E. Salinas, *Studies of Magnetic Fields at the Transmission and Distribution Stages*
Accepted for publication (August, 2001) in Journal of the IES on M&E Special Issues.

Paper G
E. Salinas, *Conductive and Ferromagnetic Screening of 50 Hz Magnetic Fields from a Three-Phase System of Busbars.*
To be published in Journal of Magnetism and Magnetic Materials, 2001, Vol. 226-230 (2001), pp 1239-1241.